UNIVERSITÉ DE MONTRÉAL

BLADDER VOLUME DECODING FROM AFFERENT NEURAL ACTIVITY

ARNALDO MENDEZ

INSTITUT DE GÉNIE BIOMÉDICAL

ÉCOLE POLYTECHNIQUE DE MONTRÉAL

THÈSE PRÉSENTÉE EN VUE DE L'OBTENTION

DU DIPLÔME DE PHILOSOPHIAE DOCTOR

(GÉNIE BIOMÉDICAL)

AOÛT 2013

UNIVERSITÉ DE MONTRÉAL

ÉCOLE POLYTECHNIQUE DE MONTRÉAL

Cette thèse intitulée :

BLADDER VOLUME DECODING FROM AFFERENT NEURAL ACTIVITY

présentée par : MENDEZ Arnaldo

en vue de l'obtention du diplôme de : Philosophiae Doctor

a été dûment acceptée par le jury d'examen constitué de :

M. SAVARD Pierre, Ph.D., président

M. SAWAN Mohamad, Ph.D., membre et directeur de recherche

M. MATHIEU Pierre-A., D.Sc.A, membre

M. BOUKADOUM Mounir, Ph.D, membre

DÉDICACE

To my family

ACKNOWLEDGEMENTS

I would like to express my immense gratitude to my advisor Professor Mohamad Sawan, first for believing in me since the very beginning, for his support, encouragement, generosity and advice during my Ph.D. studies in École Polytechnique de Montréal. I also thank Prof. Sawan for giving me the opportunity to work on such a difficult but fascinating subject in which we strongly believe.

I would also like to specially say thank you to Dr. Tomonori Minagawa, from Shinshu University in Japan, and Dr. Jean-Jacques Wyndaele, from University of Antwerp in Belgium, for the realization of the very difficult animal experimentation conducted at the Urology Department in University of Antwerp that provided us with neural data from the bladder. I also express my gratitude to Abrar Belghith from Enseirb-Matmeca University in France for her support in the VHDL-programming of the DSP during her internship at Polystim Neurotechnologies Laboratory. I would also like to thank my professors from École Polytechnique and Université de Montréal for allowing me to update and enhance my knowledge and evolve in a context of high-level research. I also thank sincerely Fayçal Mounaim, Marie-Yannick Laplante and Laurent Mouden for their valuable support through these years at Polytechnique. I am also grateful for support from the Canada Research Chair in Smart Medical Devices and le Fonds Québécois de la Recherche sur la Nature et les Technologies (FQRNT).

Finally, but not the least, I infinitely thank my family for their unconditional love and support, especially my wife and my three children who have waited with patience and love for Daddy during these years I have worked hard to achieve the results shown in this thesis.

RÉSUMÉ

Lorsque les fonctions de stockage et de miction de la vessie échouent à la suite de traumatismes médullaires, ou en raison d'autres maladies neurologiques, de conditions de santé ou au vieillissement, des complications graves pour la santé du patient se produisent. Actuellement, il est possible de restaurer partiellement les fonctions de la vessie chez les patients réfractaires aux médicaments à l'aide des neurostimulateurs implantables. Pour améliorer l'efficacité et la sécurité de ces neuroprothèses, il faut un capteur de la vessie capable de détecter l'urine stockée afin de mettre en place un système en boucle fermée qui applique la stimulation électrique uniquement lorsque nécessaire. Le capteur peut également servir à aviser les patients ayant des sensations affaiblies pour les aviser en temps opportun le moment où la vessie doit être vidée ou quand un volume résiduel postmictionnel anormalement élevé reste après une miction incomplète. Dans cette thèse, on présente de nouvelles méthodes de mesure, ainsi qu'un processeur de signal numérique dédié pour décoder en temps réel le volume de la vessie à partir des enregistrements neuronaux afférents provenant des récepteurs naturels présents dans la paroi de la vessie. Nos principales contributions sont rapportées dans trois articles de journaux avec comité de lecture.

On présente d'abord une revue exhaustive de la littérature comprenant des articles de journaux, des brevets et les livres les plus réputés portant sur l'anatomie, la physiologie et la physiopathologie du tractus urinaire inférieur ainsi que sur la mesure du volume ou la pression de la vessie. Cette étude nous a permis d'identifier les besoins qu'un capteur de la vessie doit satisfaire pour être utilisé dans des applications chroniques telles que celles proposées dans cette thèse. On présente aussi le résultat d'une analyse exhaustive des caractéristiques anatomiques et physiologiques de la vessie que nous avons identifiées d'avoir exercé une influence, ou même d'avoir empêché, la réalisation d'un tel capteur dans des études faites au cours des dernières années. Sur la base de cette étude et de l'évaluation systématique des méthodes de mesure pour la vessie, on a conclu que le principe de mesure le mieux adapté pour la surveillance chronique du volume de la vessie était la détection, la discrimination et le décodage de l'activité neuronale afférente découlant des récepteurs spécialisés du volume (mécanorécepteurs), au sujet desquels certains auteurs ont émis l'hypothèse de leur existence dans la muqueuse interne de la vessie.

Ensuite, on présente la méthode de mesure qui permet d'estimer en temps réel le volume de la vessie à partir de l'activité afférente des mécanorécepteurs. Notre méthode a été validée avec les

données acquises à partir de rats anesthésiés dans des expériences aiguës. Il a été possible d'estimer qualitativement trois états de remplissage de la vessie dans 100 % des essais où l'activité afférente enregistrée présentait un coefficient de corrélation de Spearman supérieur ou égal à 0,6. Par ailleurs, on a pu estimer quantitativement le volume de la vessie, et aussi sa pression, en utilisant des fenêtres de temps convenablement choisies. L'erreur moyenne d'estimation du volume fut de 5,8 ± 3,1 %. Nos résultats nous ont également permis de faire la lumière sur un sujet controversé concernant le type de réponses détectables à partir d'enregistrements afférents de la vessie. Nous avons démontré qu'il était possible de quantifier autant les réponses phasiques que les réponses toniques de la vessie lors de son remplissage lent et lors des mesures isovolumétriques, respectivement.

Enfin, on présente un processeur de signal numérique dédié (DSP, sigle en anglais) capable de surveiller le volume de la vessie en exécutant les méthodes de mesure qualitative et quantitative proposées. Le DSP exécute en temps réel la détection et la discrimination (classification) des potentiels d'action extracellulaires (PAEs) suivies par le décodage neuronal pour estimer soit trois niveaux qualitatifs de remplissage ou la valeur du volume de la vessie, en fonction du mode de sortie sélectionné. Le DSP proposé a été testé en utilisant des signaux synthétiques réalistes et des signaux réels de nerfs afférents de la vessie enregistrés au cours des expériences aiguës avec des modèles animaux. Le circuit de traitement pour faire la détection et discrimination des PAEs a donné une exactitude moyenne de 92% en utilisant des signaux contenant des PAEs avec formes d'onde fortement corrélées et avec un faible rapport signal sur bruit. Les circuits d'estimation du volume, qui ont été testés avec des signaux réels, ont reproduit les valeurs d’exactitude obtenues lors des simulations faites hors ligne en utilisant Matlab, c’est-à-dire, 94 % et 97 % pour les estimations quantitatives et qualitatives, respectivement. Pour évaluer la faisabilité, le DSP a été déployé dans le FPGA Actel Igloo AGL1000V2, qui a montré une consommation de puissance de 0,5 mW et une latence de 2,1 ms à une fréquence d’opération de 333 kHz. Ces performances démontrent qu'un capteur de la vessie implantable qui réalise la détection, la discrimination et le décodage de l'activité neuronale afférente est faisable.

ABSTRACT

Failure of the storage and voiding functions of the urinary bladder due to spinal cord injury (SCI), neural diseases, health conditions, or aging, causes serious complications in a patient's health. Currently, it is possible to partially restore bladder functions in drug-refractory patients using implantable neurostimulators. Improving the efficacy and safety of these neuroprostheses used for bladder functions restoration requires a bladder sensor (BS) capable of detecting urine volume in real-time to implement a closed-loop system that applies electrical stimulation only when required. The BS can also trigger an early warning to advise patients with impaired sensations when the bladder should be voided or when an abnormally high post-voiding residual volume remains after an incomplete voiding. In this thesis, we present new measurement methods and a dedicated digital signal processor for real-time decoding of the bladder volume through afferent neural signals arising from natural receptors present in the bladder wall. The main contributions of this thesis have been reported in three peer-reviewed journal papers.

We first present a comprehensive literature review, including papers, patents and mainstay books of bladder anatomy, physiology, and pathophysiology. This review allowed us to identify the requirements (user needs) that a BS must meet for chronic applications, such as those proposed in this thesis. An exhaustive analysis of the particular anatomical and physiological characteristics of the bladder, which we realized had influenced or prevented the achievement of a BS for monitoring the bladder volume or pressure in past studies, are also presented. Based on this study and on a systematic assessment of the measurement methods published in past years, we determined the best measurement principle for chronic bladder volume monitoring: the detection, discrimination and decoding of the afferent neural activity stemming from specialized volume receptors (mechanoreceptors), on which some authors had hypothesized about its existence in the bladder inner mucosa.

Next, we present methods that allows for a real-time estimation of bladder volume through the afferent activity of the bladder mechanoreceptors. Our method was validated with data acquired from anesthetized rats in acute experiments. It was possible to qualitatively estimate three states of bladder fullness in 100% of trials when the recorded afferent activity exhibited a Spearman’s correlation coefficient of 0.6 or better. Furthermore, we could quantitatively estimate the bladder volume, and also its pressure, using time-windows of properly chosen duration. The mean

volume estimation error was $5.8 \pm 3.1\%$. Our results also allowed us to shed light on the controversial subject of the type of responses that are detectable from bladder afferent recordings. We demonstrated that it is possible to quantify not only phasic but also tonic bladder responses during slow filling and isovolumetric measurements, respectively.

Finally, we present a dedicated digital signal processor (DSP) capable of monitoring the bladder volume running the proposed qualitative and quantitative measurement methods. The DSP performs real-time detection and discrimination of extracellular action potentials (on-the-fly spike sorting) followed by neural decoding to estimate either three qualitative levels of fullness or the bladder volume value, depending on the selected output mode. The proposed DSP was tested using both realistic synthetic signals with a known ground-truth and real signals from bladder afferent nerves recorded during acute experiments with animal models. The spike-sorting processing circuit yielded an average accuracy of 92% using signals with highly correlated spike waveforms and low signal-to-noise ratios. The volume estimation circuits, which were tested with real signals, reproduced the accuracies achieved by offline simulations in Matlab, i.e., 94% and 97% for quantitative and qualitative estimations, respectively. To assess feasibility, the DSP was deployed in the Actel FPGA Igloo AGL1000V2, which showed a power consumption of 0.5 mW and a latency of 2.1 ms at a 333 kHz core frequency. These performance results demonstrate that an implantable bladder sensor that detects, discriminates and decodes afferent neural activity is feasible.

TABLE OF CONTENTS

LIST OF TABLES

LIST OF FIGURES

LIST OF ACRONYMS AND ABBREVIATIONS

ATD	Absolute Thresholding Detection
AIC	Akaike's Information Criterion
ANOVA	Analysis of variance
ASIC	Application Specific Integrated Circuit
BIR	Bin-integrated-rate
BW	Bin-width
BS	Bladder sensor
BVD	Bladder Volume Decoder
BCI	Brain-Computer Interface
BC	Bulbocavernosus muscle
CNS	Central Neural System
CVI	Cerebral Vascular Incident
CAPs	compounded action potentials
CV	Conduction velocity
CUSUM	Cumulative sums
DSD	Detrusor-sphincter dyssynergia
DSP	Digital Signal Processor
DWT	Discrete Wavelet Transform

DRG	Dorsal root ganglia
EIP	Electrical Impedance Plethysmography
EIT	Electrical Impedance Tomography
EEG	Electroencephalogram
EMP	Electromagnetic plethysmography
EMG	Electromyogram
ENG	Electroneurogram
ED	Euclidian Distance
EUS	External urethral sphincter
FPGA	Field-programable gate array
FIR	Finite input response filter
FSM	Finite State Machine
FR	Firing rate
FIFO	First In First Out
FES	Functional electrical stimulation
FES	Functional Electrical Stimulation
GR	Gray rami
HoQ	House of Quality
IIR	Infinite input response filter

ICS	International Continence Society
IP	Intraperitoneal injection
IVP	Intravesical Pressure
IC	Ischiocavernosus muscle
LFP	Local field potentials
LUT	Lower urinary tract
MRI	Magnetic Resonance Imaging
MCU	Microcontroller
MEA	Multi-Electrodes Array
NBO	Neurogenic bladder overactivity
NCU	Neurostimulator Control Unit
NEO	Nonlinear Energy Operator
OAB	Overactive Bladder
OSR	Overall Success Rate
PAG	Periaqueductal gray matter
PC	Personal Computer
PMC	Pontine micturition center
PVR	Post void residual urine
PCA	Principal Component Analysis

PDF	Probability Density Function
QFD	Quality Function Deployment
RAM	Random Access Memory
ROC	Receiver Operating Characteristic
RBI	Rectifying and bin integration
RMS	Root Mean Square
RMSE	Root Mean Square Error
SNR	Signal to noise ratio
SAR	Specific Absorption Rate
SPH	Sphincter
SCB	Spike Classifier Block
SDB	Spike Detector Block
SRI	Spike Rate Integrator
SCI	Spinal cord injury
SPLN	Splanchnic nerves
SGP	Strain-gauge plethysmography
SPC	Superparamagnetic clustering
TEO	Teager Energy Operator
tfLIFE	thin-film Longitudinal Intra-Fascicular Electrode

UI	Urinary incontinency
UTI	Urinary tract infection
USEA	Utah Slanted Electrode Array
VHSIC	Very-high-speed Integrated Circuits
VHDL	VHSIC Hardware Description Language
WUS	Wearable ultrasonography
WED	Weighted Euclidian Distance
WR	White rami

LIST OF APPENDICES

INTRODUCTION

Nowadays there is an ongoing revolution in the field of neuroprosthetics devices that extend to different applications, allowing a total or partial rehabilitation of patients suffering from different neural diseases as consequence of spinal cord injury, stroke, traumatic brain injury, cerebral palsy, deafness, blindness, paralysis, movement disorders, and some mental illness and seizure disorders, among other diseases or non pathologic conditions as aging.

As consequence of the vertiginous development over the last decades, a new field of engineering known as neuroengineering or neural engineering emerged. This new field make use of all knowledge and cumulated experience of different fields of engineering and medicine with the aim of learn, understand, restore or augment functions and treat neural system diseases which includes both motor and sensory prostheses.

The introduction of new neuroprosthetic devices to the current clinical practice has been slower than other biomedical technology because of the high degree of complexity of the neural system and current technology limitations. One of the reasons of the restricted extension of recent neuroprosthetics devices is the limited efficacy controlling muscles, or organs like the urinary bladder, through open-loop systems due to the lack of a signal to feed back the neuroprosthetic device with the ongoing sensory information about the state, position or speed during muscles contraction and relaxation. Therefore, it can easily be deduced that the sensory feedback is crucial to effectively mimic the natural control of the targeted muscles or organs.

It has been show that the extraction of useful information from muscles (Electromyogram - EMG), nerves (Electroneurogram - ENG) and brain (Electroencephalogram - EEG) to feed back or command neurostimulator devices is an effective way to improve the Functional Electrical Stimulation (FES) efficacy restoring the lost or reduced capacity in handicapped patients [1]. These signals coming from natural receptors found in the skin, muscles, tendons, and joints are still present in many patients suffering from the diseases or conditions mentioned above. Capturing and interpreting reliably these signals by means of implanted interfaces in chronic applications is a great challenge due to the limited knowledge of the neural system and technological issues not solved yet.

The EEG, EMG and ENG signal can be used as source to command or feedback implanted neurostimulators depending on where the signal extraction is made and which the intended use of the FES device is. In clinical experiences with neuroprosthesis the EEG and EMG have been commonly considered as command signal, whereas ENG have been mainly used as feedback [1]. To achieve this goal real-time signal recording and sensory decoding is required.

The intelligent or smart neuroprosthesis with feedback capabilities are composed by two basic parts: the implanted unit (IU) and the external unit (EU). Usually both units are connected through a wireless link. The UI comprises mainly the recording subsystem that performs the front-end signal processing of the signals conveying sensory information, the neurostimulation subsystem implementing the FES approach, and a control logic driving both subsystems and the communication circuits with the EU. The IU sends the full recorded signal, or properly selected snips, to the EU unit that performs the back-end processing of the recorded signals and sends back the commands. The EU may also implement the implant-user interface and the implant-computer interface. The amount of information to exchange between the implanted and the external unit is limited by the wireless-link bandwidth and the maximum dissipated power allowable for a safe implant operation. The required power to the implanted device is typically supplied by the external unit by employing the same wireless-link with the data encoded properly.

The research conducted in this thesis is part of a larger project of the Polystim Neurotechnologies research group at the École Polytechnique de Montreal that for several years have been working under the direction of Prof. Mohamad Sawan in the search for solutions to restore urinary functions of paraplegic patients who underwent an spinal cord injury. Particularly, this thesis was focused on the research of an effective sensory feedback from the urinary bladder able to be used either as an embedded bladder sensor in a closed-loop system neuroprosthesis or as a standalone sensor able to advise patients with impaired sensations when the bladder need to be emptied. It is worth noting that in spite of the attempts done in past years, chronic bladder monitoring by an implantable device was not achieved due to limited knowledge and technological challenges that were undertaken in this work.

Motivation

FES has been studied over the last two decades to treat neurogenic bladder dysfunction [2-16]. Implantable FES devices were able to partially restore the bladder functions in patients who were considered refractory to more conservative treatments or those who could not tolerate the side-effects of prescription drugs [17],[18].

FES therapy can improve the patients' quality of life by preventing overactive bladder symptoms, non-obstructive urinary retention and bladder-sphincter dyssynergia [10],[17],[19]. This therapy can also reduce the frequency of urethral catheterization performed several times a day to empty the bladder, which causes much suffering to patients, recurrent urinary tract infections, and economical and physiological troubles. However, important side-effects of bladder FES therapy have been reported, such as an irreversible sacral deafferentation (dorsal rhizotomy), nerve-tissue injury produced by the continuous electrical stimulation, uncomfortable or painful sensations, infections, and changes in bowel function, among others [17],[19].

The restoring electrical neurostimulation performed by devices researched in past and those currently used in clinical practice is applied continuously without any sensory feedback ('blind stimulation'). Nevertheless, sensory feedback can improve the neuroprostheses effectiveness with the implementation of a conditional neurostimulation approach based on the ongoing bladder volume or pressure. This approach in turns provides the intrinsic self-regulation advantages of the closed-loop control systems [1],[8]. An FES device implementing a conditional neurostimulation approach applies the electrical stimuli as and when needed, thus favoring energy saving and minimizing the deleterious effects on the neural tissue caused by continuous electrical stimulation [20]. Thereby, chronic monitoring of the bladder volume is required to improve the effectiveness, tolerability and safety of the neuroprosthetic devices used for restoring bladder functions. Attempts over the past few years, which are comprehensively reviewed in Chapter 2, have been made to find a suitable method for continuous bladder monitoring. However, a reliable, precise and robust device for providing feedback with sensory information from the bladder had not yet been identified.

Moreover, a sensor for chronic monitoring of bladder volume can also be useful as a standalone device able to provide early warnings to patients with impaired sensations when the bladder is approaching its capacity or when abnormally high post-voiding residual volume remains after an

incomplete voiding. Such a sensor may also be helpful in bladder differential diagnosis, bladder disease research and in the choice of best suited clinical therapy approaches.

Objectives

Our main objective was to find an effective method for chronic bladder volume monitoring with the aim of supplying an FES device with the feedback information required to restore bladder functions in a safe and effective manner. To accomplish the general objective, the following specific objectives were developed:

1. Identify user needs that a sensor for chronic bladder volume monitoring must fulfill for the intended application.
2. Determine whether a measurement principle based on artificial sensors or on natural receptors is best suited to satisfy the user needs.
3. Propose a bladder volume measurement method based on the selected measurement principle.
4. Validate the proposed measurement method for bladder volume monitoring using *in vivo* recordings from rats.
5. Assess the feasibility of an electronic device deploying the proposed bladder measurement method.

Thesis works

To clarify the problem, it was necessary to identify the main issues of chronic bladder volume monitoring while considering the anatomical and physiological characteristics of the lower urinary tract (LUT) and its innervation. Thus, an exhaustive review was conducted of updated literature from the different sources indexed in the PubMed, Compendex, Inspec and Derwent Innovation Index on-line databases and the recent editions of well-known reference books on clinical urology practice and neurophysiology [21-26]. The most relevant achievements and pitfalls in the bladder monitoring studies performed in the past years were identified from this analysis.

Once the problem was clarified and the challenges were recognized, the user needs were identified. These are the medical, technical, and ergonomics needs that should be satisfied by a

bladder volume monitoring device to provide the information about bladder volume or pressure. This identification was a crucial step toward the proposition of the measurement method to be used in the implementation of such a device.

The identified needs were translated into technical specifications, also known as target specifications, using the quality function deployment (QFD) methodology [27]. Some published studies and the standards defined by the International Continence Society (ICS) [28],[29], were used as references during this process.

Next, a functional decomposition of the measurement system was performed to identify the critical sub-functions and to focus the search for their solutions. A comprehensive literature review was performed with this goal, and all measurement principles and methods for volume measurement in medical and non-medical applications, particularly the methods used in past research for monitoring bladder volume or pressure, were compiled.

Subsequently, the compiled volume measurements methods were evaluated to identify those that better satisfied the needs and specifications defined in the preceding analyses. The evaluation criteria were obtained from the most important user needs and carefully matched with relative importance weights. An initial screening was performed to keep the most promising methods for the next analysis. These methods were chosen based on the expected feasibility, the technological availability and the go/no-go test that used the most relevant user needs as a threshold. A much more refined selection process was completed using evaluation matrices with the selection criteria and the corresponding weights. To ensure that the method selection was robust enough, i.e., less dependent on the variation of the assigned weights, various sets of weights were used, and the final score was calculated by averaging the resultant score for each set, while keeping the rating given to each method. To rate each measurement method, a qualitative scale was employed. This methodology allowed best methods to be chosen more objectively, overcoming the most evident bias that is often present in any researcher analysis.

From the results of the comprehensive literature review, user needs identification and an exhaustive analysis of all possible measurement methods, we concluded that the bladder mechanoreceptors were the best choice for the primary transducer for chronic monitoring.

The hypothesis and research questions were defined based on the published experimental results about the afferent activity of bladder mechanoreceptors in validated animal models (rats, cats,

dogs, and pigs). These types of studies have not been done in humans due to the highly invasive nature of the experiments needed to draw conclusions about the functioning of the mechanoreceptors. The conclusions from some of these studies suggested that volume-specific mechanoreceptors should exist in the bladder wall for properly controlling the bladder [30] and that the activity of these receptors increases with different response patterns during the bladder filling [31-34].

The initial evidence for the power feasibility of implantable circuits for real-time neural source discrimination was obtained from a theoretical study based on simulations [35]. Nevertheless, we did not find any study demonstrating the feasibility of real-time neural source discrimination together with sensory information decoding, both of which are required for the standalone (autonomous) operation of implantable neural sensors.

Consequently, we defined the two main thesis hypotheses as follows:

> H1. When the local nervous system is intact, the bladder volume monitoring can be performed by decoding the afferent mechanoreceptors activity using an implantable device.
>
> H2. The measurement method is deployed in a standalone, implantable system that estimates the ongoing bladder fullness state with an accuracy of 75% or better.

We chose 75% as an acceptable value of accuracy for a difficult measurement to be performed by an implantable device monitoring a physiologic variable in real-time.

The respective research questions underlying these hypotheses were as follows:

1. Can the afferent activity of bladder mechanoreceptors be detected and decoded in real-time to monitor the volume or pressure?
2. Is the measurement method electronically feasible and effective for a standalone implantable device considering power and real-time constraints?

As is customary in the research process, we performed an iterative search of the proper method for sensory decoding of bladder volume or pressure from neural afferent activity. We started with a preliminary method proposition, and we performed experiments using animal models.

Subsequently, the estimation methods were improved gradually to achieve the targeted objectives. Finally, the measurement methods and the thesis hypothesis H1 were validated.

Acute experiments with rats were carried out to record bladder mechanoreceptor afferent activity along with the pressure and the known volume of the infused saline. Three types of experiments were performed with particular objectives. The first type of experiment allowed us not only validation of the proposed measurement methods but also to research the afferent activity during the resting, filling and voiding phase using a saline infusion pump with a physiologic filling rate and the instruments required for pressure and neural signal recordings. The second type of experiments was performed to research the reversibility of the mechanoreceptor afferent response by passively withdrawing the infused saline using a second infusion pump. The last experiment type allowed us to research whether the bladder showed phasic and tonic responses during the slow filling and during the isovolumetric measurement phase when the bladder was filled to different level of fullness. Important conclusions were drawn from the experimental results, which demonstrated the feasibility of bladder volume and pressure estimation from the mechanoreceptor afferent activity, the hysteretic mechanoreceptor response and the presence of both phasic and tonic responses. The latter response is a controversial subject we noticed during the literature review.

Two decoding methods were proposed to estimate the bladder volume in real-time. The first method allowed qualitative volume estimations, i.e., three levels of fullness defined as low-volume, comfortable level; medium level, the need-to-void within a proper timeframe; and high level, the urge-to-void because there is a risk of an imminent leaking. The second, a quantitative method, allowed the real-time estimation of the bladder volume or pressure value.

The qualitative method required low-computational cost and only a few hardware resources for its electronic implementation and yielded a high accuracy estimation of the bladder volume. The three qualitative levels defined appear to be sufficient for proper feedback of an FES device for restoring bladder functions and for advising patients with impaired sensations. On the other hand, the quantitative method can accurately compute the bladder volume for future applications, such as patient warning, differential diagnosis, and clinical research. The quantitative method was implemented by a regression model optimized to run in real-time with much lower computational

cost than those found in published works for decoding sensory information from neural recordings.

Both methods required neural source detection and discrimination in real-time, also known as on-the-fly spike sorting. This is a high demanding task even for a powerful personal computer and commonly requires human supervision, which are huge limitations that prevented the use of such algorithms in our intended application. Therefore, new algorithms were proposed and optimized to run unsupervised in real-time with low-computational cost to detect extracellular action potentials (spikes) immersed in noisy signals and to perform the on-the-fly spike sorting process.

The estimation methods were designed to run in two phases to reduce the system complexity and the amount of hardware resources required by the implantable device for real-time bladder volume monitoring. The first is a training phase that is executed offline, and the second is the monitoring phase in which the unsupervised real-time volume estimation is performed. The training phase is used to determine the parameters required for the real-time monitoring phase. During the training phase, the most suitable algorithms were executed, regardless of their complexity, to compute the optimal parameters; whereas the monitoring phase, which is to be implemented in an electronic system, used lower complexity and much faster algorithms. Using this approach, some of the complexity from the monitoring phase could be transferred to the training phase without affecting the estimation accuracy.

The simulation and validation tests of the methods were realized in Matlab/Simulink with a real-time-like signal processing approach using realistic synthetic signals with known ground-truth to test the spike sorting process and real recordings from the *in vivo* experiments to test and validate the measurement methods.

To deploy the method in a standalone electronic system that could be implanted in the lower abdomen or near the targeted spinal root, several algorithms for the detection, classification and decoding of neural signals were designed and optimized to run unsupervised in real-time using few hardware resources and low-power consumption. An improved digital circuit was designed for detecting the spikes in signals with high background noise by estimating the instantaneous energy and comparing it with a self-tuned detection threshold. Furthermore, a digital circuit was designed for the spike classification using the template matching technique with a new metric

that allowed unsupervised on-the-fly spike sorting with high classification accuracies, even for highly correlated spike waveforms.

The new algorithms implemented by the real-time signal processing circuits were previously tested in Matlab/Simulink using custom-written software. Fixed-point arithmetic was chosen to reduce the signal processing retrieval times (latency) as much as possible and also the hardware burden compared with those required for floating-point arithmetic implementation. The number of bits for number representation was carefully determined using simulations performed with the Fixed-point toolbox of Matlab/Simulink to account for the trade-off between the amount of hardware required and the computation accuracy.

The electronic system was implemented in a dedicated digital signal processor (DSP) using a low-power field-programmable gate array (FPGA) to account for the trade-off between a fast and cost-effective R&D process for the bladder sensor and the overall performance required for future tests in chronic experiments. Finally, the results of the validation tests, which were also performed using the realistic synthetic signals and the signals from animal recordings, allowed us to validate the research hypothesis H2 by showing that an implantable low-power bladder sensor is feasible and accurate for the intended application.

Note: Throughout the document, the International System of Units was used for all measurements except for pressure. We used centimeters of water (cmH_20) instead of Pascal (Pa) because cmH_20 is the standard unit for research on this subject and for urodynamic clinical diagnostic tests. For references purposes, 1 cmH_20 (4°C) = 98.0638 Pa.

Contributions

The thesis contributions were reported in three peer-reviewed journal papers. The two major contributions of our research works were as follows:

1. New measurement methods for decoding the bladder volume and pressure from the neural afferent activity arising from the bladder mechanoreceptors. The achievement of this contribution required original research based on the data gathered from experimentation

with animal models. No previous study has demonstrated the feasibility of volume estimation using the afferent activity of the bladder mechanoreceptors.

2. On-chip implementation of a dedicated DSP capable of performing in real-time the spike sorting process and the neural decoding with low-power consumption. To the best of our knowledge, this is the first time that such a DSP performing all these complex tasks, usually run on a personal computer, is reported.

Other important contributions that allowed the achievement of these two major contributions are summarized below:

- Identification of the user needs that a bladder sensor must meet to be effective, safe and tolerable. This comprehensive list of needs was obtained from a thorough study of the specialized medical literature and was crucial for achieving our objectives. This user needs list may also help in future related research.
- Selection of the bladder volume measurement method best suited for neuroprosthetic implants. This selection was not evident from the commonly used pros and cons analyses found in past studies focused on this subject. Some of these studies showed some issues in their methodological approaches and misunderstanding of the bladder neurophysiology. The review, assessment and selection of the measuring method for bladder monitoring were reported in [36].
- Based on the results of specially designed *in vivo* experiments and the subsequent signal processing and statistical analyses, we showed that it is possible to measure accurately the tonic and phasic responses of the bladder detrusor muscle using the proposed method. The experiments with animal models and the neural signal processing used for the real-time decoding of the sensory information arising from the bladder were reported in [37].
- To demonstrate the feasibility of an implantable bladder sensor that deploys the proposed decoding methods, several interesting solutions were found to meet the real-time and low-power consumption constraints imposed on the implantable sensors. The main contributions reported in [38] on this subject were as follows:

- Accurate detection of action potentials (spikes) immersed in signals with a low signal-to-noise ratio using a self-adjusted threshold circuit.
- Accurate spike discrimination using a method that does not require the customary processing sequence comprising spike feature extraction, dimensional reduction, and clustering, thus allowing for a frugal deployment of a digital circuit with low-power consumption.
- Digital implementation of the decoding method with fixed-point arithmetic that was accurate enough using a readily accessible input parameter, such as the spike-rate count, within a time-window of optimally chosen duration.

Social and economic impact

Patients suffering from urinary dysfunction are a topic of high interest because it affects millions of people all over the world [39]. The huge number of patients living with this problem and the economic impact is overwhelming. In just the United States, an estimated 34 million community-dwelling men and women have an overactive bladder. Managing urinary incontinence and overactive bladder costs $19.5 billion a year [40],[41].

The urinary incontinency (UI) prevalence in the Canadian population is estimated to be 3.3 million (10%) [42]. UI is a common condition in the elderly, affects 30% to 60% of patients over 65 years of age, and increases exponentially with age [43]. The projections of Statistics Canada estimate that the number of seniors will double by 2031. There are nearly 4 million of people aged 65 or older in Canada today, but in 30 years there will be 8.7 million, with 2.3 million who are at least of 80 years old. Age is strongly associated with the onset of chronic bladder conditions, which can lead to activity limitations, disabilities, and institutionalization. Therefore, it is expected that this growth in the elderly population will exert increasing pressure on the health care system [42]. Furthermore, there are 85,556 patients in Canada living with spinal cord injury (SCI) [44], which is a major cause of bladder dysfunction [40],[41].

These are, indeed, staggering economical and epidemiological statistics, but it also important to consider the social impact of disease and the patients' impairment. Stigmatization, isolation, loss of self esteem, depression, and risk of institutionalization are present in many patients suffering

from bladder dysfunction. A study with data from the Canadian Community Health Survey shows that urinary incontinence is a major cause of depression in Canadian women with an average prevalence of 15.5%, which increases to 30% in women with ages between 18 and 44 years [45]. Moreover, a recent study demonstrated that the UI has a negative impact on the psychological burden of family caregivers [46].

With this thesis research, we aimed to improve the quality of life and life expectancy and to reduce the high cost of patient care for those suffering from urinary dysfunction due to different diseases, neurological disorders, and other non-pathologic conditions such as aging. We intended to achieve these goals by providing new knowledge and solutions for an unsolved problem, such as the chronic monitoring of bladder volume and pressure. We hope that the result presented in this thesis can help in bladder dysfunction treatment and diagnosis.

Thesis organization

The thesis comprises this Introduction, four chapters, and a final chapter with a general discussion and conclusions. We present the following work: a careful study of the targeted biological system (lower urinary tract), a literature review, an assessment of the measurement methods used in past studies, the proposal of new measurement methods based on recorded afferent neural activity, and the deployment of the proposed dedicated electronic system deploying the measurement method researched.

The first chapter of the thesis introduces the reader to the fundamentals of the anatomy, physiology and physiopathology of the urinary bladder that are necessary for a better understanding of the thesis work, the scope, objectives, impact and contributions. Particular emphasis is given to the neural control of the urinary bladder due to its relevance for the approach adopted in our research.

The second chapter presents three important subjects related to bladder volume monitoring: 1) a comprehensive review of the previous measurement method for monitoring the bladder volume and pressure; 2) the anatomical and physiological characteristics that we found to have the greatest impact in past studies that failed to find a solution for the bladder monitoring problem; and 3) an assessment of all of the measurement methods used in past studies, which allowed us to determine the method that was most suitable for our research objectives.

The third chapter first describes the acute experiments we performed in anesthetized rats and then proposes two measurement methods. These methods, one qualitative and another quantitative, estimated the bladder volume or pressure from the afferent neural activity arising from bladder mechanoreceptors. Finally, the result of the validation tests of these estimation methods and other test runs are presented.

The fourth chapter explains the design of the electronic system for the proposed measurement method to estimate in real-time the bladder volume or pressure from the recorded neural activity using an on-chip dedicated digital signal processor implemented in a low-power FPGA. Each processing block and the whole system is described and validated using both realistic synthetic signal and real signal recordings, thus showing the feasibility of such a system intended to be used in intelligent neuroprosthetic devices.

The fifth and last chapter discusses the thesis results. Finally, conclusions and recommendations for future work are presented.

Four Appendices are presented at the end of this thesis. Appendix 1 presents the list and the weightings of all of the identified user needs; Appendix 2 lists of all of the targets specification obtained using the QFD method; Appendix 3 presents the values of the weights and rates used in the assessment of the measurement methods; and finally, Appendix 4 shows the result of the analyses performed to choose the correlation coefficient better suited to identify the best unit for bladder volume decoding.

CHAPTER 1 OVERVIEW OF THE URINARY BLADDER

The urinary bladder presents challenging characteristics that have greatly hampered the achievement of a sensory device capable of monitoring urine volume and vesical pressure. Understanding the anatomy, physiology and physiopathology of the urinary bladder is crucial for accomplishing any successful work concerning sensory recovery and restoration of the storing and voiding functions.

An overview of these subjects, with a particular emphasis on the neural control involved in bladder functions, is provided to facilitate the understanding of the thesis works. Finally, the clinical practice standards for evaluating the bladder urine volume are introduced to show their particularities and limitations for chronic bladder monitoring.

1.1 Bladder anatomy and physiology

The urinary bladder is part of the urinary system, which is also composed of the kidneys, the ureters, and the urethra (Figure 1-1). The function of urinary systems is to regulate the water and ionic composition of the body, to excrete waste and potentially toxic products of metabolism, to remove foreign chemicals and to produce several hormones.

The bladder functions are the storing and voiding of urine in a coordinated and controlled manner. The bladder must store a socially adequate volume of urine until voiding is voluntarily elicited. To store urine, the bladder smooth muscle (detrusor) must be relaxed, and the sphincter must be contracted (closed). In contrast, emptying the bladder requires synchronous activation of all detrusor muscles because contracting only one part would stretch the uncontracted compliant (flexible) areas, thus preventing the increase in pressure necessary for urine to be expelled through the urethra. At the same time, these contractions must be followed by sphincter relaxation and opening to discharge the urine.

The bladder detrusor is a smooth muscle that is more adaptable than skeletal muscle and is able to adjust its length over a much wider range. For instance, if the bladder is filled to 400 mL with a diameter of 30 cm and is then emptied to a residual volume of 10 mL with a diameter of 8 cm,

the diameter would have decreased ~75%; thus, the detrusor would have a change in muscle length of same magnitude [47].

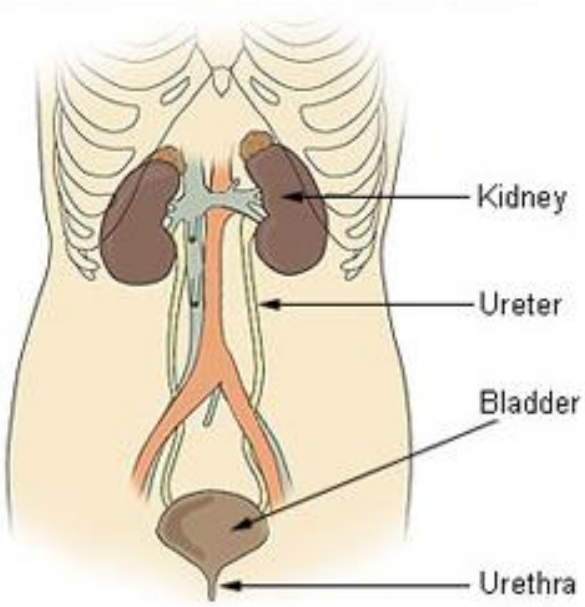

Figure 1-1 Components of the urinary system, from [48].

The bladder can be divided into two parts: a body lying above the ureteral openings and a base consisting of the trigone and bladder neck. The bladder outlet is composed of the bladder base, the urethra, and the internal and external urethral sphincter (rhabdosphincter), as shown in Figure 1-2.

The urethra and the sphincter system (Figure 1-2) play an important role in the two principal bladder functions of storing and voiding. These components not only provide controlled urine conduction way but also play an important role in the guarding and micturition reflexes.

There are anatomical and functional differences between the male and female urethral sphincter systems. Males have an internal sphincter composed of smooth muscle at the level of the bladder neck that is innervated by the sympathetic nervous system to prevent retrograde ejaculation. The female urethra is much shorter than that of the male. This is one factor which accounts for the higher prevalence of incontinence in females.

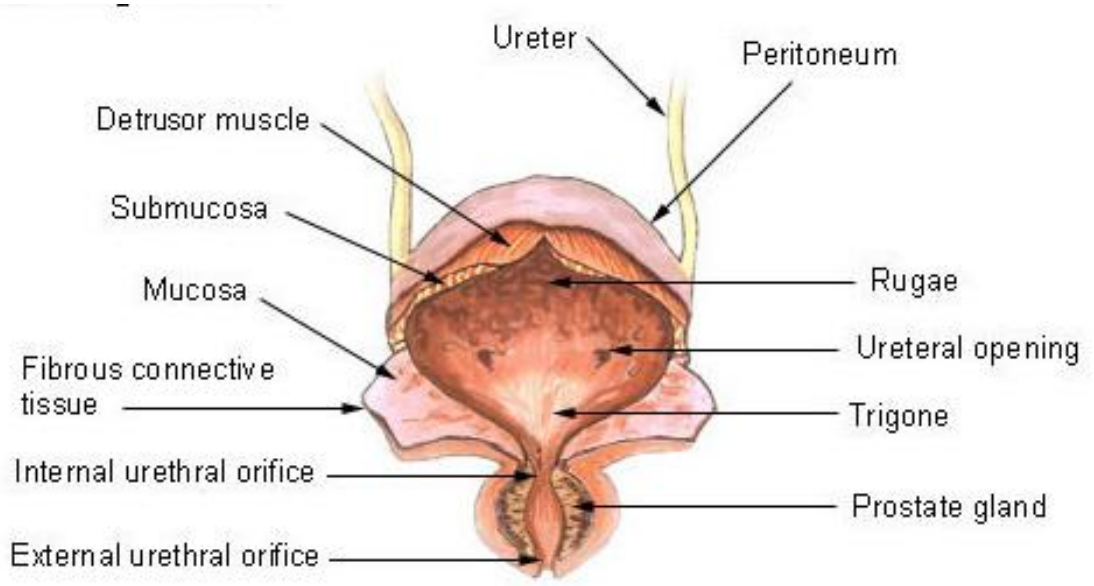

Figure 1-2 Anatomy of the urinary bladder, from [48]

Both the external urethral sphincter (EUS) and the internal urethral sphincter (IUS) allow the control of the opening for urine discharge. The EUS is composed of striated muscles that allow voluntary control of micturition by somatic innervation. In contrast, the IUS, which is composed of smooth muscle, is controlled by autonomic innervation.

The bladder has a storage capacity of approximately 400 – 600 mL, which can accommodate the production of 1 – 2 L of urine per day, in an average adult. The bladder is typically emptied 5 – 7 times a day, often at much smaller volumes. The average urine flow time is less than 30 seconds; thus, the bladder is actively emptying less than 1% of the time. Therefore, the predominant function of the bladder is storing urine [49].

1.2 Bladder biomechanics

The fundamental mechanical properties of the bladder include the stress-strain relationship, viscoelasticity, and deformation of bladder tissue. Whole-bladder properties include bladder shape, mass, and distention.

Basic bladder hydrodynamics and biomechanical properties depend on the relationship between bladder shape, size, pressure, and tension, as expressed by Laplace's law, which is shown in equation (1-1). There is a direct relationship between the wall tension and the intravesical pressure and bladder size. In this equation, T is the bladder wall tension, P_{ves} is the intravesical pressure, R is the bladder radius, and d is the wall thickness. During normal bladder filling, P_{ves} increases very slowly. When the bladder is completely distended, the wall thickness d decreases significantly relative to the other parameters unless a hypertrophied wall exists. At this point, a further increase in P_{ves} will produce high wall tension and strong afferent activity.

$$T = P_{ves}\frac{R}{2d} \tag{1-1}$$

The bladder compliance (C) is defined as the ratio between the variations in the bladder volume and detrusor pressure (P_{det}) as shown in equation (1-2).

$$C = \frac{dV}{dP_{det}} \tag{1-2}$$

The viscoelastic behavior of the bladder and urethra depends on both neuromuscular and mechanical properties. The mechanical properties rely on the magnitude of the wall stretch (distention) and the tissue structure and composition. The bladder is mainly composed of smooth muscle, 50% collagen and 2% elastin [47]. The collagen content increases with injury, obstruction, and denervation, leading to decreased bladder compliance. Conversely, the compliance will be higher when the elastin content exceeds the collagen content. A decrease in compliance or in the efferent neural input modifies the wall tension, causing an abnormal increase in the afferent activity, which may disturb normal bladder sensations and the threshold volume for micturition.

The bladder is typically modeled as a spheroid; however, this organ exhibits one of the most irregular anatomic shapes, especially when it is full, due to the contact with surrounding pelvic structures. Estimating the volume by instrumentation principles based on bladder geometry becomes more difficult because of this shape irregularity.

The bladder intravesical pressure depends on both the abdominal (P_{abd}) and detrusor (P_{det}) pressures, as shown in equation 1-3. Bladder emptying depends on the detrusor contraction for increasing P_{det} without a significant increase in P_{abd}.

$$P_{ves} = P_{det} + P_{abd} \tag{1-3}$$

P_{ves} measurement during bladder filling shows low and relatively constant bladder pressures (6 to 10 cm H_2O in humans) when the bladder volume is below the threshold for inducing voiding. The accommodation of the bladder to increasing volumes of urine is primarily a passive phenomenon that depends on the viscoelastic intrinsic properties of the vesical smooth muscle and the quietness of the parasympathetic efferent pathway.

1.3 Bladder innervation

Bladder innervation involves both the autonomic (involuntary) and the somatic (voluntary) nervous system. Pelvic parasympathetic nerves, which are located at the sacral level of the spinal cord, drive micturition reflexes by contracting the detrusor muscle and relaxing the urethra. The sympathetic nerves, which are located in the lumbar zone, have an opposite action: they promote the storing reflex by relaxing the detrusor muscle and contracting the bladder base and the urethra. The pudendal somatic nerve, which contains afferent sensory axons and efferent motor axons, excites the EUS.

In humans, the afferent axons in the pelvic, hypogastric, and pudendal nerves transmit information from the lower urinary tract to the lumbosacral spinal cord from L1 to S4 roots. The location of these nerves varies from one experimental model to another. The protocols for studying bladder innervation are consequently adjusted.

The bladder wall contains sensory receptors that work as physiological transducers, transforming natural energy into a train of all similar action potentials where sensory information is encoded in the time interval between them. Most of these receptors respond only to one type of energy (mechanical, thermal, or chemical), but others can respond to a combination of different types of energy. Mechanoreceptors respond to bladder wall distension and contraction by increasing or decreasing their firing frequency. Trough the afferents pelvic, hypogastric and pudendal nerves,

these action potentials are reaching the spinal cord at L1 to S4 levels and are relayed to the pontine storage and micturition centers, as shown in Figure 1-3.

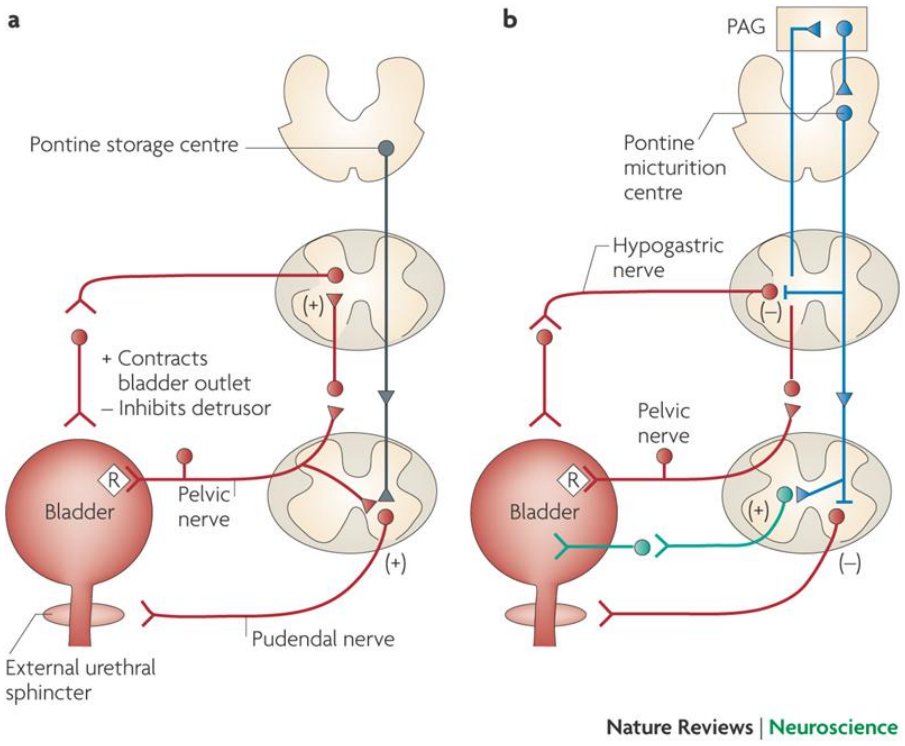

Figure 1-3: Neural circuits controlling the storage and voiding reflexes. A) Storage reflexes pathways. B) Voiding reflexes pathways. PAG: Periaqueductal grey, R: receptors on afferent nerve terminals [50].

The mechanoreceptors can be slow- or fast-adapting receptors. The slow-adapting mechanoreceptors detect changes in pressure, while the fast-adapting mechanoreceptors respond to rapid changes and vibration. The frequency of action potential discharge is proportional to the intensity of the stimulus. The sensitiveness threshold (minimum pressure required to excite the mechanoreceptor) of the physiological pressure in humans is between 5 and 40 cmH_2O. This pressure is in the range of the compliant part of the pressure-volume curve (25 - 75%). This threshold is well correlated with the point where the first sensation of filling is normally detected, although the threshold can be higher, for example, 95 cmH_2O after a spinal cord injury [22].

In the pelvic and hypogastric nerves of rats and cats have been found axons of mechanoreceptors that respond to bladder contraction and distention, known as in-series tension mechanoreceptors [25],[47]. Furthermore, afferent nerves that respond only to bladder distention during filling but not to detrusor contractions have been identified in the rat bladder and appear to be volume receptors that are possibly sensitive to the inner mucosa stretching [30].

The pelvic nerve, which conveys information about bladder volume, is composed of myelinated Aδ fibers and unmyelinated C fibers. The latter are silent fibers that show no activity in a normal individual during the bladder filling but become active during neuropathic and inflammatory conditions. In contrast, C fibers are normally active in animal models such as rats but not in humans [32],[33].

The storing and voiding reflex pathways controlling the bladder are depicted in Figure 1-3 [50]. These pathways, comprising superior brain centers and the spinal cord, ensure a reciprocal relationship between the bladder and the urethra. During the urine storage phase, Figure 1-3a, bladder distention produces low-level bladder afferent activity that stimulates both the sympathetic discharge to the bladder outlet (base and urethra) and the pudendal nerve discharge; these discharges keep both urethral sphincters closed. Both responses are driven by spinal-reflex pathways and represent the guarding reflexes that maintain continence. The sympathetic activity also inhibits the detrusor muscle and neural transmission in bladder ganglia.

The voiding reflex mechanism is shown in Figure 1-3b. Voluntary micturition is initiated by somatic (voluntary) relaxation of the EUS. At the beginning of micturition, intense vesical afferent activity turns on the pontine micturition center (PMC) in the brainstem. The PMC inhibits the spinal guarding reflexes mediated by the sympathetic and pudendal outflow to the bladder base and both urethral sphincters. The PMC activation stimulates parasympathetic outflow to contract the bladder detrusor and to relax the smooth muscle of the IUS internal urethral sphincter. The voiding reflex is maintained by the ascending afferent input from the spinal cord that passes through the periaqueductal gray matter (PAG) before reaching the PMC [50].

1.4 Bladder dysfunction

There are several causes of storage and voiding dysfunction, which is often multifactorial [25]. Both the bladder and the urethra are involved in the failure to store and void urine. We introduce an overview of some bladder dysfunctions that can be treated using FES devices [24].

Injuries or diseases affecting the nervous system can disrupt the voluntary micturition control, causing the re-emergence of the infant micturition reflex (uncontrollable emptying of the bladder). This reflex leads to detrusor overactivity and incontinence of a different nature; for instance, stress, urge, mixed, false or overflow incontinence [22],[51]. Bladder-sphincter dyssynergia may also occur, producing a urine reflux to the kidneys, which leads to dilation, overpressure, infections and eventual renal failure [49].

Failure of the storing function produces incontinence as result of a variety of diseases or neurologic disorders that lead to a condition known as neurogenic bladder overactivity (NBO) [42]. NBO is a common condition affecting the storing function with or without incontinence, which is usually associated with increased daytime frequency and nocturia (the need to get up in the night to urinate). Factors leading to NBO include the following: birth defects, interruption of cortical inhibitory circuits, disruption of basal ganglia function during Parkinson's disease, damage to the pathways from the brain to the spinal cord, multiple sclerosis, spinal cord injury, benign prostatic hyperplasia, and sensitization of bladder afferent nerves [25].

NBO is one of the conditions that can be treated by sacral neuromodulation using FES devices to suppress detrusor overactivity. Sacral electrical stimulation can be used to inhibit the somatic and the autonomic afferent activity of the bladder reflexes by suppressing the interneuronal relay in the spinal cord. This suppression blocks the transmission of the information between the bladder and the PMC, thus preventing the incontinence but retaining control of voluntary voiding. Another approach is electrical stimulation of the pudendal nerve to inhibit preganglionic neurons in the bladder. The inhibition is achieved by turning off the bladder reflexes by directly suppressing the somatic activity arising from the spinal cord.

Immediately following an SCI, there is a period known as spinal cord shock. This period is characterized by muscular flaccidity and total loss of the spinal reflexes. Following this period of approximately three weeks in humans, recovery of the reflexes below the level of the lesion

depends on the location and degree of cord damage. For instance, detrusor-sphincter dyssynergia (DSD) was found in 70% to 96% of patients who underwent an SCI [52]. DSD produces high intravesical pressure, incomplete bladder emptying, urinary tract infections (UTI), and kidney function deterioration. Other after-effects follow SCI and cause bladder spasticity and the loss of voluntary control [22].

Voiding failure results from reduced bladder contractility, an anatomical obstruction of the outlet (e.g., enlarged prostate), external sphincter dyssynergia, or an alteration in one of the reflex mechanisms presented in Figure 1-3b; these reflexes are required for initiating and maintaining normal detrusor contraction. Failure to properly empty the bladder can also lead to high residual volume, thus lowering functional capacity and consequently augmenting voiding frequency and the risk of incontinence [25].

Failure of the bladder functions invariably lead to severe deterioration of the health and quality of life [42].

1.5 Bladder volume assessment in clinical practice

Traditional techniques for bladder volume evaluation in clinical practice are abdominal palpation, bimanual digital vaginal examination, contrast radiology, radionuclide scans, and bladder catheterization. These techniques can be inaccurate, impractical or expensive [53].

Transurethral catheterization is a simple and low-cost method that is considered the *gold standard* when other bladder measurement techniques are assessed. It is employed in patients with voiding dysfunction using a catheter that is introduced through the urethra into the bladder to relieve the obstruction of the urine outflow. Catheters can also be passed above the pubis through the abdominal wall (suprapubic catheterization) directly into an enlarged bladder if urethral catheterization is not possible. The urine is drained and measured employing direct or indirect accurate methods, such as the volumetric method using calibrated containers or the gravimetric method using accurate scales. However, some complications, such as physical discomfort, infringement of urethral trauma, and urinary tract infections, could arise and worsen with repetitive long-term catheterization [54].

Over the past two decades, ultrasound has been developed as a convenient non-invasive method of measuring bladder volume, primarily for measuring post-void residual (PVR) urine as an alternative to catheterization. Ultrasound is a well-studied technique worldwide with mixed results. Although a standard ultrasound machine with the appropriate software can be used to assess bladder volume, a specialized portable (non-wearable) machine is commonly used in current clinical surveillance of patients suffering from urinary retention.

The *BladderScanner*® series manufactured by Verathon Medical Inc., Bothell, Washington, is the more extensively used machine. Several clinical studies have shown that this machine is sufficiently accurate for evaluating PVR in adult patients when the machine is used by well-trained personnel [55]. However, the effectiveness in children and other patients, for instance, patients with a prostatectomy or hysterectomy, has not been conclusively shown [56]. Thus, urethral catheterization is still recognized as the most accurate and reliable technique.

CHAPTER 2 CHRONIC MONITORING OF BLADDER VOLUME: A CRITICAL REVIEW AND ASSESSMENT OF MEASUREMENT METHODS

In this chapter, we present the published paper that first introduces the problem of chronic monitoring of bladder activity and its possible applications. Afterward, the paper describes the experimental setup and protocol commonly used for studying the bladder and summarizes the most important anatomical and physiological characteristics of the bladder that we identified as causes that hampered the achievement of a suitable device to chronically monitor the urine volume stored in the bladder. Afterward, the methods proposed in past studies for measuring the bladder volume or pressure are reviewed. The achievements, drawbacks, methodological problems, and controversy among authors regarding important subjects, relevant information for development of a bladder sensor, and experimental methods that are useful for our research objectives are introduced. Finally, a summary of the assessment results of the possible methods to monitor the bladder volume or pressure using wearable or implantable devices, are presented and discussed. Based on the assessment results and discussion, we indicate the method that we consider most suitable for use in continuous bladder monitoring but acknowledge the current limitations that must be overcome to use the method in subsequent research.

The information gathered and summarized in this chapter was essential to propose a method for monitoring bladder volume with the required efficacy and safety. This review included mainstay books in urologic physiology and clinical medicine; core journals in biomedical sciences, electrical and biomedical engineering; and patents.

The review was particularly focused on the methods that have been researched in past studies for bladder monitoring using wearable or implantable devices. Other methods, which have been used to measure volume in other biomedical applications, were also analyzed to avoid skipping over some possible or interesting measurement principles. These other methods included volume displacement plethysmography, indirect volume measurement from flow integration, and indicator dilution methods (e.g., marker concentration, thermodilution, radionuclide imaging, first pass, dynamic recording and gas dilution) [57],[58]. However, after a careful analysis of new

measurement concepts that we identified based on the combination of some of them, these methods did not pass the first screening stage of the go/no-go test, which used the most important user needs to assess feasibility. Therefore, those methods were not considered in subsequent analysis.

Due to space limitations, the published paper did not include the entire exhaustive and systematic analysis we performed to draw the conclusions about the best method to monitor bladder volume. In fact, the user needs identification, evaluation, and weighting was an important stage to clarify the problem and to focus the research on the most important issues. The medical, technical and ergonomic needs identified during this analysis, which are required to the design of an implantable bladder sensor, are presented in Appendix 1.

The users were considered not only patients with bladder dysfunction (primary users) but also other stakeholders such as physician, nurses, and caregivers. The user needs just describe ‘what’ is necessary to be performed in order to achieve the main goal but without specifying how to achieve them. The ‘how’ was reserved for the next stages of the research process, thus preventing, as far as possible, any bias in the proposed solution. All technical specifications and methods to be developed in later stages should satisfy, as close as possible, the identified needs but also consider current medical and technological limitations. A proper weighting of the identified needs was required to keep the focus on the most important aspects while considering the goals, limitations, trade-offs, and feasibility. The selection criteria for choosing the measurement method that was best suited for implementing implantable bladder sensor were drawn from the most important user needs.

We determined that the bladder sensor, like other sensors used in biomedical or industrial applications, should comprise two transduction stages: the primary and secondary transduction stages, as shown in Figure 2-1. The primary stage transduces the mechanical stretching of the bladder into a change in energy or in a physical property depending on the principle of the measurement, whereas the second transduction stage converts this intermediate output into electrical energy output. The reviewing process presented in this chapter was also focused on finding the principles for both stages. Figure 2-1 also summarizes the possible principles that can be used to realize each transduction stage.

The technical specifications are the translation of the user needs into metrics that we used to assess the artificial sensors. As artificial sensors we considered all volume sensors that are different from the natural receptors in the bladder wall. The technical specifications for the bladder sensor were obtained using the quality function deployment (QFD) method and the worksheet known as House of Quality (HoQ). Both the technical specifications and the HoQ are presented in the Appendix 2.

The evaluation matrix with the rates and the sets of weights used to assess the measurement principles assessed in section 2.4 are presented in Appendix 3.

Both the user needs and the technical specifications can be useful in future studies of bladder dysfunction and the research for possible therapies, regardless the chosen approach.

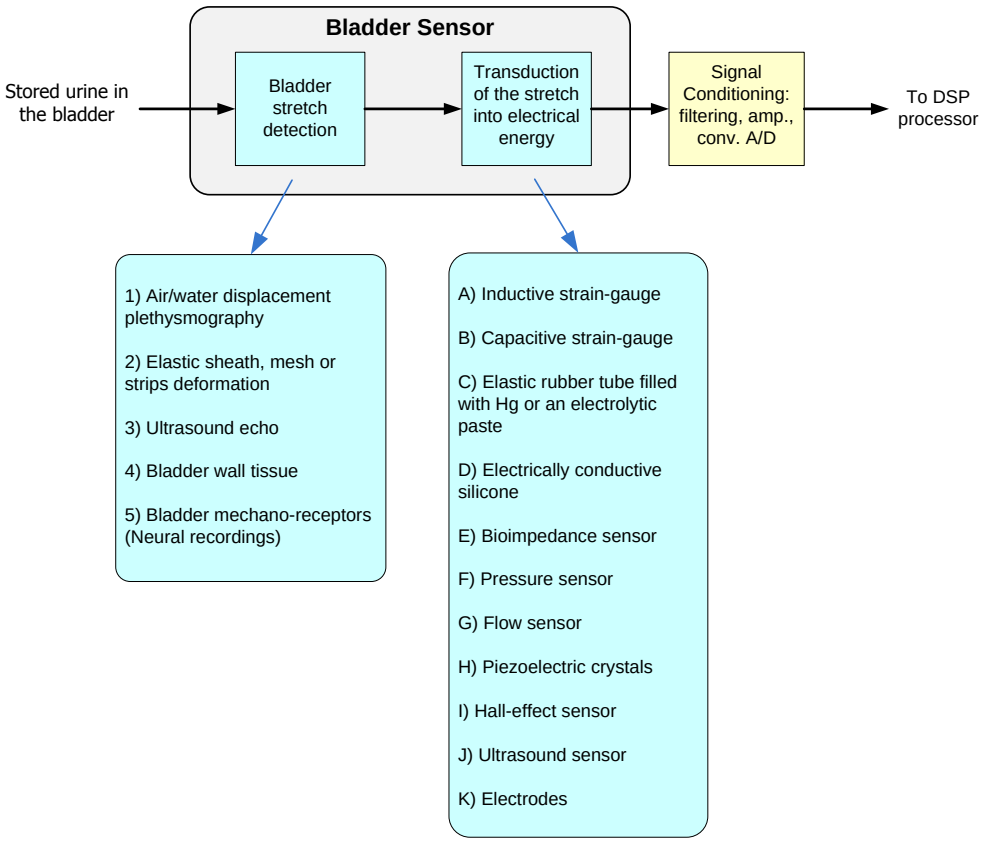

Figure 2-1: Primary and secondary transduction stages of the bladder sensor. A summary of the potential measurement principles that may be used in implementing each stage is also shown.

Chronic Monitoring of Bladder Volume: A Critical Review and Assessment of Measurement Methods

(The published paper is reproduced here)

Publication source: Mendez, A. Mendez, and M. Sawan, "Chronic monitoring of bladder volume: a critical review and assessment of measurement methods," *The Canadian journal of urology*, vol. 18, no. 1, pp. 5504-16, 2011. [36]

Arnaldo Mendez[1], Mohamad Sawan[1]

[1]*Polystim Neurotechnologies Laboratory, Ecole Polytechnique de Montreal, Quebec, Canada*

Abstract

Chronic monitoring of bladder volume can improve the clinical diagnosis and the choice of therapeutic approach for patients suffering from urinary dysfunction. It can also be employed to notify patients or healthcare personnel when the bladder should be emptied. An early warning can be triggered either when functional bladder capacity is reached or when an abnormally high post-voiding residual volume remains in the bladder after an unfinished voiding. Currently, neuroprosthetic implants are used in the treatment of refractory patients with overactive bladder, with urgency-frequency or with voiding complications. These implants can further enhance their performance, and also reduce their adverse-effects, by implementing a conditional stimulation based on the ongoing information of bladder volume. In this paper, we review the measurement methods used in past studies, we analyze and assess them, and lastly we pinpoint the one that we consider the optimal one for chronic monitoring of bladder volume.

Key words: bladder volume, chronic monitoring, conditional stimulation, neuroprosthetic implants, overactive bladder, urgency-frequency, voiding dysfunction.

2.1 Background

The bladder functions of storing and voiding urine can fail as a consequence of several causes, ranging from a simple and reversible urinary tract infection to more severe diseases or conditions. Without pretending to write an exhaustive list, we can mention the following [25],[40],[41],[49]: prostatic hypertrophy or bladder cancer, Spinal Cord Injury (SCI), strokes and other Cerebral Vascular Incidents (CVIs), neurological diseases (e.g., Parkinson's, multiple sclerosis, Alzheimer's, etc.), arthritis, iatrogenic incontinence (e.g. following radical prostatectomy or hysterectomy), nocturnal enuresis, fistula, neuropathic bladder and nonorganic causes, urethral hypermobility with or without associated pelvic organ prolapse, prostatitis, pharmacologic side-effects, weak or damaged pelvic floor muscles or nerves, and neurologic dysfunctions anywhere along the neuraxis from the brain to the spinal cord, or in the peripheral nerves or ganglia. As a result of bladder malfunction owing to any of the above mentioned causes, serious complications in a patient's health and a continuous deterioration in their quality of life will occur.

Chronic monitoring of bladder volume will allow a more suitable clinical diagnosis and a better choice of therapeutic approach. It can also be employed to notify the patients or the healthcare personnel when the bladder should be emptied. This situation can arise either when functional bladder capacity is reached or when an abnormally high post-voiding residual volume remains after an incomplete micturition.

Nowadays, there are alternative therapeutic approaches that are being used in patients who do not respond to, or could not tolerate conservative treatments. These approaches are based on implanted neuroprosthesis that perform electrical stimulation of the Lower Urinary Tract (LUT) nerves. The electrical stimulation of these nerves helps the patients with urge incontinence or abnormal urgency-frequency due to an Overactive Bladder (OAB), and it can also assist patients with urinary retention owing to non-mechanical obstructions [17]. Some studies published in recent years have proposed different approaches based on the permanent stimulation of LUT nerves [13],[15],[16],[59-61].

It has been stated that conditional stimulation, i.e. depending on the ongoing bladder state, can improve overall performance and prevent or reduce adverse effects [62]. The conditional stimulation can also decrease the deleterious effects produced by a continuous electrostimulation, for instance, the noxious electrochemical reactions at the electrode-tissue interface and nerve

degeneration [20]. Moreover, it has been affirmed that supplying the neurostimulation device with sensory information could significantly improve the neuroprosthesis effectiveness [1]. In this way, a closed-loop control can be implemented, adding intrinsic auto-regulation advantages, which allows considering the differences of the physiological responses among patients or even in the same patient over time.

Despite the few attempts carried out the last few years, which will be reviewed and analyzed in the next sections, to date, there is no device for a continuous and reliable monitoring of bladder volume [62].

We found that some physiological and anatomical characteristics of the urinary bladder have been the principal causes that could account for the failure of past attempts. These characteristics will be summarized in the following section. Furthermore, the complexity of the bladder's autonomic and somatic neural system as well as the technical limitations of today's available technology for the chronic monitoring of biological variables, have greatly hindered the development of such a device.

In this paper, we analyze the published studies related to bladder volume measurement, and also we assess several measurement methods, in order to pinpoint the most promising one for chronic monitoring of bladder volume. The analysis was carried out by critically and exhaustively reviewing up-to-date literature from different sources indexed by Medline-PubMed, Compendex, Inspec and Derwent Innovation (patents), as well as the websites of companies that sell neuroprosthetic devices. To ensure, as far as possible, an unbiased analysis of the measuring methods, we used evaluation matrices with weighted criteria that will be briefly described below.

2.2 The Anatomical and Physiological Characteristics of the Bladder that Challenge Chronic Monitoring

In the past, many attempts to monitor bladder volume have failed or have not overcome the laboratory boundaries due to difficulties arising from the complexity of bladder anatomy and physiology and the proper decoding of its neural activity. The main difficulties that we found influencing failures in bladder volume monitoring were:

1) The low change in intravesical pressure during filling due to high bladder compliance (viscoelasticity) and wall accommodation (<10 cm H_2O).
2) The substantial changes in the size of the bladder during filling and voiding (~75% of surface variation).
3) The irregular shape of the bladder when full due to the influence of the surrounding pelvic organs.
4) The variations in bladder pressure depending on the patient's posture and the influence of many stress conditions, e.g. coughing, sneezing, vomiting, etc.
5) The chemical properties of urine, e.g. its high corrosiveness, variable conductivity, its high concentration of salts that can adhere to any sensor or device inserted into the vesical lumen, etc.
6) Bladder smooth muscle is less electrically coupled than other smooth muscle.
7) The high complexity of bladder control, partly because the bladder is the only smooth muscle organ driven by both the somatic and the autonomic neural system.

2.3 An Exploration of Methods Used for Bladder Volume Monitoring

The methods that could be used for chronic monitoring of bladder volume will be explored and analyzed in the following paragraphs in order to assess their efficacy in a subsequent analysis.

Most of the *in vivo* studies that will be analyzed below used the typical setup depicted in Figure 2-2, with roughly similar kind of equipment and accessories. This setup allows mimicking bladder filling and voiding (with known limitations), performing a similar procedure to that used in urodynamic studies.

The procedure usually performed with the setup depicted in Figure 2-2 consists of injecting saline (NaCl 0.9% at 37 ^{o}C) into the bladder through one barrel of a double-lumen transurethral catheter. However, in small animal models like rats, a double lumen cannula is inserted through

the bladder dome. An infusion pump allows setting up different filling rates (physiological or fast filling) depending on the experiment goals and on the functional bladder capacity of the experimental model (relatively high filling rates generally elicit overactivity). The second barrel is connected to a pressure transducer to record simultaneously the intravesical pressure (P_{ves}). In some studies the abdominal pressure (P_{abd}) can also be measured. To perform this measurement a balloon is inserted into the rectum and connected to a second pressure transducer. This allows determining the pressure exerted by the detrusor (P_{det}), because as known, P_{ves} results from the addition of pressures produced by the contraction of the detrusor muscle and the abdominal musculature, i.e. $P_{ves} = P_{abd} + P_{det}$. Thus, P_{abd} measurement allows detecting artifacts produced under several physiological circumstances. In more recent studies, P_{ves} and P_{abd} data have been fed into a computer through a data acquisition system that amplify, filter and convert this data to digital values. Once inside the computer the signal is processed and the results are displayed conveniently.

Depending on the goals of the experiment different types of transducers or electrodes can be used to measure variables such as pressure, displacement, elongation and also images can be obtained using ultrasound transducers. Electrodes, which essentially are ionic to electronic current transducers, are used to inject or to record electrical current, to or from the tissue (bladder wall or nerves). A generic representation of these transducers and electrodes placed on the bladder dome is shown in Figure 2-2 (A and B). However, their specific location in the lower abdomen varies from study to study. As will be described below, the transducers or the electrodes can be sutured onto the bladder wall, inserted into the vesical lumen or embedded in the submucosal layer. A special type of electrode (cuff-electrode) can be wrapped around the bladder nerves or around the sacral roots to record neural signals produced by bladder distension and contraction. Typically, the ultrasound transducers are externally fixed to the lower abdomen using belts or elastic pants.

Specialized electronic interfaces (Figure 2-2) are used to properly drive the transducers or the electrodes and connect them to the computer by means of the data acquisition system. All gathered signals from the transducers and the electrodes are stored in computer memory to be processed on-line and displayed in real-time, or to be further processed off-line using more complex algorithms. Generally, the researcher try to find out a relationship (correlation) between bladder activity and the signals recorded from the transducers.

2.3.1 Intravesical Pressure Measurement

This method is based on the principle that if we know the value of P_{ves} it could be used to indirectly assess bladder volume. For instance, if we determine in a previous cystometric study the value of P_{ves} along with the volume that elicits a voiding sensation, then we could detect, by mean of an implanted pressure transducer, when the bladder has reached its functional capacity.

Past studies have assessed the feasibility of this approach for monitoring the bladder pressure or volume. However, Westerhof et al. showed that bladder pressure variation does not correlate well with the urge sensation [63]. On the other hand, it is known that a detectable pressure increase arises only when a threshold value is reached [26].

A model proposed by Korkmaz et al. [64] allowed describing the stress–strain behaviour of the bladder wall during the filling and voiding cycle. By means of this model, and using the data collected from real cystometry and uroflowmetry of different patients, the authors verified that the stress in the bladder wall during the filling and voiding cycle is characterized by a curve with hysteresis, which results from the viscoelastic properties of the bladder. Additionally, they showed that during the filling phase, stress relaxation is the most important issue that accounted for the small increase in the intravesical pressure.

Some experiments performed on dogs in order to track bladder pressure, considering different physiological situations, were carried out by Takayama and coworkers [65]. Pressure transducers were embedded in the submucosal layer of the anterior bladder wall. The authors reported a small increase in intravesical pressure during the bladder filling phase, but they also mentioned that undesirable artifacts produced by animal's movements hindered the extraction of reliable information, which is required to follow the bladder pressure with enough precision.

It has been shown by Koldewijn et al. [66] that it is possible to use pressure transducers affixed with non-absorbable sutures in the peritoneal surface of the bladder's dome. However, they reported that the transducers can erode into the vesical lumen or can detach from the wall.

An autonomous monitoring system that measured the intravesical pressure using a capacitive pressure transducer inside the bladder was proposed by Coosemans et al. [67] However, they did not make the packaging for the electronic system required to carry out *in vivo* experiments to evaluate the efficacy of this device in real conditions.

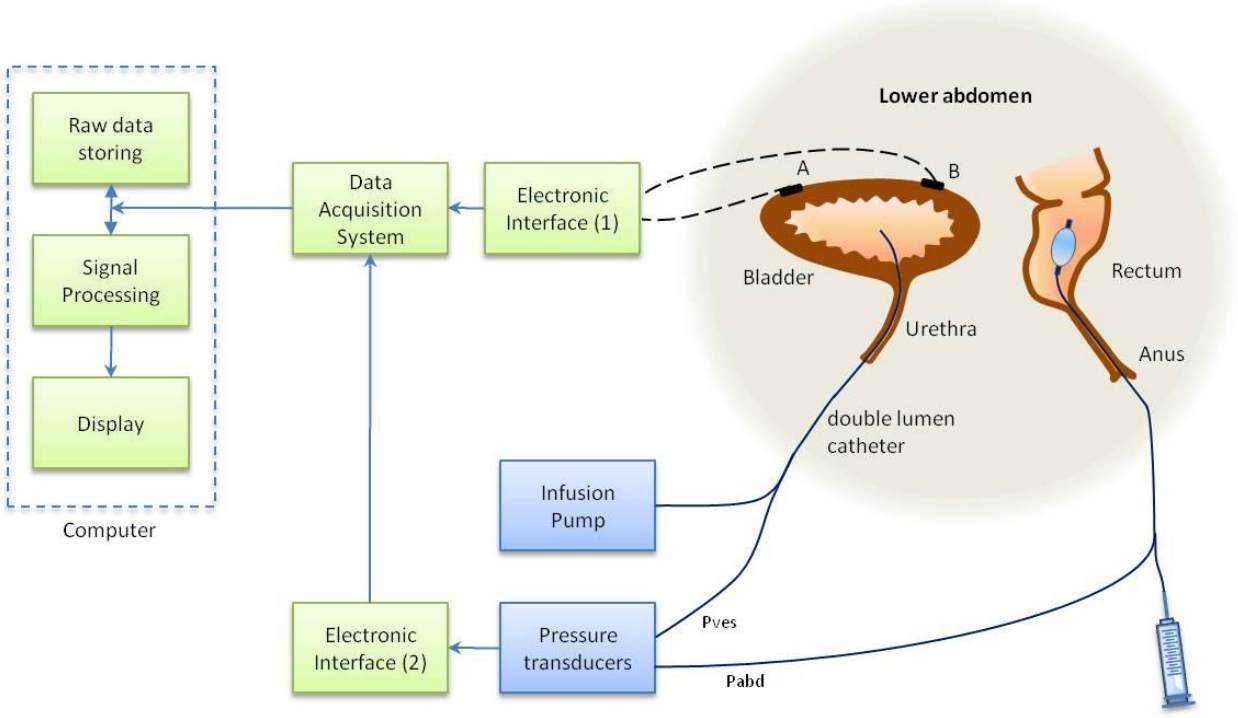

Figure 2-2: Typical setup used for studies of bladder activity. A and B are generic transducer or electrodes located on different parts of the lower abdomen depending on experiment goals.

Results from these and other studies confirm that it is difficult to extract volume information from the intravesical pressure, but Jezernik et al. [20] showed that it is possible to spot onset bladder contractions detecting a sudden increase in P_{ves}. However, the P_{ves} variation is also produced by stress conditions such as on voiding, coughing, defecating, vomiting and postural changes between the standing and sitting position, etc., [65]. These conditions can produce false positives if they are not detected.

2.3.2 Electrical Impedance Plethysmography

Plethysmography is a method for measuring volume changes in specific parts of the body or of the whole body. There are three types of plethysmographic techniques: 1) volume displacement using air or water outside the body; 2) measurement of the electrical impedance or admittance of a body part (bioimpedance); and 3) image plethysmography using X-rays, ultrasound or

Magnetic Resonance Imaging (MRI). The volume displacement technique seems to be impractical for bladder monitoring purposes. A type of image plethysmography, i.e. wearable Ultrasonography, will be described later.

Electrical Impedance Plethysmography (EIP) is typically carried out by injecting a controlled AC current into the tissue. This current passing through the tissue produces a voltage drop between the electrodes (generally one or two pair) placed on the lower abdomen skin or directly on the organ. This voltage can be measured using a specialized amplifier. Then, it is possible to calculate the tissue bioimpedance, since the values of the injected AC current and the voltage drop are known [68].

Over the last few decades, several studies used EIP for assessing bladder volume. Some of them were focused in whole body impedance measurement while others in bladder impedance measurement. The hypothesis underlying these studies states that there is a correlation between bladder bioimpedance and the volume of urine stored. Nevertheless, the published results are quite controversial, as will be shown below.

The feasibility of the direct impedance measurement method to assess bladder volume was tested by Waltz et al. [69]. The authors found a linear relationship between bladder volume and the impedance recorded with an implanted device, using two electrodes attached to a dog's bladder. The measured sensitivity was 7 Ohms per 100 ml. The reproducibility and the long-term stability of the method were not reported in this study.

Other researchers have used EIP for measuring bladder volume in a non-invasive way. Denniston and Baker [70] also found a linear relationship between bladder volume and bioimpedance measurements, but using spot (snap) electrodes on the abdomen skin of anaesthetized dogs. They described the advantages of a new arrangement of the spot electrodes placed nearer to the bladder boundaries. These authors also reported a linear response but with a lower sensitivity (0.7 Ohms per 100 ml). Similar results were reported by Doyle and Hill [71] but conducting experiments in humans, which showed a linear response but with even a lower sensitivity (0.1 Ohms per 100 ml).

A comprehensive research using this approach was carried out by Abbey and Close [72]. They conducted studies in men and women (two groups of 20 patients) for measuring several variables simultaneously, using four spot electrodes with the patients resting in the supine position. Their

results showed a weak relationship between the impedance and bladder volume during the bladder filling and voiding phases. However, the results were greatly influenced by some patients' specific factors and their sex; in both men and women, the baseline impedance was influenced by the skin surface and by the skin fold thickness, but in women, this baseline also correlated with the time since the last menstrual period (oestrous cycle). Nevertheless, they did not report any results concerning the accuracy of the method used for bladder volume measurement.

Other studies focused their efforts in the detection of bladder fullness. Yamada et al. [73] worked on a device for detecting bladder fullness using a pair of spot electrodes placed on the surface of both femoral joints, and another pair near the bladder area. They concluded that a remarkable stability and reproducibility can be achieved using specially designed electrodes placed in those places to detect the urge threshold. However, in their experiments and subsequent analysis they did not consider known issues mentioned in other studies [72],[74], which could interfere with or modify the results.

The Electrical Impedance Tomography (EIT) technique, which produces images from bioimpedance measurements, has also been used for measuring bladder volume. In a study conducted by Hua et al. [75] an array of 48 surface electrodes and a 2D-dimensional computer model was used to display a finite element image of the bladder. This study aimed to show the feasibility of this technique; however, no result was found concerning the effectiveness of the proposed method.

A device based on bioimpedance measurement to estimate bladder volume was proposed by Provost et al. [76] This device was designed to provide feedback to an implantable electrical stimulator [77] intended to drive a neurogenic bladder. The device tried to detect when the urge volume threshold was attained. The authors showed interesting results from the analysis of their measurements using four pairs of electrodes placed on dog's bladder. However, since then they foresaw difficulties in correctly assessing this threshold during the *in vivo* experiments, due to the changes in urine conductivity and the zeroing problems that arose from residual volume. In fact, those issues are still some of the hardest to be addressed by this technique. On the other hand, it is known that bladder smooth muscle is less electrically coupled than other smooth muscles [25], which could hinder the accuracy of the bioimpedance measurements of the bladder.

In another study carried out by Kim et al. [78] in 13 patients with SCI, using surface electrodes placed on the lower abdomen, additional limitations of this method for detecting small changes in bladder volume in long-term measurements were shown. The major limitations found were the influence of body fat and the interference arising from fluid and fecal movements as well as fecal accumulation in the bowels.

A more recent study executed by Keshtkar et al. [79] assessed the relationship between the measured bioimpedance and the bladder volume, in *ex vivo* and *in vivo* experiments, using urine-like solutions with different conductivity that could affect the measurements. They concluded that the bladder tissue bioimpedance decreased when it was stretched and all mucosal folds became flattened. The authors also showed that at lower frequencies, the measured impedance increased with bladder volume, i.e. an opposite sign slope. Moreover, an insignificant, weak relationship was found.

A comprehensive study conducted by Gill et al. [74] also assessed the feasibility of fluid conductance for measuring bladder volume. Several *in vitro* experiments were developed using four electrodes, latex vessels and bladders excised from pigs, filled with a urine-like saline solution at different temperatures and concentrations. The authors showed that the conductance increased with temperature and concentration but was different for each pair of these variables, except at low concentrations where this relationship was no longer valid. They also showed that the measured conductance was determined by the fluid conductivity, and lastly, that the conductance increased linearly at low volume but approached asymptotically to the high values. Therefore, in order to use this method in practical applications, the authors suggested that it required a real-time compensation of the fluid conductivity for the dynamically varying properties of urine and also an improvement in sensitivity.

As seen above, the EIP has been one of the most used measurement method for monitoring bladder volume by means of electrodes placed on the lower abdomen skin or on the bladder wall, with a preference for the former. Some authors showed the feasibility of using the EIP method to estimate bladder volume, while others have shown that, despite the fact that it is barely possible to correlate bladder bioimpedance with volume, several issues must be addressed in order to use this method for reliably estimating bladder volume. Moreover, electrodes placed on the bladder, continuously exciting the tissue with a current (required for the bioimpedance measurement), can

lead to permanent damage and induce changes in the physiological behaviour of the bladder wall. Additionally, electrode migration toward the bladder lumen or electrode detachment is possible. Thus, we can state that none of the studies reviewed implementing EIP demonstrated any effective solution for the chronic monitoring of bladder volume.

2.3.3 Strain-gauge plethysmography

This method uses transducers that change their impedance or their electrical charge pursuant to the modification of the shape produced by external forces. The measuring principle of these transducers can either be resistive, capacitive, inductive or piezoelectric. Specifically, for this application, the elongation or the contraction of the transducer placed on the bladder will generate a variation in the impedance or in the charge (piezoelectric case). This variation can be measured by a proper electronic circuit (e.g. a bridge or a charge amplifier), then translated into distance, and lastly into volume units.

Few studies using this approach have been published, even if this could be one of the most interesting principles for a reliable monitoring of bladder activity and volume. In fact, this principle is based on the direct measurement of a primary variable, i.e. the bladder distension/contraction. Therefore, these measurements should correlate well enough with bladder activity and volume and not be dependent on the patient's health condition.

We can speculate and say that the small number of studies with this approach might be related to unsuccessful attempts in the past, mainly as consequence of the low reproducibility and the low stability of measurement achieved using this approach, as will be shown below.

An interesting measurement method using this approach was proposed by Rajagopalan et al. [80]. They measured the changes in electrical resistivity of a polypyrrole (a polymer) deposed on a highly elastic fabric used like a pouch covering the bladder. Their results showed that when the fabric with the impregnated polymer was stretched, it produced a linear resistivity change in a range of 20-40%. The *in vitro* experiments, carried out in a phantom bladder, showed the feasibility of using such a sensor to measure bladder volume, displaying some advantages inherent to the measurement method. However, some fabrication issues should be solved in order to use this sensor in long-term measurements, because after few days its sensitivity became null.

On the other hand, no *in vivo* experiment was performed with the goal of assessing the conductivity, the accuracy, the reproducibility, the stability and the biocompatibility under real conditions.

A patented sensor for measuring changes in any anatomical part, but especially designed for the mammalian bladder, was proposed by Upfal et al. [81]. The transducers were made of a silicone elastomeric sheath containing a pair of helically coiled conductive wires. The limited results published in the patent application are not enough to assess the effectiveness of this device. Moreover, an analysis of the known issues affecting this method was omitted. We did not find any additional related studies, either from these authors or from the company that owns the patent.

In order to meet the requirements of chronic monitoring, the materials used for covering and supporting the sensor on the bladder wall should be soft and elastic. These properties allow the transducer to follow the large changes of the bladder's surface during its distension and contraction, but without overloading it. In fact, an increase in the effort required to stretch the bladder wall could substantially affect the measurements, and also overall bladder behaviour, particularly in overactive bladders. Additionally, the material should fit properly the irregular shape of the bladder, have high endurance and also be biocompatible. These material requirements, and the intrinsic invasiveness of this method, are identified as the major issues to be addressed in order to use this method in practical applications.

2.3.4 Wearable ultrasonography

Ultrasound or ultrasonography is a well known medical imaging technique that uses sound waves of high frequency and its echoes for determining tissue boundaries by means of image processing algorithms. This technique produces animated 2D or 3D, black and white or color images. Ultrasonography has become a useful non-invasive method for measuring bladder volume. Currently, it is a common method for measuring Post Void Residual urine (PVR). It is an alternative to indwelling catheterization, the most accurate and the gold standard technique but with known adverse effects.

Whereas a standard ultrasound machine with the appropriate software can be used to assess bladder volume, a new type of specialized portable machine today is widely used (e.g. Bladder Scanner series from Verathon Medical Inc., Washington, USA). This machine helps in the clinical surveillance of patients suffering from urinary dysfunctions.

The above mentioned devices cannot be considered wearable, which is a must for chronic monitoring of the bladder. By definition, a wearable device should be very easy to wear, thus a wearable device for measuring bladder volume should be lightweight, smaller, and more ergonomic than a portable one.

A few studies have used the ultrasound technique for continuously monitoring bladder volume by means of a wearable device. Petrican et al. [82] proposed a miniaturized ultrasonic bladder volume monitor for children with enuresis. The aim of this device was to alert the patient when the urge threshold was reached during the night. The device was affixed to a belt fastened around the patient's lower abdomen. It was tested in 41 patients showing more than 70% accuracy in determining volume under well controlled conditions. However, a number of shortcomings were found during the testing phase in obese patients, in patients that had undergone abdominal surgery, or were sitting, constipated or had liquid stools. Improved solutions were suggested by the authors based on the use of an array of ultrasound cells affixed to elastic pants that fit the patient better.

These suggestions were taken by Beauchamp et al. [83], who reported that a clinical evaluation carried out in ambulatory patients showed only 40% success. They also mentioned measuring problems arising from even slight changes in probe orientation, which caused artifacts that incorrectly triggered the alert. In a new study [83], the same authors were seeking a device for preventing bed-wetting, i.e. for alerting enuretic patients before and not after the micturition. The device showed good results in phantom bladder testing, but no clinical trial was carried out to test the measurement robustness.

Kristiansen et al. [84] also proposed a similar solution with the same goal. They designed a wearable ultrasonic bladder volume monitor that used 7 phased-array ultrasonic transducers in a circular pattern device. The data collected was sent wirelessly (through a Bluetooth channel) to a portable computer for further processing. They reported good results with their *in vitro* test using a prototype apparatus and a phantom bladder. The measurements showed a mean absolute error

of 2.9%, good reproducibility; low drift over time and with temperature and a good correlation vs. a volume estimation obtained by MRI. Despite the good results shown under well controlled conditions, none of the intrinsic limitations of this method mentioned above [82], were analyzed.

As has been seen so far, the results yielded by this method are greatly affected by the patient's conditions and have only been shown to be effective under well controlled conditions. On the other hand, bladder activity monitoring is more complicated using this method, owing to the small, rapid variations that must be detected by the data processing algorithms. Moreover, the image processing requires a powerful computer for executing the complex algorithms in real-time and for displaying the measured volume. Therefore, for this method to have a practical application in chronic bladder monitoring, an improvement in measurement robustness as well as in the ergonomics issues is required.

2.3.5 Electroneurographic signal recording and processing

This method uses information gathered from the bladder's natural sensors (mechanoreceptors) for monitoring its activity. Several studies have shown the presence of mechanoreceptors that respond to the bladder distension and contraction and others that respond, more specifically, to bladder volume [30],[32],[33]. The sensory information produced by these mechanoreceptors during the filling and voiding cycle, coded as action potential firing frequency, is carried by the bladder afferent nerves (i.e. the pelvic, hypogastric and pudendal nerves). These nerves are part of the complex organization of sympathetic, parasympathetic, and somatic pathways of the pelvis nerves shown in Figure 2-3. The recording of this neural activity is known as an Electroneurogram (ENG). The ENG signal arises from the superimposed or compounded action potentials (CAPs) of several firing units present in the nerve.

The recorded ENG signal is processed using algorithms with different degrees of complexity depending on the application. The most common ENG processing method is the signal averaging and low-pass filtering, which is technically known as Rectifying and Bin Integration (RBI). This method allows one to extract rough sensory information from the ENG amplitude envelope [85]. The sensing interface most commonly used in this type of recording has been tripolar cuff-

electrodes. These electrodes are formed by three rings of metal (platinum or stainless steel) supported by a cylindrical cuff generally made of silicone or its derivatives [86].

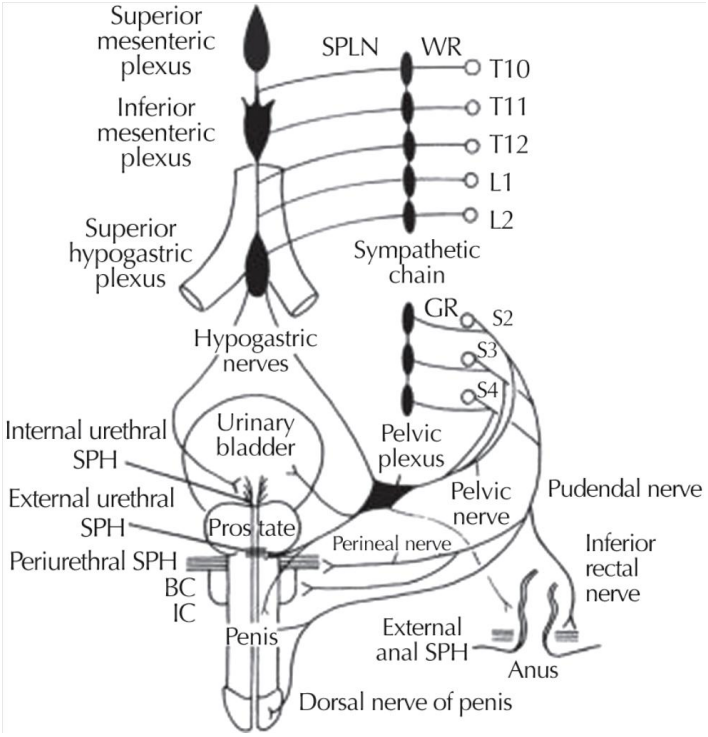

Figure 2-3: Neural pathways of the pelvis showing the afferent nerves commonly used the ENG recordings (see text). SPLN, splanchnic nerves; GR, gray rami; WR, white rami; BC, bulbocavernosus muscle; IC, ischiocavernosus muscle; SPH, sphincter. From [49], reproduced with permission from John Wiley and Sons.

The RBI has shown to be a feasible and quite robust technique for detecting onset bladder contractions using tripolar cuff-electrodes wrapped around pelvic nerve and sacral roots [20],[87-90], albeit it has been less effective at the pudendal nerve [90]. The application of different detection algorithms such as the constant threshold, the adaptable (variable) threshold and the cumulative sums (CUSUM) [90],[91], have allowed detecting the sudden increase of P_{ves} due to a detrusor contraction.

A few studies have been conducted with the main goal of establishing whether it is possible to extract volume information from the ENG recorded from the afferent bladder nerves. A

preliminary study performed by Harb et al. [92] recorded the ENG using tripolar cuff-electrodes on the sacral root S2 in dogs with the spinal cord transected at the supralumbar level. The authors, using the RBI technique, showed an increase in S2 neural activity in dogs during the bladder filling, with some lag explained either by a volume threshold required to trigger nerve activity or by a delayed bladder response to filling.

The feasibility of bladder activity monitoring from ENG activity was assessed by Jezernik and coworkers in acute experiments performed in pigs [87]. They showed the possibility of recording bladder afferent activity by mean of tripolar cuff-electrodes placed on the pelvic nerve and on the sacral root S3. Their results revealed that bladder response was more phasic than tonic, since the recorded activity was higher during fast filling or during detrusor contraction than during isovolumetric volume measurements or slow filling. This behavior was considered good for detecting bladder contraction (e.g. overactivity) but it was considered bad for detecting bladder fullness.

A study carried out by Sinkjaer et al. [89] in one human patient with a suprasacral SCI also showed that passive filling and bladder contraction activity can be detected from the ENG of the sacral dorsal root S3 using tripolar cuff-electrodes.

A comprehensive study performed in cats by Jezernik et al. [20] stated that monitoring the bladder fullness (volume) directly from cuff recordings of the sacral root S1, using the RBI technique, was not feasible. However, the authors suggested that maybe it was possible by measuring the time elapsed between reflex contractions in overactive bladders. Nevertheless, the single result shown is not enough to confirm this. Moreover, they commented on the limitations of the cuff-electrode recordings in achieving higher signal levels, a better signal to noise ratio (SNR) and also the shortcomings due to the low selectiveness of sacral root recordings. As was mentioned above, these signals arise from the superposition of the efferent and afferent activity from the bladder, rectum and dermatomes. Therefore, they suggested that recording of the pelvic nerve activity could improve the selectiveness, eliminating some interference from visceral and dermatome activity. However, the long-term effects of placing cuff-electrodes on the pelvic nerve have not yet been assessed.

Another important study carried out in human patients with SCI, was performed by Kurstjens et al. [88]. The authors investigated the afferent activity of the bladder, the rectum and the skin

(dermatomes), performing intraoperative recording of the ENG elicited by these sources in the extradural sacral root S3. They showed the feasibility of performing these recordings in humans using cuff-electrodes and confirmed or questioned some previous published results. For instance, the authors confirmed that the ENG signal recorded using tripolar cuff-electrodes was influenced by the number of fibers, by the diameter, and by the proximity of the firing axons to the electrode surface. They found that skin responses were larger than those from the bladder and the rectum, depending on the type of conducting fibers. The authors also showed that during bladder filling, both the phasic and the tonic responses were elicited. Conversely, Jezernik et al. [87] observed mainly phasic responses in animal models, as was mentioned above. In fact, Kurstjens and coworkers questioned the extension of this conclusion to humans, based on the tonic response that they recorded for P_{ves} over 40 cm H_2O. However, this is not sufficiently supported in their publication, and a final conclusion similar to that given by the Jezernik et al. [87] was stated, favoring the detection of bladder contraction based on the phasic nature of neural response. Lastly, they considered difficult to monitor bladder volume from the ENG recordings of the sacral roots S3 using tripolar cuff-electrodes.

More recently Saleh et al. [93] published an interesting acute study performed in anesthetized dogs. They proposed a method that recorded the voltage drop (V_{out}) across a section of the extradural sacral root S2 when a sinusoidal constant low current (4 μA p-p, 30 Hz) was applied to it by means of a tripolar cuff-electrode. The authors reported a correlation between bladder volume and the V_{out} amplitude recorded, which can be roughly observed in some graphic results. However, no analysis of the specificity of the processed signal was presented. Lastly, the authors stated the feasibility of bladder volume measurement based on recorded nerve activity when a sinusoidal current was applied to the S2 sacral root. Even so, more exhaustive analysis and experiments should be done to test the robustness of the proposed method.

None of the above reviewed studies have shown robust results demonstrating the feasibility of bladder volume monitoring from ENG recordings. In fact, there are few published studies whose principal goal was the detection of bladder volume from the ENG recording, while in other related studies this feasibility was marginally analyzed. Some possible shortcomings could be identified, e.g. inaccuracies in the methodology used and in the analysis of the results. For instance, in some acute experiments performed with anaesthetized animals the spinal cord was

transected at a supralumbar level to produce a SCI, and immediately the researchers started the recordings of the ENG activity in the targeted nerve.

It is known that after a spinal cord trauma (i.e. SCI) a spinal shock period will arise. This period is characterized by motor paralysis, by a loss of sensation and the by the abrupt disruption of the reflex pathways, which lead to a condition of hyporeflexia or areflexia [22]. It might take three to four weeks on average to recover some reflexes, depending on the SCI site and its extension. Thus, the information recorded during the spinal shock period could yield misleading results. Moreover, some studies reviewed did not establish either the specificity of the measured signal or the identification of animal's physiological conditions (e.g. bladder compliance), which could greatly influence the results.

Furthermore, very low levels of ENG signals (under 10 μV) should be detected to measure the amplitude variation in the processed signal. However, it was shown that recordings performed using tripolar cuff-electrodes feature a low Signal-to-Noise Ratio (SNR). The measurements are also affected by the low selectiveness of sacral root recordings using tripolar cuff-electrodes, because they result from superimposed action potentials of efferent and afferent nerves from different viscera and dermatomes. This hinders the extraction of bladder information because the signal produced by the bladder afferents is the weakest. Consequently, the low selectiveness of the recording could lead to erroneous signal interpretation.

Recent studies have shown that it is possible to improve the quality and the selectiveness of the ENG recording of the peripheral neural system using different types of multicontact electrodes [94] and more complex processing algorithms [95-97]. Therefore, the ENG recording method requires more in depth research to determine whether it is suitable for bladder volume monitoring using other electrodes and processing techniques.

2.3.6 Electromagnetic Plethysmography

The measurement of the distance between points by means of Hall Effect crystals sutured onto the bladder wall was used to estimate topographical bladder movement during isovolumetric reflex activity. The approach correlated the distance with changes in magnetic flux emanated from a permanent magnet also affixed in the bladder wall and then sensed by nearby Hall Effect

transducers. This setup was used by Woltjen et al. [98] for monitoring bladder activity during isovolumetric reflexive contraction in cats and dogs. They measured a displacement between the Hall Effect transducer and the permanent magnet with a precision error in a range of 0.5 to 3 mm and the speed of contractions was estimated in a range of 2 to 4 cm/s. These results could be useful for bladder volume monitoring, if it is possible to establish a correlation between the measured distances and bladder volume. However, the authors did not report any results concerning bladder volume measurement.

A more recent implementation of this measurement principle was carried out in dogs by Wang et al. [99]. A permanent magnet sutured onto the anterior bladder wall was magnetically coupled to an external warning unit sutured onto the inferior abdominal wall. The external unit contained a compass-like switch that triggered a buzzer when the magnet movement showed that the volume had reached the programmed threshold. This method has been reported by the authors to be effective under very well controlled lab conditions, but no test in humans has been published to prove its efficacy, or patient's tolerance or comfort. Moreover, robustness is a pending issue because the positioning of the magnet on the bladder wall and the sensor in the reading unit is critical. Thus, any relative displacement between them will yield wrong results.

In general, this measurement method, as well as others mentioned above, still has major issues to be addressed; i.e. the long-term stability of fixing the sensor to the bladder wall. As was shown [66], any sensor or electrode affixed to bladder wall can detach or migrate toward the bladder lumen. Therefore, for long-term or chronic monitoring, an improvement in the method for fixation to the bladder wall is required.

Once this issue is resolved (a hard task), another interesting and potentially effective method could be applied to monitoring bladder volume; i.e. sonomicrometry. This technique uses several tiny piezoelectric crystal sensors attached or embedded in an organ (e.g. the cardiac muscle) forming a network. One crystal sends an ultrasound wave that is detected later by another crystal. The time elapsed between the emission and the reception of the ultrasound wave can be related to the distances between the crystals. By properly calibrating the system and using the information from all of the crystals in the network, it is possible to measure several mechanical variables such as the volume, the pressure, and the speed of the distension or contraction, etc. Currently, this method is considered the gold standard for the measurement of mechanical cardiac variables in

acute studies [100] because of its accuracy and reproducibility. It has been proposed for use in Medtronic pacemakers to improve their performance, according to a patent owned by the company [101].

2.4 Assessment of the Measurement Methods

In order to assess the methods described above and to pinpoint the one with the greatest promise to succeed in chronic monitoring of bladder volume it is necessary to define some evaluation criteria, then assign a weight to them, and lastly to evaluate each measurement method accordingly. This evaluation methodology allows quantitative analysis to select the optimum method more objectively than, for instance, pros vs. cons, thereby overcoming the most evident bias always present in the researcher, his analysis and his preferences.

The International Continence Society (ICS) has published some standards [28],[29] for the measurement of volume and pressure of the bladder, which could be used as references during this evaluation process. However, it must be taken into account that these standards have been suggested for urodynamic equipment used in the diagnostic of LUT diseases, for non-chronic applications under very well controlled conditions. Consequently, the ICS standards could hardly be met by such a type of chronic monitoring device, considering the limitations of both medical knowledge and technological feasibility. On the other hand, it is known that monitoring devices do not always have to meet the same specifications that diagnostic devices do (commonly less demanding), because the clinical purpose and the operating conditions are often quite different.

The following evaluation criteria have been established from the analysis of the measurement methods for chronic monitoring of bladder volume:

- Effectiveness in chronic use;
- Ease of implantation (minimally invasive);
- Reproducibility of volume measurements;
- Immunity to postural changes, urge stress, urine conductivity, temperature, and other artifacts;
- Detection of bladder overactivity;

- Safety in use with minimal deleterious effects;
- Accuracy of volume measurements (more important for diagnostic than for monitoring);
- Ease of set-up, calibration, and adjustment to the patient's particularities;
- Low power consumption (from a battery);
- Availability and cost of materials and components required for its implementation.

An analysis based on an evaluation matrix was carried out to pinpoint the monitoring method that best meets the criteria mentioned above. The results of this analysis are shown in Table 2-1 and the computation of the scores was performed as described below.

To rate each method, we employed a qualitative scale ranging from 1 to 5 (very poor, poor, passable, good and very good). Consequently, the final score is given on this scale as well as a total percentage. The methods were rated from 1 to 5 for each individual criterion. Then, each method’s rate was multiplied by the weight assigned to the criterion. To ensure that the selection of the optimum method was robust enough, i.e. less dependent on small weighting variations, five sets of appropriate weights were used. The final score, which appears in the cells of Table 2-1, was calculated averaging the score for each set while keeping the rate given to each method.

Lastly, the total score for the measurement method is the sum of each rate (column sum). Note that for the sake of simplicity only the final score obtained using this procedure is shown in Table 2-1.

Considering its consistency throughout the analysis, the recording of the ENG afferent activity of the bladder mechanoreceptors has been identified as the chronic bladder volume monitoring method that best satisfies the evaluation criteria defined in this paper.

Table 2-1 Methods Assessment results

	Measurement method					
Selection criteria	**IVP**	**EIP**	**SGP**	**WUS**	**EMP**	**ENG**
Effectiveness in chronic use	0.2	0.2	0.3	0.3	0.4	0.5
Immunity to postural changes, urge stress, urine conductivity and temperature and other artifacts	0.1	0.1	0.4	0.2	0.2	0.4
Ease of calibration and adjustment to the patient's particularities	0.2	0.2	0.1	0.2	0.1	0.2
Ease of implantation (minimally invasive)	0.4	0.4	0.2	0.6	0.4	0.5
Safety in use with minimal deleterious effects	0.4	0.1	0.4	0.6	0.5	0.5
Efficacy of volume measurement (accuracy)	0.1	0.2	0.4	0.3	0.3	0.2
Precision of volume measurement (reproducibility)	0.1	0.2	0.6	0.5	0.5	0.4
Detection of bladder overactivity	0.5	0.3	0.5	0.4	0.3	0.4
Low power consumption	0.3	0.2	0.1	0.2	0.5	0.5
Availability and cost of materials and components	0.4	0.5	0.1	0.4	0.4	0.4
Total Score (over 5)	2.7	2.4	3.1	3.7	3.5	3.9
Score percentage	53%	49%	62%	75%	70%	77%
Rank	5	6	4	2	3	1

(IVP: Indirect volume measurement from intravesical pressure; EIP: Electrical Impedance Plethysmography; SGP: Strain-gauge Plethysmography; WUS: Wearable Ultrasonography; EMP: Electromagnetic Plethysmography; ENG: Electroneurographics recordings)

2.5 Discussion

Knowing and understanding the anatomy, the physiology and the neural control of LUT is essential to accomplishing any successful work in bladder monitoring. We found that some studies overlooked very important elements of bladder physiology, which either were ignored at the time of publication or perhaps were considered irrelevant. It might happen that the eagerness to quickly get results sometimes leads the researchers to skip over essential steps.

For monitoring bladder volume, two types of sensing options have been used; those based on artificial sensors (pressure, displacement, ultrasound, etc.) or those that use the natural sensors present in the bladder wall (mechanoreceptors). The information gathered from the artificial bladder sensors is more independent of the patient's condition, so it can be more reproducible over time in the same patient and among different patients. Furthermore, accuracy could potentially be higher than that provided by natural receptors. Major drawbacks are the decreasing reliability over a long period of time, a higher degree of invasiveness, the problems arising from their location within the lower abdomen on or near a moving organ, and the biocompatibility of the materials employed. On the other hand, the information gathered from natural mechanoreceptors is more reliable, the implantation procedure of the neuroprosthesis is less invasive and the cuff-electrodes used as interfaces for ENG recordings are well tolerated in chronic applications [1]. However, in the pathologic bladders of patients with SCI and other neural conditions, bladder cancer, cystitis, etc., the information collected from mechanoreceptors could be misleading. Additionally, the selectiveness and the signal to noise ratio of recorded ENG signal using tripolar cuff-electrodes are still pending issues.

Analyzing the results of the studies reviewed concerning bladder volume monitoring, it can be stated that the sensory information produced by the bladder mechanoreceptors is rather more related to the detection of bladder fullness and pain than of a specific volume, particularly when P_{ves} is below the threshold value.

The firing frequency of the tension mechanoreceptors increases during bladder distension, but a relatively rapid adaptation of these receptors along with the viscoelastic accommodation of the bladder, have prevented the extraction of volume information from the measurement of P_{ves}. This is in accordance with the finding of the prevalence of phasic over tonic response of the bladder

mechanoreceptors. Thus, the mechanoreceptors that specifically respond to bladder volume should be a better target to relate their outflow activity with bladder volume.

It was not evident to pinpoint the optimum method for monitoring bladder volume, considering the anatomical and physiological particularities of the bladder, as well as the discussed limitations of the methods based on natural or artificial sensors, and bearing in mind the technological constraints. As could be seen in Table 2-1, none of the measurement methods proposed in past years completely met the evaluation criteria. The ENG recording of bladder afferent activity, which could reflect the bladder distension and contraction as well as the volume information, appears to be the most suitable method for this biomedical engineering challenge. Nevertheless, more studies are required to demonstrate its feasibility. An improvement in selectiveness and in the signal to noise ratio seems to be mandatory for success in a new endeavour.

The choice in no way means that this is the only valid method but that it is the most suitable candidate to be studied in future research. Thus, this result should not discourage future works that may use the other methods that have not been favoured in the present analysis, provided that the mentioned limitations could be addressed.

Considering the enormous economic and social impact of urinary bladder dysfunctions, which affect millions of people around the world and cost several billion dollars each year [40],[41],[102] future research should be carried out to find out new therapeutic methods and to improve the currently available ones.

2.6 Conclusion

We can confirm that there is currently no available method having the effectiveness required for use in current clinical practice for chronic monitoring of bladder volume. This is a critical requirement for more successful application of the neuroprosthetic implants in patients with bladder dysfunctions.

ENG recording was found to be the method that best met the user's needs. However, more studies are required to determine whether this method can be used for bladder volume monitoring.

It is expected that the present study can facilitate the development of a safe and effective method and apparatus for the chronic measurement of bladder volume, clinically useful for patient monitoring or as part of a neuroprosthetic device.

2.7 Acknowledgement

The authors would like to thank the Canada Research Chair of Smart Medical Device and the Natural Sciences and Engineering Research Council (NSERC) of Canada and to Le Fonds Québécois de la Recherche sur la nature et les technologies (FQRNT) for their support.

CHAPTER 3 ESTIMATION OF BLADDER VOLUME FROM AFFERENT NEURAL ACTIVITY

From the literature review and the assessment of measurement methods, we concluded that recording the neural activity (ENG) of the bladder was the most suitable approach for chronically estimating the bladder volume. However, the few studies that targeted the bladder volume estimation from ENG recordings were not able to ascertain the feasibility of this approach due to several drawbacks that were presented and discussed in the preceding chapter.

In this chapter, we present the published paper of the study that we performed to assess the feasibility of estimating bladder volume from the neural activity produced by specialized receptors that respond to bladder stretching during filling. We describe the setup and protocol of the acute experiments performed in anesthetized rats, an accessible and well-documented animal model for this type of study.

To perform these difficult *in vivo* experiments collaboration from other research groups with the required expertise was needed. Due to the specificity of this type of experiments, we could not find locally the research group with the lab facilities and the particular skills to conduct the experiments in rats. The Urology Department of the Faculty of Medicine in University of Antwerp, Belgium, which has been working over several years on studies that required this type of experiments, accepted to collaborate with us. The acute experiments with rats were performed by Dr. Tomonori Minagawa under direction of Prof. Jean-Jacques Wyndaele. They provided us with the recordings of the neural activity and the bladder pressure during the different types of experiments that we designed at the École Polytechnique de Montréal.

Two measurement methods for decoding sensory information from the afferent activity recordings are explained, illustrated and validated throughout the chapter. Both methods are based on neural source detection and discrimination (classification) of the recorded activity. One method was proposed for qualitatively detecting three level of bladder fullness. This method requires a minimum of operations and can be implemented using few hardware resources. The second method quantitatively estimates the bladder volume using a regression model of programmable order. We also show that it is also possible to estimate the bladder pressure using

appropriate parameters in the regression model that was implemented in the method. The quantitative estimation method can also be used to deploy a closed-loop system by providing continuous feedback about the bladder state to the FES control unit and to provide timely warnings to patients with sensory impairments, among other possible applications.

Additional test runs were performed to study the mechanoreceptor behavior under special conditions. The results from these test runs allowed us to clarify the contradictions found in the literature concerning both the existence of specialized bladder receptors and the detection of bladder tonic and phasic responses.

The proposed methods are executed in two phases: an offline training phase and a second phase that is executed in real-time to estimate both the qualitative and quantitative values of the bladder volume. The training phase was used to learn or identify the parameters required for real-time volume monitoring. During the training phase, the most suitable algorithms can be executed regardless of their complexity and execution time. Hence, in the real-time monitoring phase, we can use algorithms of lower complexity that are still effective thanks to the previously executed phase. The algorithms of lower complexity that are used in the real-time monitoring phase allow for subsequent electronic implementation with fewer hardware resources and less operation cycles, thus favoring the reduction of the power consumption, which is a major constraint for any implantable device.

The accuracy and reproducibility of the estimation results obtained from the validation tests using the *in vivo* recorded signals allowed us to demonstrate the feasibility of both methods. Therefore, our hypothesis H1 was validated.

In Appendix 4, we present an interesting analysis we performed to choose the most suitable correlation coefficient for detecting the afferent nerve that conveys sensory information about bladder volume or pressure. This analysis was not included in the paper due to space limitations.

Three different correlation coefficients were computed and analyzed to find the most suitable one for nerve selection: the Pearson's, Spearman's and Kendall's correlation coefficients. The Pearson's correlation coefficient assesses a linear relationship between variables, while the Spearman's and Kendall's *rank* correlation coefficients rather assess a monotonic dependence. The results of the Multiple Comparison test among the groups of coefficients using a one-way ANOVA are shown in the Appendix 4. The results of this analysis show that the Spearman's rank

correlation coefficient is a good choice for this type of correlation analysis when a non-linear relationship between the variables is expected.

Estimation of Bladder Volume from Afferent Neural Activity

(The published paper is reproduced here)

Publication source: Mendez, A., Sawan, M., Minagawa, T., & Wyndaele, J. J. Estimation of Bladder Volume from Afferent Neural Activity. *Neural Systems and Rehabilitation Engineering, IEEE Transactions on*, vol. 2 no.5, 2013. doi: 10.1109/TNSRE.2013.2266899

Arnaldo Mendez[1], *Member, IEEE*, Mohamad Sawan[1], *Fellow, IEEE*, Tomonori Minagawa[2,3], and Jean-Jacques Wyndaele[2]

[1] École Polytechnique de Montreal, [2] University of Antwerp, Belgium, [3] Shinshu University, Japan

Abstract— Refractive urinary dysfunction in individuals suffering from neurogenic bladder syndrome can be treated with implanted neurostimulators that restore, to some degree, the control of the urinary bladder. A sensor capable of relaying feedback from bladder activity to the implanted neurostimulator is required to implement a closed-loop system to improve overall implant efficacy and minimize deleterious effects to neural tissue caused by continuous electrical stimulation. In this paper, we present a method that allows real-time estimation of bladder volume from the primary afferent activity of bladder mechanoreceptors. Our method was validated with data acquired from anesthetized rats in acute experiments. It was possible to qualitatively estimate three states of bladder fullness in 100% of trials when the recorded afferent activity exhibited a Spearman's correlation coefficient of 0.6 or better. Furthermore, we could quantitatively estimate bladder volume, and also its pressure, using timeframes of properly chosen duration. The mean volume estimation error was 5.8 ± 3.1%. Our results also demonstrate that it is possible to quantify both phasic and tonic bladder responses during slow filling and isovolumetric measurements, respectively.

Index Terms— Bladder volume, Bladder pressure, Neural prosthesis, Biomedical signal processing, Biomedical monitoring

3.1 Introduction

Urinary dysfunction can result from injuries or pathologies that affect the local or central neural system (e.g., spinal cord injury) or from nonpathologic conditions such as aging [25]. Any major disruption in the autonomic reflex pathways that drive urinary bladder storage and voiding functions, leads to loss of bladder control, resulting in severe deterioration in patient health and quality of life.

For over a decade, implanted neuroprostheses have been used in refractive patients who do not respond to or cannot tolerate conservative treatments for urinary dysfunction. These implants can restore bladder control to some degree, although they have known side-effects [19]. To the best of our knowledge, none of the implants currently used in clinical practice are capable of performing conditional neurostimulation. However, stimulation based on ongoing bladder activity can improve the overall performance of neuroprostheses by providing feedback for a closed-loop system [8]. Adding intrinsic auto-regulation advantages can also reduce power consumption and prevent deleterious effects caused by continuous electrical stimulation [103].

Studies published over the past years have attempted to identify a suitable method for chronic monitoring of bladder activity, i.e. the volume or pressure variation over time. Challenging characteristics arising from the bladder's anatomy and physiology, among other factors, have hampered the achievement of such a goal [36].

The most common methods used in past to monitor bladder have been the followings: indirect volume estimation from intravesical pressure, electrical impedance plethysmography, strain-gauge plethysmography either resistive or capacitive, imaging plethysmography using ultrasound sensors, electromagnetic plethysmography, and electroneurographic recordings (ENG) form peripheral nerves. The choice of whether to use artificial sensors or natural sensors (bladder mechanoreceptors) for chronic monitoring of bladder volume or pressure was not immediately evident by simple pros and cons analyses. Therefore, to choose an optimal method that balanced considerations for dealing with the challenging natural characteristics of the bladder with the patients' needs, we performed an exhaustive analysis of the published literature [36]. We concluded that the recording from bladder afferent nerves was the most suitable method for chronic monitoring of the bladder volume.

The ENG recordings have been used in rehabilitation applications as command and feedback signals for Functional Electrical Stimulation (FES) devices, for instance to correct foot-drop in hemiplegic individuals and to control hand grasp in tetraplegic individuals [1]. Past studies have also shown that ENG recordings using tripolar cuff-electrodes from pelvic nerves and sacral roots, with subsequent signal processing using the rectification and bin integration (RBI) or cumulative sums (CUSUMs) techniques, can detect sudden changes in pressure produced by overactive bladder contractions [20],[87-90].

The whole-nerve ENG recorded using cuff-electrodes is a composite signal formed from superimposed action potentials arising from several firing units in the nerve that also carries information from other sources (e.g. rectum and dermatomes), where the contribution of the bladder afferents is the weakest [88]. Moreover, signal processing of ENG recorded from cuff-electrodes has to deal with extremely low signal-to-noise ratios, which hampers the detection of the very small increase in the composite ENG signal level produced during the bladder filling [20]. Therefore, from this compounded and noisy signal it is not possible to identify reliably the source and to quantify accurately the afferent activity, which is essential to extract sensory information of the bladder volume.

In contrast, by measuring activity recorded with penetrating electrodes in the appropriate dorsal root, S3 in humans [88], it is possible to record and discriminate extracellular activity stemming specifically from the bladder mechanoreceptors [104] and not from activity of other afferents projecting into the same dorsal root ganglia (DRG). Recent studies have demonstrated that the Utah Slanted Electrode Array (USEA) can properly record the afferent activity in peripheral nerves during chronic experiments [105],[106]. Moreover, the thin-film longitudinal intra-fascicular electrode (tfLIFE) has also shown to be capable of recording selectively afferent activity from specific aferent nerves [95],[107].

It is known that in the bladder wall there are specialized receptors (mechanoreceptors) that produce afferent activity upon stretching and contraction [34]. Afferents nerves that respond specifically to bladder filling have also been identified in animal models. These appear to be volume receptors that are sensitive to the stretching of the inner mucosa [30]. The afferent activity we are interested in travels through the pelvic nerves and the DRG to a specialized reflexive center in the spinal cord. Moreover, studies performed with animal models (rats) have

demonstrated that the firing rate (FR) of a single afferent fiber conveying sensory information from the bladder mechanoreceptors increases with the volume [30],[32],[33].

Relatively few studies have targeted chronic bladder monitoring based on artificial or natural sensors. Most of them focused on detecting pressure changes. Those that have sought to estimate bladder volume are even fewer, and their results have not conclusively demonstrated that monitoring bladder volume from afferent neural activity is feasible. Therefore, we have performed a study to assess the feasibility of monitoring bladder volume from the primary afferent activity of bladder mechanoreceptors.

To validate our bladder monitoring method, we used Sprague-Dawley rats, a practical and accessible animal model for studying the lower urinary tract (LUT) [108]. Although the urinary system is quite similar among mammals, there are always differences with humans that must be considered to conduct well-controlled experiments and properly analyze the results [32],[33].

3.2 Experimental Methods

3.2.1 Experimental setup

A total of 40 intact female Sprague-Dawley rats (203 – 287 g) were used. Immediately before the experiments, animals were anesthetized with urethane (1.5 g/kg IP), an anesthetic known to spare the bladder afferent activity [109]. After the experiments, animals were euthanized by overdose with urethane. The protocol for the experiments was approved by the Animal Ethics Committee of the University of Antwerp, Faculty of Medicine (No. 2012-05).

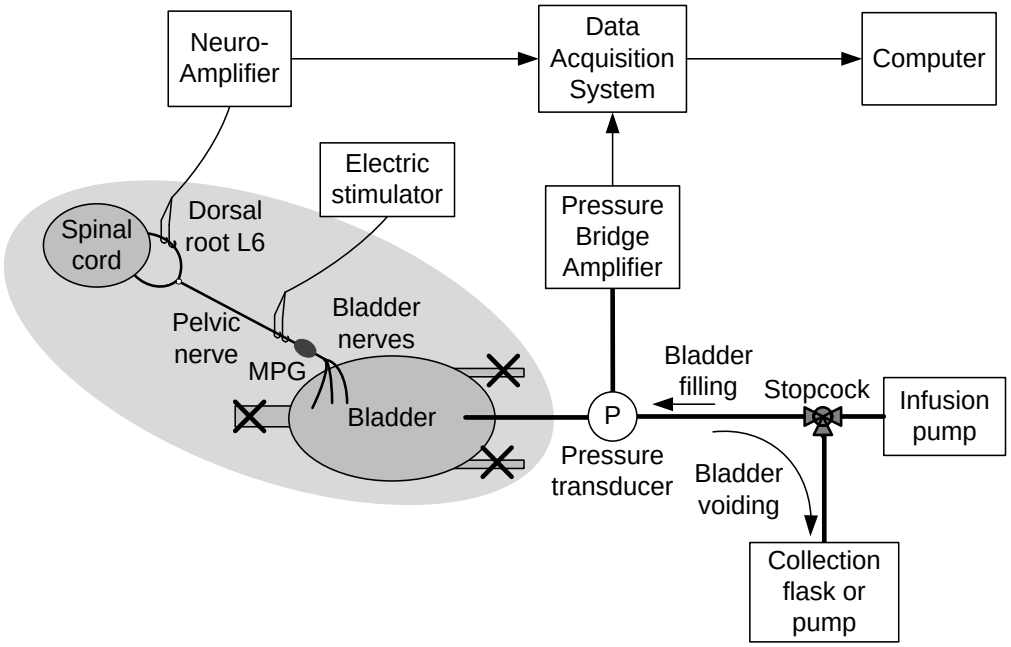

Figure 3-1: Experimental setup used for identification of bladder afferent nerves projecting into the L6 root and for recording the afferent activity during a filling cystometry. (MPG: Major Pelvic Ganglion).

The setup used throughout our experiments is depicted in Figure 3-1. Because it is not possible to place penetrating microelectrode arrays in rat spinal roots, mechanoreceptor afferent activity was recorded following the technique described in [108]. Briefly, we describe this technique as follows. The pelvic structures were exposed, the ureters were ligated and the urethra was clamped. The left pelvic nerve was then isolated, and a pair of Teflon-coated silver electrodes with bared tips forming a hook were placed around it and sealed with Wacker Silgel (Wacker Chemie, Munich, Germany). A catheter (Clay-Adams PE-50, NJ) was inserted into the bladder through the dome and secured by silk suture. The catheter was attached to a stopcock connected to a pressure transducer (DX-100, Nihon Kohden, Tokyo, Japan) and an infusion pump (NE-1000, ProSense, Netherlands) for recording the intravesical bladder pressure and infusing saline into the bladder, respectively. Next, the lumbosacral spinal cord was exposed by laminectomy and the dura mater was opened. The dorsal skin was sutured to form a pool that was filled with body temperature (38°C) paraffin oil (Fisher Scientific, Loughborough, UK). Finally, both L6 dorsal roots were cut. Fine filaments dissected from the left L6 dorsal root were placed across shielded silver bipolar electrodes.

The recorded afferent activity was pre-amplified with a low noise AC differential amplifier (10x), filtered (60–5,000 Hz), further amplified (10,000x) and digitally converted (Micro-Plus CED, Cambridge, UK). The neural signal was sampled at 24 kHz and the pressure at 100 Hz. Afferent fibers originating from the bladder were identified by electrical stimulation of the pelvic nerve (0.5-msec square wave pulses, SEN-3301, Nihon Kohden). The nerve filaments were teased until a maximum of three clearly distinct unitary action potentials were evoked by the electrical stimulation. The extracellular action potentials, known as spikes, were recorded along with the intravesical pressure using Spike2 software (CED, Cambridge, UK), which can also be used for online spike discrimination.

3.2.2 Acute experiments

The afferent activity, hereafter referred to as ENG (Electroneurogram), and the vesical pressure (Pves), were recorded throughout a measurement cycle. Different bladder volume curves were used depending on the specific goals of the experiments, as shown in Figure 3-2.

Profile (A) was used in all the trials for determining the feasibility of volume estimation from ENG signals. Profile (B) was used to assess the reversibility of mechanoreceptor responses when the bladder was passively voided by withdrawing saline with an additional infusion pump. Profile (C) was used to assess the tonic responses of mechanoreceptors by recording the ENG during an extended isovolumetric measurement phase. The first phase for each profile was always a resting phase (empty bladder). Within the first half of this phase, electrical stimulation was applied, as described above, to identify the bladder afferent fibers. The spikes generated by this stimulation were treated as artifacts. These types of artifacts are normally present during neuroprosthetic device stimulation, thus the system must be able to address them. The other half of the resting phase was used for detecting the ongoing resting activity (i.e., the baseline). In contrast to humans, rats exhibit bladder afferent activity when empty that must be considered [32].

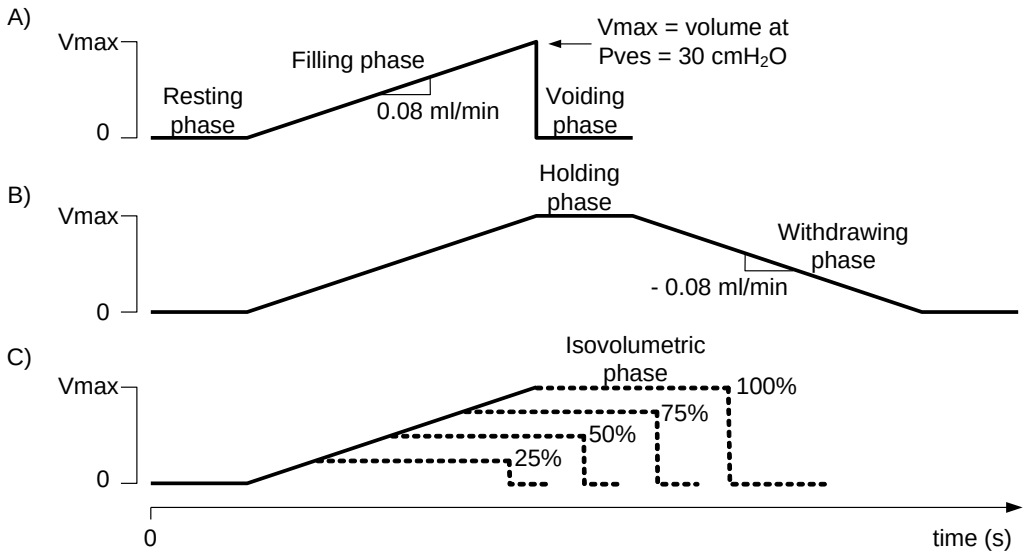

Figure 3-2 : Filling profiles used in three types of experiments. A) Standard filling-voiding cycle. B) Standard filling and passive withdrawing. C) Filling to different levels followed by an isovolumetric phase.

The second phase in each cycle consisted of a constant filling cystometry using a low filling-rate of 0.08 mL/min of saline at room temperature. This slow filling rate is used to mimic, as far as possible, a physiological filling rate and prevent undesirable changes in bladder natural responses [110]. In the experiments with profiles (A) and (B), infusion continued until the Pves reached 30 cm H_2O (2.94 kPa). In the experiments with profile C, the bladder was filled to four different degrees of fullness: 25%, 50%, 75% and 100% of the maximum volume reached at Pves = 30 cmH_20. The third phase was profile specific. For profile A, the volume was voided by opening the stopcock. For profiles B and C the volume was held for 60 s and 180 s, respectively. During the fourth phase in profile (B), a passive voiding (withdrawing) at -0.8 mL/min was performed using an additional infusion pump. In all of the experiments, the filling-voiding cycle was repeated three or more times, when possible, on the same fiber. At the end of each cycle a final electrical stimulation confirmed that the signal source was intact.

Conduction velocity (CV) was calculated from the latency of the response to electrical stimulation and the distance between the stimulation and recording sites. Fibers with a

CV < 2.5 m/s were classified as unmyelinated C-fibers. Fibers with a CV ≥ 2.5 m/s were classified as myelinated Aδ-fibers.

Offline signal processing and statistical analysis were executed using custom-written software in MATLAB, Mathwork Inc., MA.

3.3 Bladder volume estimation method

To reduce the system complexity and the amount of hardware resources required by the implantable device for real-time monitoring of the bladder volume, we developed a method which requires two phases: 1) an offline training phase; and 2) an unsupervised real-time volume estimation (monitoring) phase. The training phase is used for identification of the parameters required for real-time monitoring.

3.3.1 The training phase

1) Digital data conditioning. The ENG data were band-pass filtered between 300 Hz and 3 kHz using a non-causal linear phase finite input response (FIR) filter. This finite response filter, unlike the infinite response (IIR) filter, prevents spike shape distortion. Additionally, FIR filters are more suitable for electronic implementation using fixed-point arithmetic because they avoid error accumulation over successive arithmetic operations without retroaction.

2) Identifying the afferent unit exhibiting the best correlation with bladder volume. Identification of the optimal afferent unit was performed only during the training phase. This identification was designed to spot the unit (afferent neuron) that exhibited the best correlation between ENG and bladder volume. As described in section 4.2.1, a preliminary selection was performed by isolating the filament connected with the bladder pelvic nerve. However, this fine filament typically contains more than one active unit (up to three were detected) as shown in Figure 3-3, which may or may not show good correlation. Multiunit activity is always present in recordings acquired from microelectrode arrays such as the USEA and tfLIFE. These electrodes arrays seem to be the best available options for this kind of recordings in future experiments. Consequently, detection, alignment and classification of the spikes, known as spike sorting or discrimination, were

performed using software custom-written in Matlab. This software used the superparamagnetic clustering function provided by Waveclus software [111].

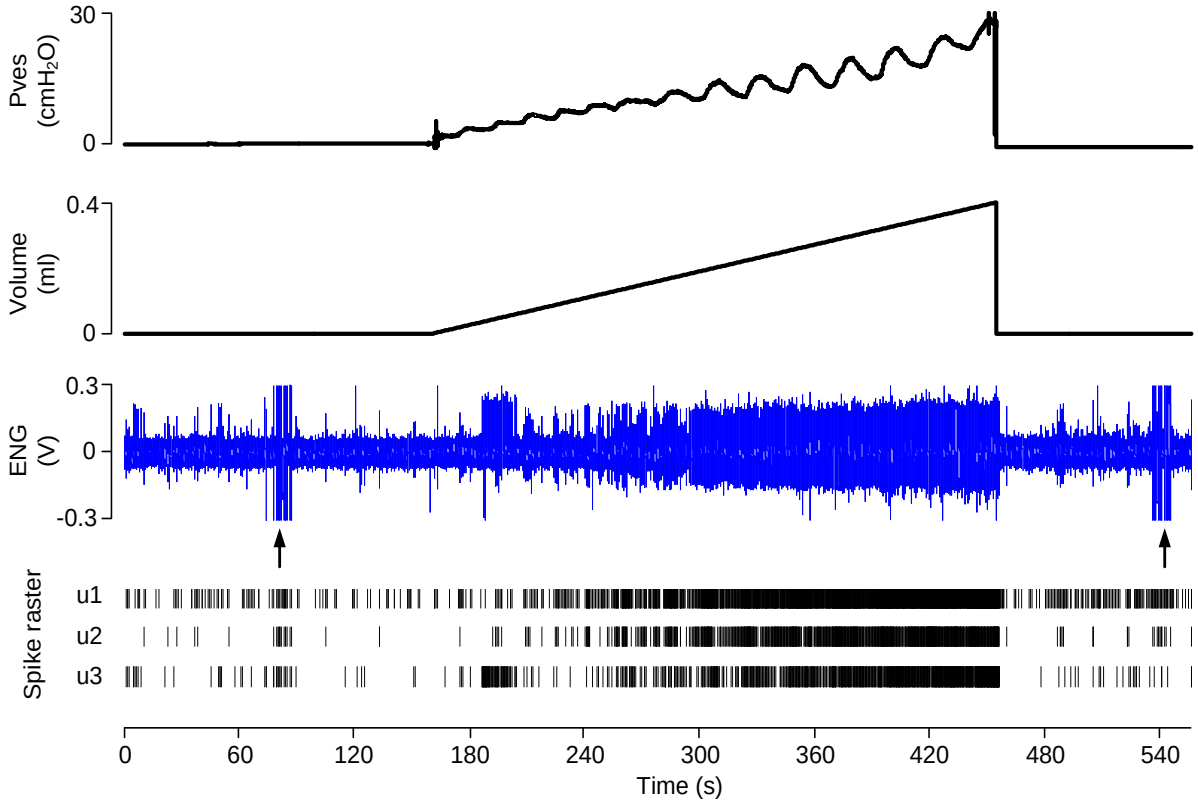

Figure 3-3: Bladder afferent activity recordings (ENG) using filling profile A (from animal No. 15, Aδ-fiber). The arrows point to the artifacts elicited by electrical stimulation. The spike raster of the three units identified is shown.

Next, we computed the number of spikes detected within a time window of one second for each detected unit throughout the measurement cycle.

To identify the unit that exhibited the best correlation with volume, we used the Spearman's *rank* correlation coefficient (ρ). Unlike the more commonly used Pearson's correlation coefficient (r), which measures a linear dependence between two variables, the Spearman's rank coefficient rather assesses a monotonic dependence that is not necessarily linear. Taking bladder physiology into consideration, this coefficient is better suited for the relationship between ENG and volume,

providing more robustness for our estimation method. Lastly, the unit class displaying the FR vs. volume with the highest ρ was chosen for subsequent processing.

The Spearman's rank correlation coefficient was computed by using (3-1), where ρ_k is the Spearman's coefficient of the unit of class k; k is the number of classes detected; n is the number of timeframes used through the recorded signals, hereafter referred to as bins; $FR_{i,k}$ stand for the ranked values of the units' firing-rate per second; $V_{i,k}$ is the mean value of the volume within the same bin; and $\overline{FR}_k$ and $\bar{V}_k$ are the mean values of all firing rates and volume bins for the class k, respectively.

$$\rho_k = \frac{\sum_{i=1}^{n}\left(FR_{i,k}-\overline{FR}_k\right)\left(V_{i,k}-\bar{V}_k\right)}{\sqrt{\sum_{i=1}^{n}\left(FR_{i,k}-\overline{FR}_k\right)^2 \sum_{i=1}^{n}\left(V_{i,k}-\bar{V}_k\right)^2}} \tag{3-1}$$

3) Estimating the ongoing resting activity. As mentioned above, rats exhibit resting activity that must be considered during the estimation process. Thus, a baseline was calculated by averaging the FR during at least 60 s before starting bladder infusion with saline. Any FR activity below this base line was assumed to be resting activity corresponding to an empty bladder. Baseline calculation was also helpful for suppressing the evoked spike activity produced during electrical stimulation,

4) Conversion of the volume curve into bins. In this stage, the volume and FR data were prepared for the subsequent procedure. The continuous volume curve was quantized into a finite number of bins of the same length, herein referred to as the bin-width (BW). The volume within each bin was set to the mean volume between its edges.

5) Discrete integration of the firing rate within each bin. The discrete integration of the FR within the bin edges (i.e. the spikes count within the bin) was also performed for the selected unit, herein referred to as the bin-integrated-rate (BIR). The BIR is computed in real-time using a timer with the time base fixed to the best BW and a counter of the number of spikes detected during the BW.

To find the proper timeframe duration that minimizes the estimation error, the stages 4 and 5 were performed using different BWs, ranging from 1 to 60 s using 1 s steps. The computations for a BW of 1 s were previously executed during the best correlated unit selection, thus subsequent processing started at 2 s.

6) Volume estimation. Two methods for volume estimation were developed: one for qualitatively estimation of different degrees of the bladder fullness and another for its quantification. One or both methods could be implemented in an implantable sensor depending on the intended application. The qualitative method will require fewer hardware resources than the quantitative method. Nevertheless, the latter is more suitable for monitoring applications where an accurate value is required, such as long-term follow-ups for clinical purposes and research studies.

3.3.1.1 Qualitative volume estimation

Three states representing a fraction of the full bladder were defined as low-volume (comfortable level), need-to-void (within some predefined time) and urge-to-void (risk of an imminent leaking). Correspondingly, three different thresholds for estimation of bladder fullness were set as 0.25, 0.5 and 1.0 times the maximum bladder functional capacity, which can be determined by cystometric measurements. The definition of the states and the fractions were set inspired by the actual sensations arising from the lower urinary tract in humans [32],[112]; i.e. undetectable bladder sensation due to a low-urine volume stocked, the filling sensation threshold, typically at 250−300 mL, and the detection of urinary urgency, discomfort or pain on average at 500−600 mL.

Next, using linear regression during the training phase, we found the BIR for the selected unit that best matched each of the fullness states to properly set the corresponding threshold. As result, we obtained three BIR values that were related to each fullness state, i.e. $BIR_{0.25}$, $BIR_{0.5}$, and $BIR_{1.0}$.

Qualitative volume estimation was performed by finding the minimal distance among the real-time computed BIR and the stored values ($BIR_{0.25}$, $BIR_{0.5}$, and $BIR_{1.0}$). This way each bin was assigned to one of the three bladder states defined above. The BW was swept using the intervals mentioned, and finally the length yielding the lowest qualitative estimation error (E_{Qual}) was chosen.

To compute E_{Qual} in (3-2) we used the Overall Success Rate (*OSR*) [113], which is the ratio of all correct classifications of the states over all classifications performed. The *OSR* is calculated by adding the number of bins (B_i) for which the estimated state matched the actual state and dividing by the total number of bins (n).

$$E_{qual} = 1 - OSR = 1 - \frac{\sum_{i=1}^{n} B_i}{n} \tag{3-2}$$

3.3.1.2 Quantitative bladder volume estimation

Several models were analyzed for quantitative volume estimation. The main constraint on model choice was suitability for implementation with an electronic system using a reasonable amount of hardware resources. We selected a regression model based on a polynomial of order N, as defined by the following equation,

$$\hat{V} = \sum_{i=0}^{N} (c_i * BIR^i) \tag{3-3}$$

where $\hat{V}$ is the estimated volume, *BIR* is the bin-integrated rate defined early, and c_i are the coefficients for the regression model. To compute the coefficients, we used the bisquare robust fitting method, which assigns lower weights to the outlier values during the fitting process as described in [114].

We found the optimal model order (N) by performing several simulation trials using real ENG recordings. A trade-off was present among the values of N, which could influence the amount of hardware resources to be eventually used in an electronic system, the estimation accuracy and the BW. To account for this trade-off we found the minimal N and the shortest BW that yielded the lowest estimation error.

To that end, we defined some error metrics. Ranked in the order of relevance these metric were: 1) the Root Mean Square Error (RMSE), also known as the standard error, during the filling phase ($RMSE_{Fill}$); 2) the RMSE during all cycle phases shown in Figure 3-2A ($RMSE_{All}$); and 3) the Quantization Error ($RMSE_{Qty}$), i.e., the systematic error resulting from the conversion of the continuous volume curve into bins. Both, $RMSE_{Fill}$ and $RMSE_{All}$ assess the accuracy of the

estimation, whereas $RMSE_{Qty}$ also accounts for the total error. $RMSE_{Qty}$ depends on the BW by which the minimal $RMSE_{Fill}$ error is determined. The larger the BW is, the higher the $RMSE_{Qty}$.

All mentioned error metrics were used for validating the proposed method for bladder monitoring during the real-time volume estimation phase. The RMSE in all cases was calculated by (3-4), where V_i is the actual volume of the bin *i*, $\hat{V}_i$ is the estimated bin volume value computed using (3) for the same bin *i*, and *n* is the total number of bins.

$$RMSE = \sqrt{\frac{\sum_{i=1}^{n}(V_i - \hat{V}_i)^2}{n}} \tag{3-4}$$

For both, the qualitative and the quantitative volume estimation, we computed the template of the spike corresponding to the best-correlated class by averaging the detected spikes from the same class.

All the parameters found during the training phase; i.e., the best correlated unit class along with its averaged waveform, the optimal BW, the resting activity threshold (baseline), the thresholds needed for qualitative fullness detection, the optimal polynomial order and its fitting coefficients; were stored to be used during the real-time monitoring phase.

3.3.2 Real-time volume estimation (monitoring)

During the real-time monitoring phase, the ENG signal was processed as follow: 1) digital filtering; 2) on-the-fly spike sorting, i.e., real-time detection, alignment and classification of the spikes; 3) computing of the BIR for the unit selected and using the optimal BW, both parameters found during the training phase; 4) comparing the BIR to the resting activity threshold baseline and if lower, setting the volume of the bin to zero; or otherwise, 5) computing of the online volume estimation using equation (3-3).

3.4 Results

Considering the characteristics of highly invasive method used to record afferent activity from rats, and the relatively long duration of the filling and voiding cycles required for the training and testing phases, we carried out just one experiment type with the same animal to favor reproducibility throughout successive trials. We performed 164 recordings with 45 fibers from 40 different animals. Out of 45 fibers, 25 were used for experiments of type A (n_A = 25, 107 trials), seven fibers were used for experiment type B (n_B = 7, 21 trials), and three fibers were used for experiment type C (n_C = 3, 15 trials). Ten out of 45 fibers were not useful for the experiments because they ceased to respond few minutes after they were dissected or showed negligible or no correlation with volume or pressure. The mean and standard deviation of the maximal volume from all trials were 438 ± 159 μL.

3.4.1 Bladder afferent activity detection and classification

Most of the fiber recordings exhibited one to three distinct units, but only three cases showed more than one unit with good correlation with the instilled volume ($\rho > 0.6$ for a BW of 1 s).

Pressure and volume, which exhibited high non-linear correlation between them throughout the experiments $\bar{\rho} = 0.98$, showed quite similar ρ values. However, the bladder volume was more consistently correlated with BIR than pressure when longer BWs were used (30 s and over).

Based on conduction velocities, we inferred that out of the 25 fibers in the trials for profile (A), seven were classified as Aδ-fibers (CV = 9.86 ± 1.98 m/s) and 18 were classified as C-fibers (CV = 1.33 ± 0.15 m/s). The average correlation coefficient (ρ) computed using a BW of 1 s for all Aδ-fibers was 0.88 ± 0.1, and 0.89 ± 0.08 for all C-fibers. The one-way ANOVA test showed that there were no significant differences between the two groups ($p > 0.05$).

3.4.2 Qualitative bladder volume estimation

Examples of qualitative volume estimation and the effect of optimal binning on reducing the estimation error are illustrated in Figure 3-4. Figure 3-4B and Figure 3-4C depict the volume

quantized into bins of 1 s and 30 s, respectively. The BIR for each BW was computed as described in section 3.3, and the reference volume curve used for comparison was obtained by quantizing the actual volume infused into the three states defined earlier. These states were denoted, for a shorter representation, by L, M and H (Low, Medium, and High volume). As can be seen in Figure 3-4B, for a BW of 1 s, there are many undesirable transitions between the states. This was a criterion for exclusion. The BW of 1 s (Figure 3-4B) produced an estimation error (E_{Qual}) of 13.7%, whereas the BW of 30 s (Figure 3-4C) produced an E_{Qual} of 0%. Similar error-free qualitative estimations were achieved in 50% of all trials.

The confusion matrices depicted in Figure 3-5 show the average results of the state detection from all measurement cycles performed for the experiments type A during the training (Figure 3-5A) and testing phases (Figure 3-5B). The columns (estimated states) were normalized using the actual number of positive predictions for each state. Thus, the diagonal values show the sensitivity for each estimated state ($\hat{L}, \hat{M},$ and $\hat{H}$); i.e. the True Positives Rate (TPR) [113]. The values outside the diagonal show the corresponding percentage of the states misclassification.

The E_{Qual} computed for Aδ-fibers was 2.6 ± 3.9 % and 1.8 ± 3.1 % for C-fibers. There was no statistically significant difference between the two groups ($p > 0.05$). The combined E_{Qual} regardless of the fiber type was 2.2 ± 3.5 % (n = 107) and the average of the optimal BW was 37.4 ± 11.8 s.

For validating our method during the monitoring phase, simulations of qualitative volume estimation were performed by emulating real-time reading and processing of the input data. To this end, three consecutive cycles of bladder filling and emptying were carried out with a resting interval among cycles. Figure 3-6 shows the real-time-like qualitative estimation. The first cycle (not shown in the figure) was used for training and the following two cycles were used for emulation of real-time monitoring using the parameters determined during the training cycle.

Depending on the bladder compliance, which determines the maximum volume capacity, the total recording time, including the training cycle, could last 40−50 min. Despite the difficult conditions for the dissected filaments over the long course of the experiments, which hampered reproducibility over time, the E_{Qual} was still only 9.5 ± 4.2% (n = 67).

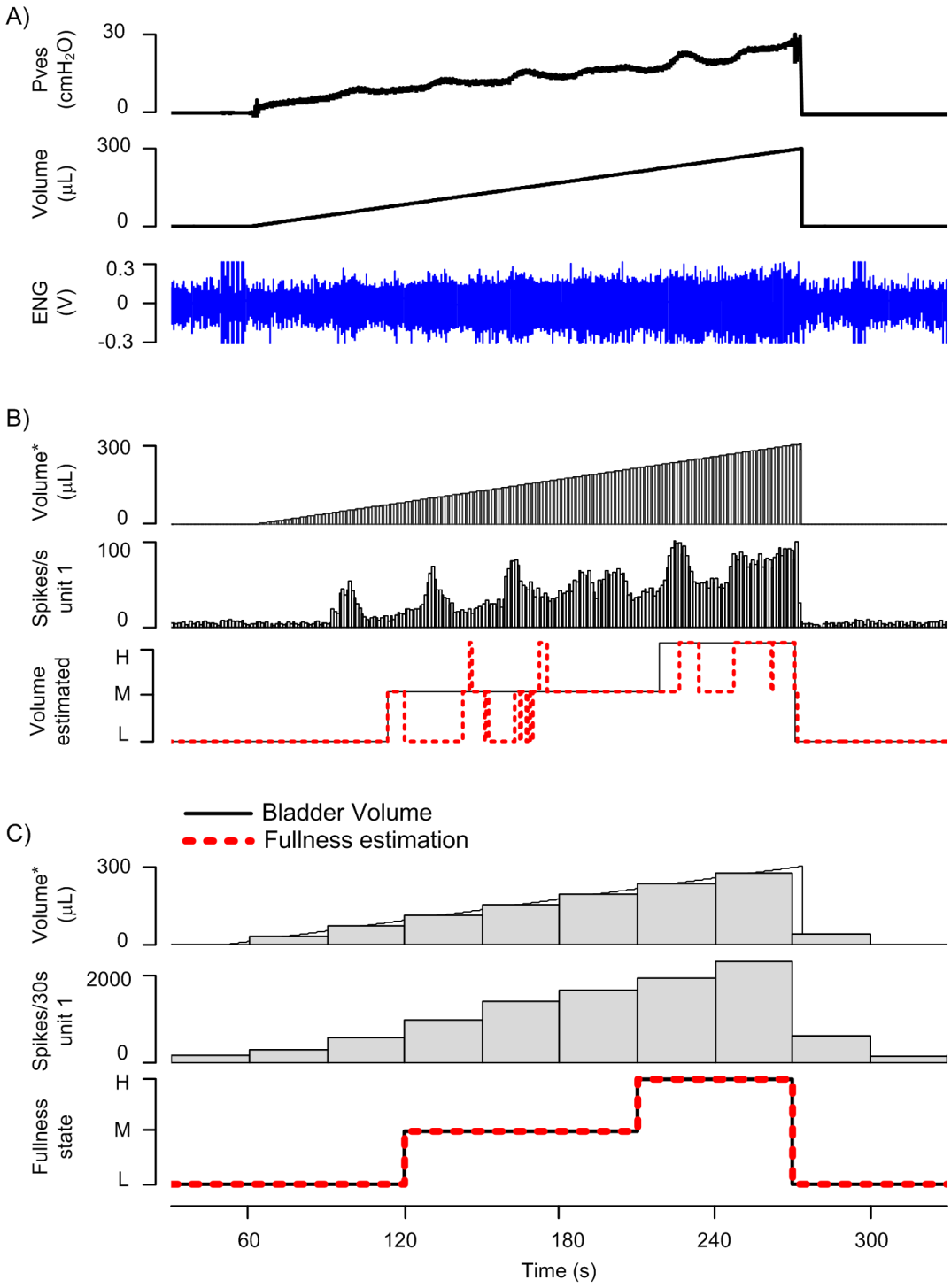

Figure 3-4 : Qualitative estimation of bladder volume (Ex. from animal No. 21, C-fiber). A) Pressure, volume and ENG recorded during a filling cystometry. The effect of the optimal BW selection is shown by a comparison of the estimation errors achieved in B) 13.7% for 1 s and C) 0% for 30 s. (Volume*: quantized volume; L: Low, M: Medium, H: High, represent the bladder fullness states, see text).

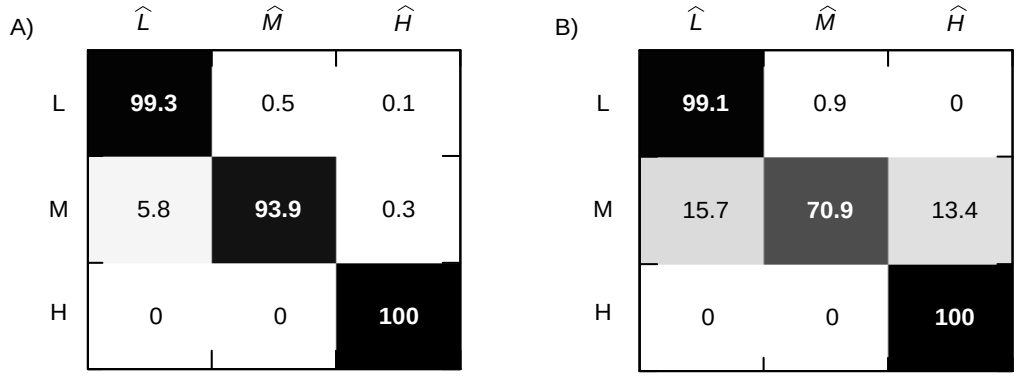

Figure 3-5: Confusion matrices with average results in percentage from all trials of the experiments type A during the training phase (A) and during the real-time-like monitoring phase (B).

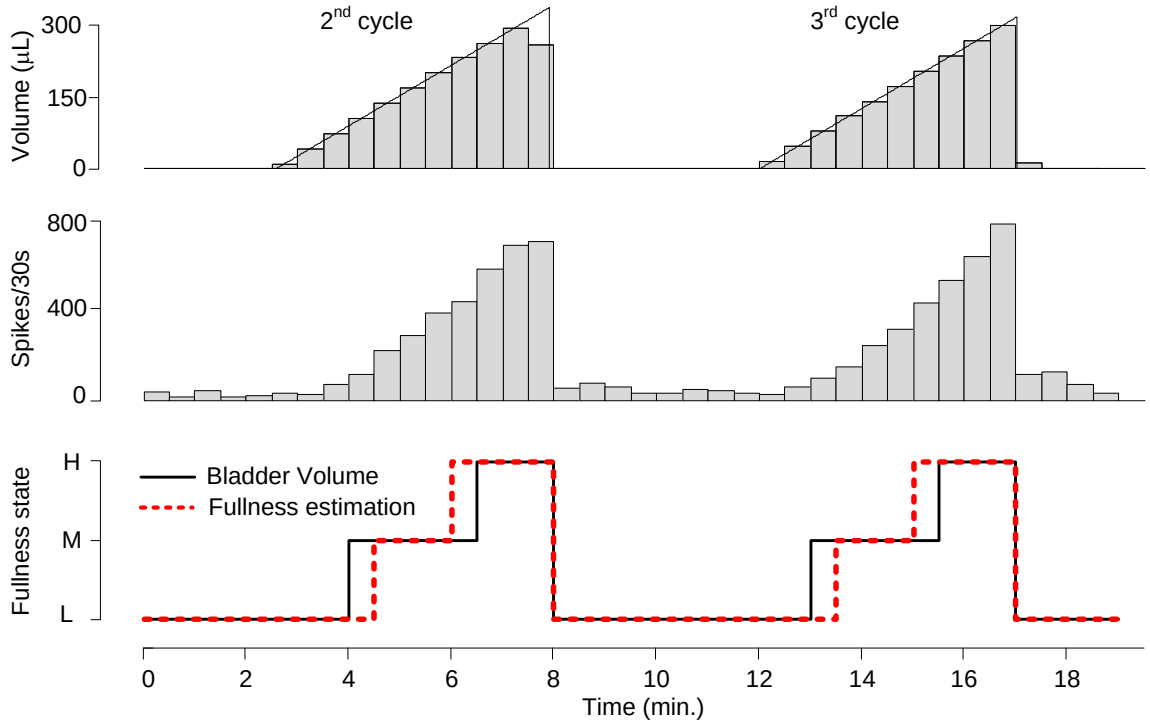

Figure 3-6: Qualitative volume estimation for simulated real-time data processing (Ex. from animal No. 25, C-fiber). The second and third measurement cycles are depicted. The first cycle was used in the learning phase. The qualitative estimation error for depicted cycles was 10.3%.

3.4.3 Quantitative bladder volume estimation

Using the ENG from the training phase, a fitting process was executed to determine the coefficients needed for the regression model implemented by (3), as well as the best BWs for polynomial orders ranging from 2 to 6. We employed data from every fiber that exhibited an acceptable correlation coefficient ($\rho > 0.6$, $n_A = 25$, 107 trials), regardless of its classification as an Aδ or C fiber. The value of $\rho > 0.6$ was set so that the mean of the estimation $RMSE_{all}$ error was under 10% (9.2 ± 5.5%).

An optimal binning process, i.e. proper timeframe selection, allowed us to find the BW yielding the minimal estimation error during the filling phase ($RMSE_{Fill}$). We chose this error as a reference because it had the greatest impact on the estimation error for all phases ($RMSE_{All}$), in turn accounting for all errors. Figure 3-7 shows an example of quantitative volume estimation using two different BWs. In Figure 3-7A, a BW of 1 s produced an $RMSE_{All}$ of 13%. This error was reduced to 4.2% by using a BW of 35 s, as shown in Figure 3-7B. This result demonstrates that at any moment it is possible to estimate the quantized volume with enough accuracy within a timeframe of 35 s.

Estimation with the minimal BW of 1 s (Figure 3-7A) allowed us to determine the time at which afferent activity started to increase once the sensitivity threshold was reached (t_{thr}). The volume at this point (V_{thr}) is the minimum detectable volume for the minimum BW employed (1 s). The value V_{thr} affects the accuracy of estimation during the filling phase. A higher sensitivity threshold means that volumes lower than V_{thr} will be estimated as zero for a longer period during the beginning of the filling phase. We computed V_{thr} as the percentage of the maximum volume reached for all recorded fibers. The Aδ-fibers yielded a V_{thr} of 14.2 ± 11%, and the C-fibers yielded a V_{thr} of 13.3 ± 10.2%. There was no statistically significant difference between the two fiber types. As shown in Figure 3-7B, the estimation after the optimal binning process reduced the error, despite the high sensitivity thresholds displayed by some fibers.

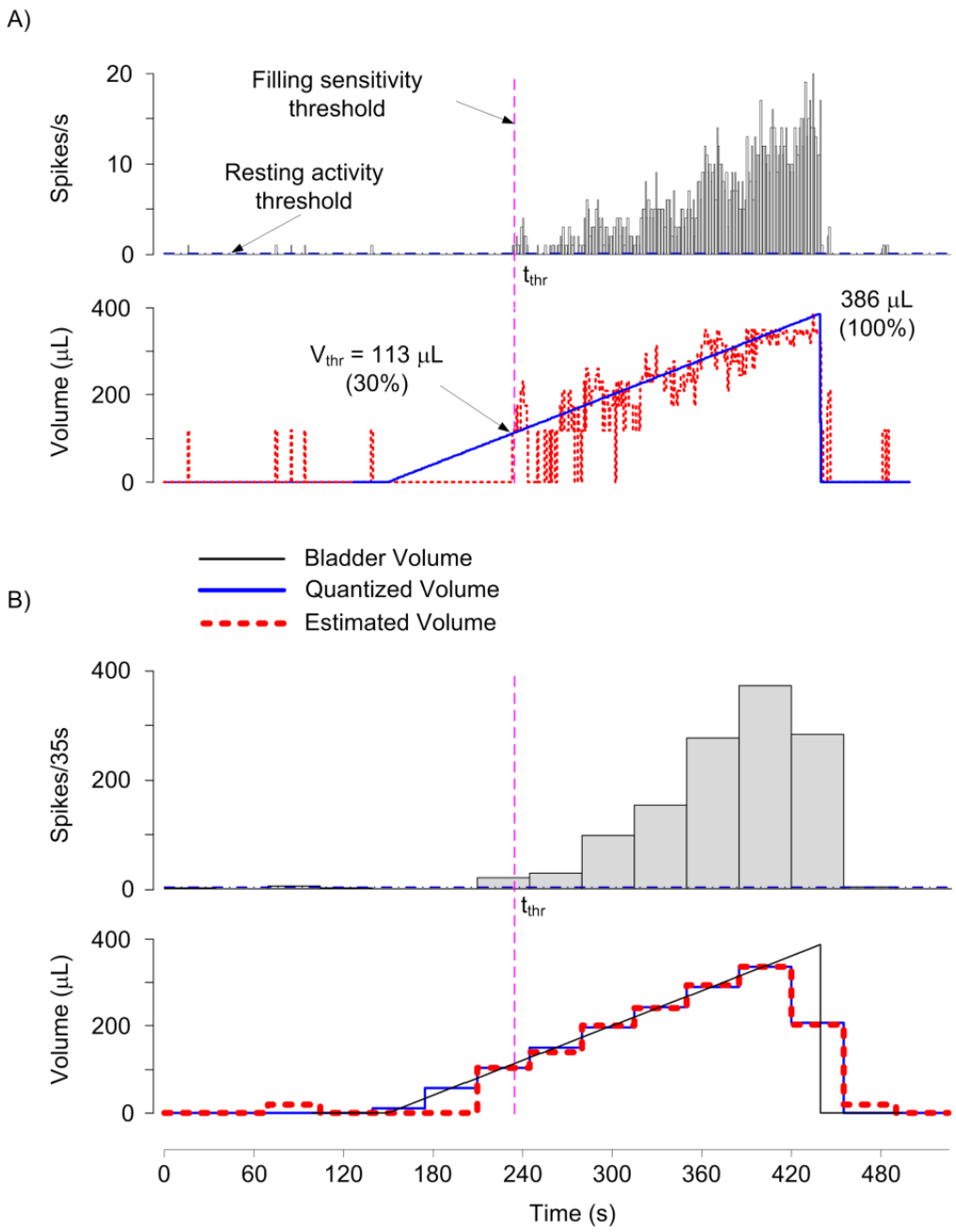

Figure 3-7: Quantitative volume estimation by the proposed method (Ex. from animal No. 18, Aδ-fiber). Comparative results for BW selection are shown. A) Estimation using a BW of 1 s yields an $RMSE_{all}$ of 50.2 µL (13%) and an $RMSE_{Fill}$ (t > tthr) of 58 µL (15%). B) Estimation using the optimal BW of 35 s produced an $RMSE_{all}$ of 16.2 µL (4.2%) and an $RMSE_{Fill}$ ($t > t_{thr}$) of 5.2 µL (1.4%).

In most of the trials, the estimation was better above the sensitivity threshold point (t_{thr}, V_{thr}). The $RMSE_{Fill\_(t>tthr)}$ was 2.2 ± 1.1% for the Aδ-fibers and 3.5 ± 2.2% for the C-fibers. These

differences were statistically significant (p = 0.049) for the $RMSE_{Fill}$ computed for $t>t_{thr}$. However, the significant difference between the two types of fibers tested for $RMSE_{All}$ vanished after the optimal binning process was performed; for Aδ-fibers the $RMSE_{all}$ was 3.6 ± 1.2 % and for C-fibers was 4.0 ± 1.8 % (p > 0.05).

An example of simulation of real-time-like volume estimation is shown in

Figure 3-8. The first measurement cycle was used as a training phase, followed by two consecutive cycles where the volume was computed from the parameters found previously. The optimal BW for this fiber was 47 s, using a regression model of order 6. These estimation results correspond to an Aδ-fiber recording, which exhibit a low sensitivity threshold (V_{thr} = 37 μL, 3.7% of V_{max}). The fitting error of the first cycle and the estimation errors of the following two cycles were very low, as shown by the $RMSE_{all}$ of each cycle: 2%, 3.9% and 4.1%, respectively.

The coefficient of determination R^2 was computed to assess the overall goodness-of-fit of each model order. In Figure 3-9A the averaged value and the standard deviation from all fiber recordings are shown. The Akaike's Information Criterion (AIC) [115], shown in Figure 3-9B, was used to measure the relative goodness of fit considering the number of parameters in the model. In both cases the model of order 6 yielded the best result maximizing R^2 and minimizing AIC. Higher orders (N > 6) produced over-fitting errors and were discarded for subsequent tests.

The $RMSE_{all}$ computed for all fibers during each optimal binning process decreased exponentially with the BW, as shown in Figure 3-10. For values above a given BW (~16 s), the $RMSE_{all}$ decreased very slowly, but not monotonically, regardless of the regression model order. If considered acceptable, BWs lower than the length yielding the minimum error can be selected.

The oscillations in plotted errors are mainly due to the time within the bin at which the volume is voided.

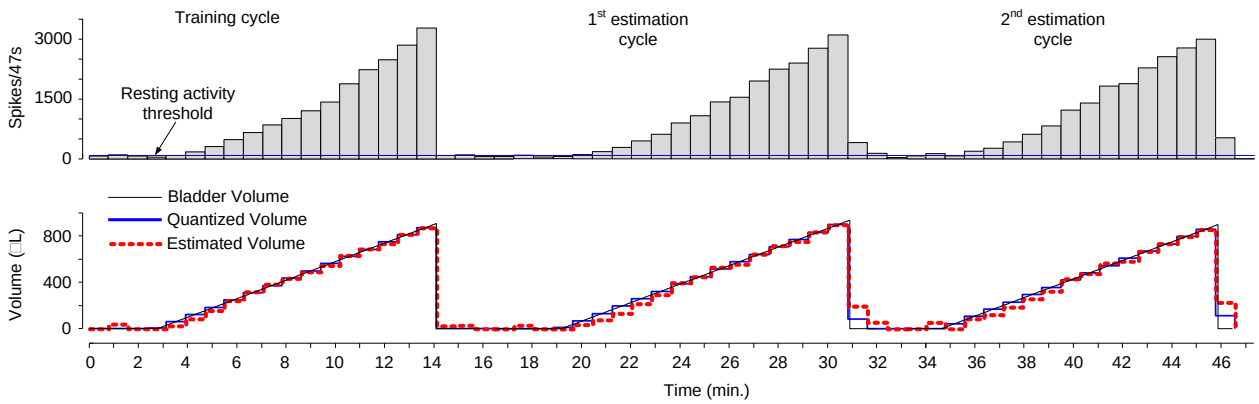

Figure 3-8: Quantitative volume estimation in a simulated real-time data processing experiments (Ex. form animal No. 31, Aδ fiber). The first cycle was used as a training period to estimate the bladder volume in two consecutives filling and voiding cycles. The resting activity threshold, the optimal BW (47 s) and a polynomial order (N = 6) were determined. The $RMSE_{all}$ was 2%, 3.9% and 4.1% for each of the three cycles, respectively.

Compilations of the fitting and estimation error means and standard deviations for all fibers are shown in Table 3-1 using the regression models for N = 6.

Table 3-1: RMS Errors (%) from experiments Type A with model order N of 6

	Best Bin-width	Filling phase	Filling phase ($t > t_{thr}$)	All phases	Quantization error
Fitting	36.3 ± 10.1	4.4 ± 2.0	3.1 ± 2.0	3.9 ± 1.6	9.1 ± 3.0
Estimation	36.8 ± 7.9	6.6 ± 4.7	5.8 ± 5.1	5.8 ± 3.1	10.0 ± 2.7

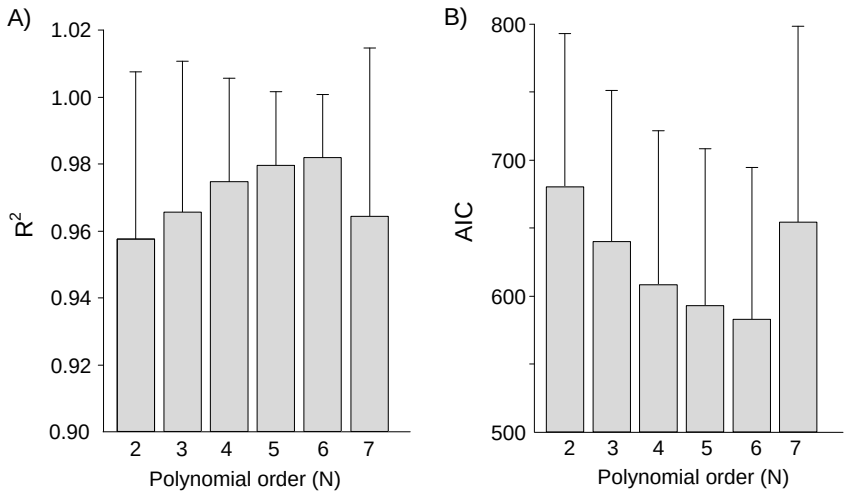

Figure 3-9: Assessment of the model goodness of fit. A) Average coefficient of determination (R^2), and B) Average Akaike's Information Criterion (AIC) for all fibers, both computed using the best BW for each model order.

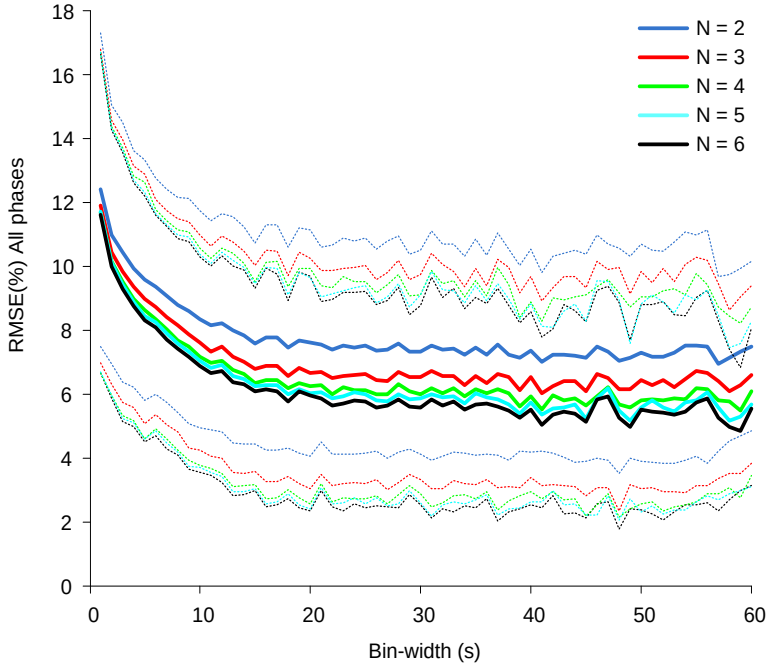

Figure 3-10: Effect of bin-width and polynomial order on the values of $RMSE_{all}$. Both parameters were swept from 1 s to 60 s and from N = 2 to 6, respectively. The averaged values (solid lines) ± standard deviation (dashed lines) computed from all fibers are shown.

In Figure 3-11A it is shown how the estimation errors decrease as the polynomial order increases to N = 5. For a higher order (N = 6), the estimation errors decrease slightly, except for the $RMSE_{Fill(t>tthr)}$. On the other hand, Figure 3-11B shows that the averaged values for the best BW for each order drop linearly with a steep slope.

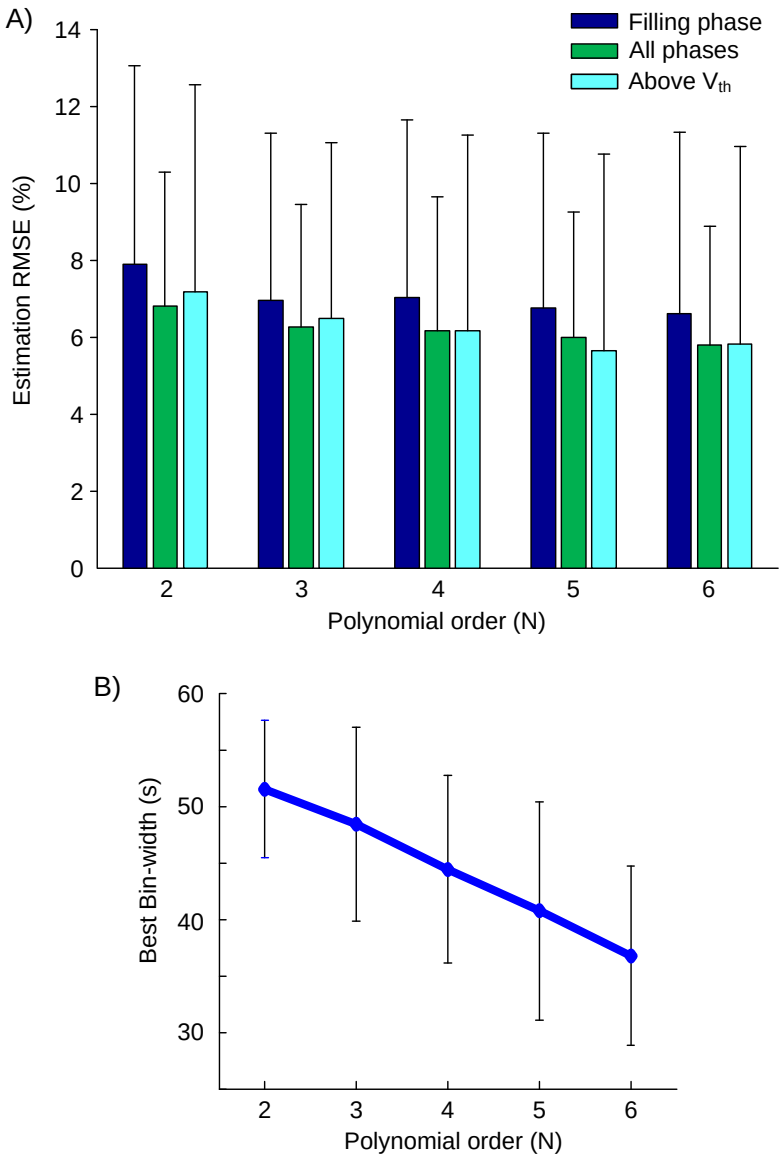

Figure 3-11 Results for volume estimation from all ENG recordings using profile A depicted in Figure 3-2 (n_A = 25, 107 trials). A) Estimation RMSEs for different model order. B) The mean and standard deviation of the best BW showing a steep linear drop with increasing polynomial order.

Considering all the above compilations, we chose an order 6 as the optimal value for real-time volume monitoring. This offered a reasonable trade-off between accuracy and BW for both fiber types.

3.4.4 Results from other test runs

In the exploratory experiments performed with profile (B), shown in Figure 3-2, the parameters gathered during the filling phase were used to estimate the volume during passive withdrawing performed using a second infusion pump. Figure 3-12 depicts an example of this type of experiment. In this example, we observed a similar behavior during the filling and withdrawing phases, which agrees with the low computed errors: $RMSE_{Fill}$ = 2.1% (fitting error) and $RMSE_{withdraw}$ = 3.1% (estimation error). However, in other trials, the estimation during the withdrawing phase was most of the time below the expected value, this way showing a hysteretic response of the bladder mechanoreceptors. Compilation of the means and the standard deviations of all the fibers (n_B = 7) yielded the following estimation errors: $RMSE_{Fill}$ = 10.3 ± 6.9% and $RMSE_{withdrawn}$ = 14.0± 6.3%.

The last type of exploratory experiments was performed with profile (C), as shown in Figure 3-2. These experiments allowed us to assess the tonic response of the bladder mechanoreceptors during the extended isovolumetric phase at different tonicity levels for the detrusor muscle. An example is shown in Figure 3-13. First, we performed a training cycle that filled the bladder to the maximum volume, which was the value reached at Pves = 30 cm H_2O (A). Next, we executed four estimation cycles filling to 25%, 50%, 75% and 100% of the maximum volume (Figure 3-13B). At the end of each filling phase, the infused saline was kept for 3 min. The estimation errors during the isovolumetric phase ($RMSE_{iso}$) in this example were 12.8%, 4.0%, 0.1% and 3.1% for the various infused volumes, respectively.

It is worth nothing that estimations for 25% fullness were not always possible because some C-fibers exhibited a sensitivity threshold (V_{thr}) higher than this value. The estimation errors from fibers with lower sensitivity thresholds were low at all fullness levels during the isovolumetric phase: 4.6 ± 3.7%, n_C = 3, 15 trials.

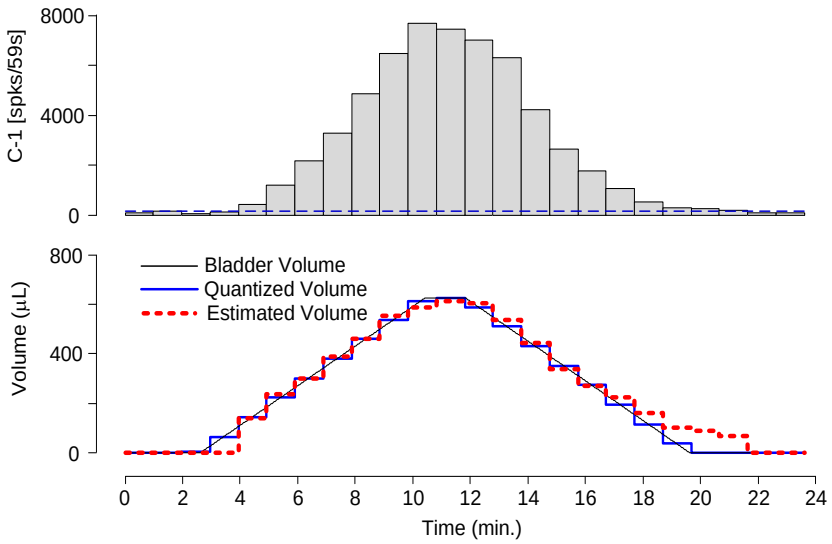

Figure 3-12: Volume estimation during passive saline withdrawing using profile B shown in Figure 3-2 (Ex. from animal No. 35, C-fiber). The resting and filling phase were used as learning periods to estimate volume in the withdrawing phase. The *RMSEs* were 2.1%, 4.1% and 3.1% for the filling, holding and withdrawing phases, respectively.

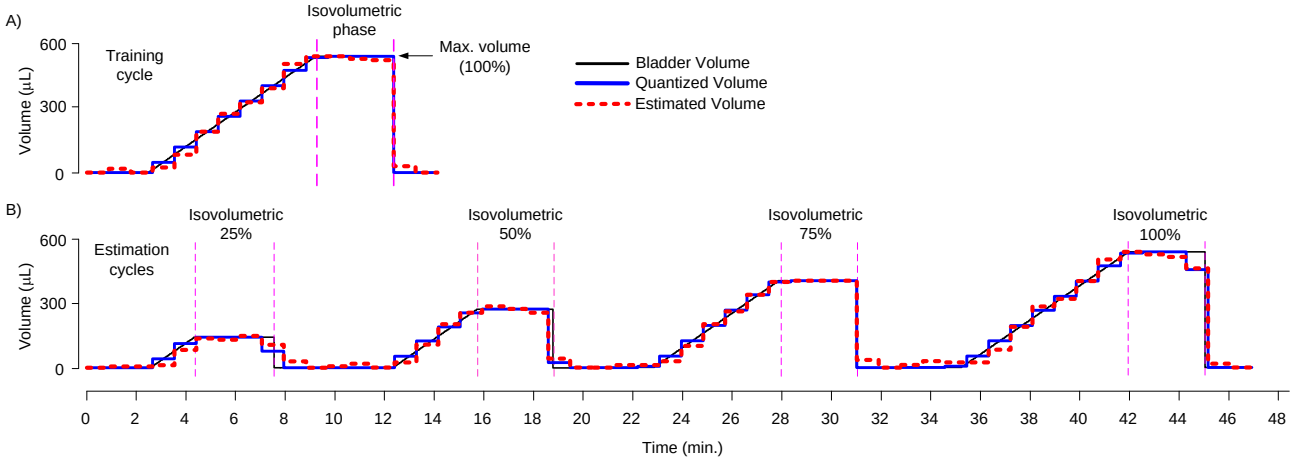

Figure 3-13: Volume estimation during the tonic response of the bladder afferent activity performed during five filling–holding–voiding cycles using profile C (Ex. from animal No. 40, C-fiber). A) The first cycle was used to compute the optimal bin-width (53 s), the polynomial order (N = 6) and the resting activity threshold. B) The isovolumetric measurements performed during the 4 holding phases yielded $RMSE_{iso}$ values of 12.8%, 4.0%, 0.1% and 3.1%, respectively.

3.4.5 Bladder pressure estimation

Considering that the pressure and the volume exhibited a high nonlinear correlation between them, as evidenced by the average Spearman's rank coefficient ($\bar{\rho} = 0.98$), our method was also tested for estimating bladder pressure. To this end it was important to consider that the dynamic responses of the bladder are different for volume and pressure. For instance, in regards to the time-constant, the values for volume are always much higher than for pressure. Therefore, shorter BWs were required for a suitable tracking of rapid changes in bladder pressure.

Most of the pressure measurements exhibited small periodic oscillations during the filling phase produced by spontaneous contractions, despite the low filling rate (0.08 mL/min) used to avoid induced overactivity. We exploited these oscillations to test Pves estimation for rapid pressure changes. For example, Figure 3-14 shows that for a BW of 3 s, the Pves estimation tracks the small contractions with an $RMSE_{Fill}$ of 7% and an $RMSE_{All}$ of 6.9%. These values decreased to 5.1% (1.7 cmH_20) when the Pves was above 10 cmH_2O. Furthermore, it was possible to detect local peaks for each of the contractions.

For longer BWs, the error decreased exponentially, similar to Figure 3-10. However, for BWs greater than half of the oscillation's period (i.e., the corresponding Nyquist frequency), it is no longer possible to track the relatively rapid Pves changes. In the example shown in Figure 3-14, the maximum allowable BW for following the small Pves changes is 3 s. However, if small variations are not relevant for the intended application, one can improve the estimation error by finding an optimal BW that properly tracks the pressure changes of interest. In Figure 3-14, the lowest estimation errors were achieved for a BW of 47 s ($RMSE_{Fill}$ = 5%, $RMSE_{All}$ = 5.2%). Table 3-2 shows the results for Pves estimation with the optimal BW using a regression model with an order of N = 6 computed from all the fiber recordings (n_A = 25, 107 trials). The $RMSE_{All}$ for Aδ-fibers was 6.2 ± 1.6 % and for C-fibers was 6.0 ± 2.5 %. Similar to volume estimation, no significant difference was found ($p > 0.05$).

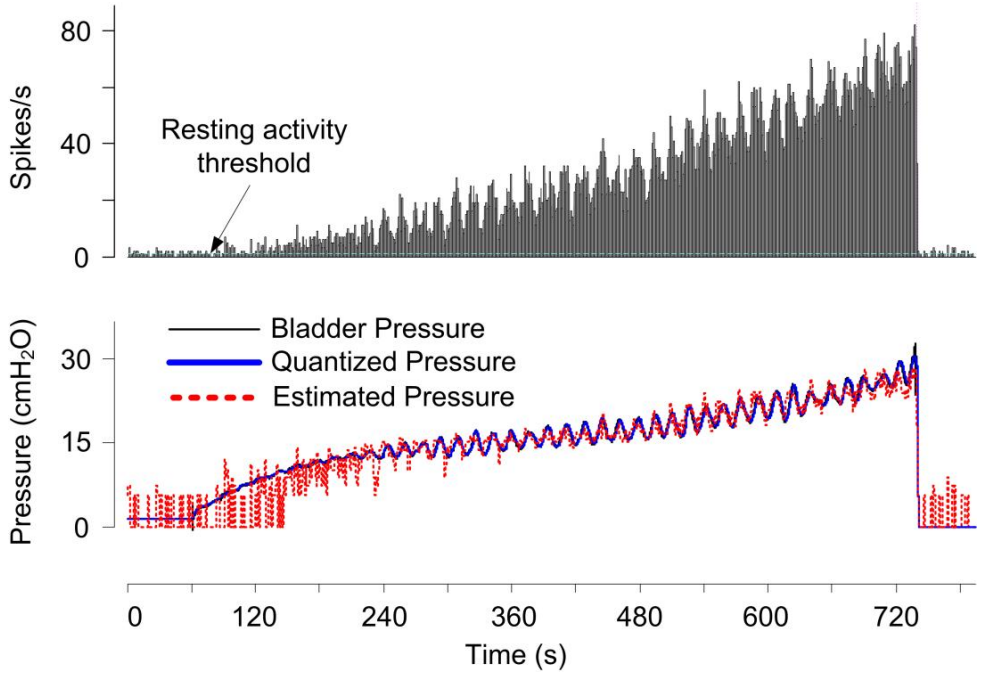

Figure 3-14: Intravesical pressure (P_{ves}) estimation during passive saline filling using profile (A) (Ex. from animal No. 31, Aδ- fiber). This estimation tracks small spontaneous bladder contractions with low errors; $RMSE_{Fill}$ = 7%, $RMSE_{All}$ = 6.9% and *RMSE for* $Pves>10cmH_2O$ of 5% (1.7cmH_20).

Table 3-2: RMS Errors (%) for bladder Pressure estimation by the best BW

	Best Bin-width	Filling phase	Filling phase ($t > t_{thr}$)	All phases	Quantization error
Fitting	36.9 ± 10.9	6.7 ± 2.8	4.1 ± 2.7	6.1 ± 2.3	9.8 ± 3.4
Estimation	36.7 ± 7.1	9.2 ± 4.4	9.7 ± 4.0	9.3 ± 2.6	9.6 ± 2.4

3.5 Discussion

In this study, we demonstrated the feasibility of real-time bladder volume monitoring from afferent activity steaming from bladder mechanoreceptors.

To propose our approach we considered past studies suggesting the presence of volume specific mechanoreceptors in the bladder inner mucosa [30] and the relatively slow dynamic response of the bladder to filling [64]. Our choice of using the bladder mechanoreceptors as primary sensors agrees with a previous study that favored the use of biopotentials from natural sensors as sensory feedback for neuroprosthetic devices [1].

We did not find a statistically significant difference between the computed correlation coefficients for myelinated Aδ-fibers and unmyelinated C-fibers, which agrees with conclusions reported in [110].

The high Spearman's coefficient values obtained after executing the binning process to find the optimal BW, which in several trials yielded the maximum value ($\rho = 1$) for relatively small BWs, may suggest that we recorded afferent activity from units that specifically responded to bladder volume. It is possible that the volume information is encoded as an average sustained activity over a given timeframe.

Some of the dissected fibers identified by electrical stimulation as bladder afferent units did not display a correlation with bladder volume. Recordings from other fibers displayed high sensitivity thresholds during the filling phase, which reduced the estimation accuracy. Such behavior agrees with the results of published studies that show that afferent activity patterns and sensitivity thresholds depend on a variety of factors; e.g., the site where axons arise from the bladder, the female estrous cycle, the chemical properties of the infused liquid [32],[33] and the presence of a spinal cord injury [110], among other factors.

The three qualitative states defined regarding the urgency level allow proper urinary urgency warnings to be issued for emptying the bladder. These states will be sufficient to feed back applications that do not require accurate or closely approximated values for bladder volume. Our approach was inspired by the actual sensations emanated from the lower urinary tract. We are not aware of the amount of volume stocked in the bladder up to the moment it approaches the filling sensation threshold, typically 250−300 mL in humans. However, once this point is reached, it is possible to detect different urinary urgency degrees and also discomfort or pain (on average at 500−600 mL), allowing us to adequately determine when it is time to pass urine [32],[112].

Using qualitative estimation, we could detect these three states of bladder fullness in 100% of cases in which an afferent nerve fiber exhibiting an acceptable value for Spearman's correlation

coefficient ($\rho > 0.6$) was identified. As shown in the confusion matrix, the average classification accuracy of the low state (L) during the training and estimation phases was very accurate and the high volume state (H) was predicted in all the experiments with a sensitivity of 100%. The accuracy classification for the in-between state (M) was considered good taking into account the difficulties to ensure reproducibility of the dissected fibers throughout long experiments. In most of the trials, the errors appeared as estimated state-transitions leading into or lagging the actual transition time for a BW period, eventually reaching the actual state. This estimation method advantageously requires minimal resources for its electronic implementation.

The volume estimation results achieved with the quantitative method were accurate and reproducible enough for chronic monitoring purposes. The errors achieved for estimating the volume during resting, filling and voiding phases surpassed our most optimistic expectations. The mean and standard deviation value achieved with the regression model of $RMSE_{all}$ was 5.8 ± 3.1%, which is equivalent to as much as 25.4 ± 13.5 μL ($\bar{V}_{max} = 438\mu L$). This is difficult to attain even with standard instrumentation other than precision weighing balances used for calculating volume gravimetrically. If the quantization error (10.0 ± 2.7%) is added to account for a special case where the instantaneous volume is required rather than the mean value during the last seconds, the estimation is still considered fairly good, in view of the inherent difficulties of such measurements.

The estimation methods proposed do not require a specific fiber type, but rather a fiber displaying good correlation with bladder volume and preferably low sensitivity threshold.

Several studies have discussed whether it is possible to detect bladder tonic responses related to fullness. For instance, in [88], the authors conclude that for high values of Pves it is possible, whereas in [87], the authors favor detection of phasic responses. The isovolumetric measurement trials performed using profile (C), show that we can accurately quantify different levels of tonic responses produced by the bladder mechanoreceptors, especially for volumes beyond the sensitivity threshold. Therefore, our method is able to detect both the phasic responses during gradual filling and tonic responses during the isovolumetric phase.

The volume estimation performed in the passive withdrawing phase in the experiments performed using profile (B) shown that bladder mechanoreceptors are capable of measuring volume during slow filling and slow voiding phases. On the other hand, comparison of the errors

for volume and pressure compiled in Table 3-1 and Table 3-2, respectively, show that estimation was more accurate for volume than for pressure, which once more suggest the existence of mechanoreceptors that specifically respond to changes in bladder volume. Further experiments, which are beyond the scope of this study, should be performed to ascertain, conclusively, this possibility.

We are presently working toward the electronic implementation of the method presented in this paper. A challenging task is the unsupervised real-time detection, classification and decoding of spikes produced by the afferent units identified during the training phase. We are optimizing new detection and discrimination approaches to perform these tasks in an implantable electronic system. Such a system should show a low-power consumption to be feasible [116],[117]. Previous studies have suggested that electronic implementation of the spike sorting process will be feasible [35]. It is worth noting that most of the existing methods are not well adapted to run unsupervised in real-time. Those that are rely on complex algorithms that represent a heavy burden even for powerful personal computers [111]. Once the electronic device is ready, chronic experiments will be carried out in larger animal models.

3.6 Conclusion

We have demonstrated that it is possible to estimate bladder volume from mechanoreceptor activity recorded at specific spinal roots that convey signals from bladder afferent nerves. The proposed method is reproducible and accurate for qualitative and quantitative determination of bladder volume when the recorded afferent activity exhibits an acceptable Spearman's correlation coefficient. We have also shown that both phasic and tonic responses related to bladder activity can be detected.

3.7 Acknowledgment

The authors would like to thank Laurent Mouden for his support to development of initial experiments.

CHAPTER 4 DEDICATED ON-CHIP PROCESSOR FOR SENSING THE BLADDER VOLUME THROUGH AFFERENT NEURAL PATHWAYS

In this chapter, the paper that describes the design and validation tests of a dedicated digital signal processor (DSP) that execute on a single chip the bladder volume decoding method described and validated in the preceding chapter is presented. To perform the decoding method, the DSP detects and discriminates the action potentials of the recorded signal in real-time. This process is also known as on-the-fly spike sorting. Once the neural source is identified, the DSP runs the decoding method depending on the output mode. It is shown, for the first time, that is possible to perform both the on-the-fly spike sorting and the neural decoding task entirely on-chip without any external support.

The general architecture and workflow showing the operation mode of the DSP is presented first for a global understanding of the system function. Afterward, the architecture and operation of each of the processing blocks are described in separate sections. At the beginning of each of these sections, the problems and challenges to be overcome, as well as the alternatives that can meet the system requirements, are discussed, and the most suitable solution for implementing the digital electronic circuits is chosen. The following signal processing blocks are described: the spike detector block that detects a spike over the background noise using a non-linear energy estimator and an adaptable threshold circuits; the spike classification block that determines the class of each detected spike; the spike-rate integrator that integrates the spike-event frequency over a given time-window; and finally, the volume decoding block that implements both volume estimation methods with optimally designed circuits. The validation tests for each of these modules are presented along with illustrations of the representative results for the spike detection, classification and volume estimation. These tests used realistic synthetic signals and real signals from neural recordings during the acute experiments with animal models presented in Chapter 3.

The good performance results for each of the circuits and the whole DSP system during these validation tests confirmed the electronic feasibility of the implantable bladder sensor that deploys the proposed method. Therefore, our hypothesis H2 was validated.

The DSP of the bladder sensor presented in this chapter will be a part of a neuroprosthetic device researched in the Polystim Neurotechnologies Laboratory. As shown in Figure 4-1, the bladder sensor provides the feedback required to implement a closed-loop system that can perform conditional neurostimulation depending on the bladder volume or pressure.

The DSP will be integrated later with a custom hybrid circuit that performs the analog signal conditioning (amplification, filtering and analog-to-digital conversion) and then packaged in an implantable device together with the neurostimulator control unit, the stimulator driver that runs the neurostimulation approach chosen, and the wireless data/power interface, which recovers energy and exchanges data in both directions with the external unit. This latter is intended for the following uses: user interface during the normal operation of the neuroprosthesis, wireless interface during the settings loading in the implanted device, and the interface with an external PC during the training phase.

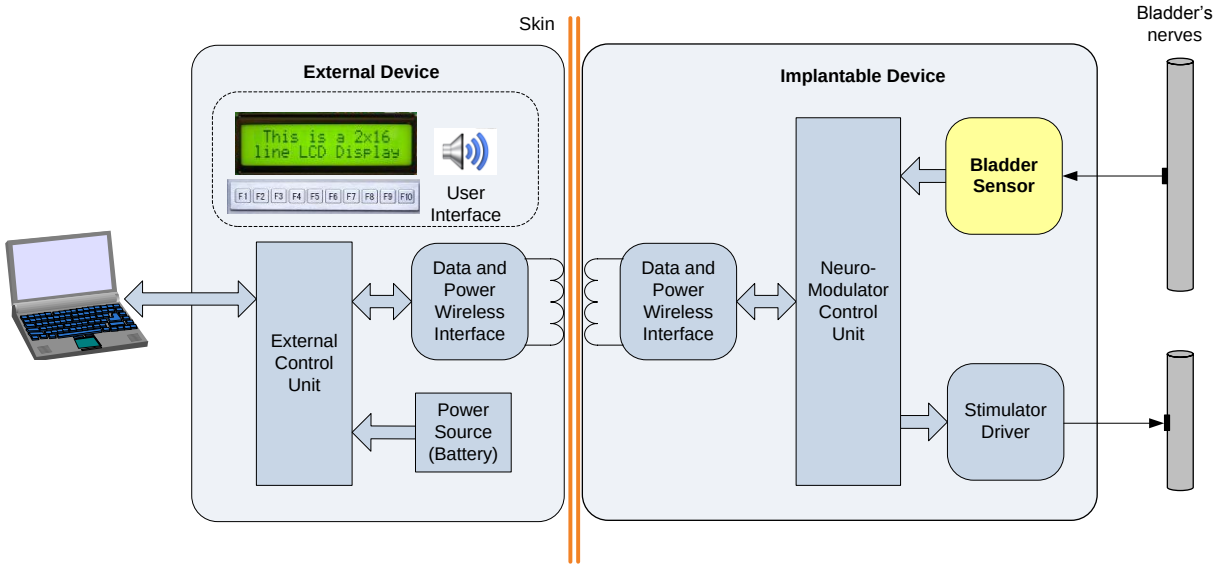

Figure 4-1: Schematic of the general architecture of the Polystim neuroprosthetic device intended to restore the storing and voiding functions of the urinary bladder in paraplegic patients.

Dedicated On-chip Processor for Sensing the Bladder Volume through Afferent Neural Pathways

Arnaldo Mendez[1], *Member, IEEE*, Abrar Belghith[1,2], Mohamad Sawan[1], *Fellow, IEEE*

[1]École Polytechnique, Montreal, Canada; [2]Enseirb-Matmeca, Bordeaux, France.

(Submitted for publication in IEEE Transactions on Biomedical Circuits and Systems, May 2013)

Abstract— In this paper, we present a dedicated digital signal processor (DSP) capable of monitoring the urinary bladder volume through afferent neural pathways. The DSP carries out real-time detection and can discriminate extracellular action potentials, also known as on-the-fly spike sorting. Next, the DSP performs a decoding method to estimate either three qualitative levels of fullness or the bladder volume value, depending on the selected output mode. The proposed DSP was tested using both realistic synthetic signals with a known ground-truth, and real signals from bladder afferent nerves recorded during acute experiments with animal models. The spike sorting processing circuit yielded an average accuracy of 92% using signals with highly correlated spike waveforms and low signal-to-noise ratios. The volume estimation circuits, tested with real signals, reproduced accuracies achieved by offline simulations in Matlab, i.e., 94% and 97% for quantitative and qualitative estimations, respectively. To assess feasibility, the DSP was deployed in the Actel FPGA Igloo AGL1000V2, which showed a power consumption of 0.5 mW and a latency of 2.1 ms at a 333 kHz core frequency. These performance results demonstrate that an implantable bladder sensor that perform the detection, discrimination and decoding of afferent neural activity is feasible.

Index Terms—Biomedical transducers, Biomedical monitoring, Neural prosthesis, Biomedical signal processing, Bladder volume.

4.1 Introduction

Neuroprosthetic implants can be used to restore urinary functions in patients who suffer from spinal cord injury (SCI) or neurological conditions that affect sensations and the voluntary control of the bladder necessary to store and void urine properly. Millions of people around the world suffer from bladder dysfunction [118]. Untreated urinary dysfunctions can lead to serious health deterioration. For instance, urinary retention can result in renal failure, and incontinence can severely affect the quality of life [25].

The overall effectiveness and safety of an implantable neuroprosthesis can be improved by sensing the bladder volume and pressure to adapt the functional electrical stimulation (FES) to the ongoing bladder state [1]. This approach, known as conditional stimulation, requires feedback to create a closed-loop system [8]. To the best of our knowledge, none of the implants currently used in clinical practice to treat urinary dysfunction are capable of performing conditional stimulation.

After a comprehensive study to choose the best method for monitoring the bladder activity, we concluded that natural sensors, rather than artificial sensors, are best suited for chronic applications [36]. We have proposed a new method to sense the bladder volume and pressure by using the afferent neural activity stemming from bladder mechanoreceptors that respond to stretching during bladder filling and voiding [37]. In this paper, we show only the results for the bladder volume. The bladder pressure estimation uses the same method and hardware implementation but with different parameters. The measurement method was specially designed to be deployed in an electronic sensor that provides feedback to an implantable neuroprosthetic device that is intended to restore autonomously the bladder functions. Such a sensor should be able to record, detect and decode sensory neural activity in real-time, with low-power consumption.

Neural signal processing begins with a front-end recording stage that amplifies microvolt level signals and filters out undesired background noise and local field potentials (LFP). The signal contains extracellular action potentials, known as spikes, from different neurons. Subsequently, the spikes should be detected and classified into different classes, a process known as spike sorting, to identify the activity source.

Several authors have previously published results showing continuous improvement on the performance of the front-end processing stage using Application Specific Integrated Circuits (ASICs) [119-123]. These ASICs envisaged different applications requiring Brain-Computer Interfaces (BCIs), and other interfaces with the peripheral neural system, that can record signals using different types of Multi-Electrodes Arrays (MEAs) [124],[94].

Lately, an increasing number of authors have incorporated on-chip preprocessing, which was usually performed at the back-end stage [116],[125-134]. The primary modifications introduced were that the front-end preprocessing was extended to include the on-chip spike detection, features extraction, and wireless transmission of the isolated spike, the spike features, or both. However, we found few works that tackled the on-chip classification of the detected spikes in real-time [96],[135],[136]. It is worth mentioning that in some of the works that reported spike sorting capability, only spike features extraction with off-chip classification using a personal computer (PC) were realized. We did not find any work reporting on-chip, real-time neural signal decoding. However, both system capabilities, i.e., the spike sorting and sensory decoding, are essential for the standalone operation we are looking for a bladder neuroprosthetic implant that do not require the transmission of any data to an external unit nor the reception of corresponding commands to function properly.

This may be because most of the existing methods for full spike-sorting and sensory activity decoding are not well adapted to run unsupervised in real-time [137]. Those that are rely on complex algorithms, which represent a heavy burden, even for powerful PCs. In addition, devices implanted on the cortex must comply with a maximum allowed power density to avoid tissue damage. The upper limit assumed for some authors was 80 mW/cm^2, initially reported in [138]. However, there is not enough research to accurately establish that this is the upper limit in the Central Neural System (CNS) [139]. Most of the long-term studies have shown that a 2°C temperature increase of 40 mW/cm^2 heat flux, with 1.6 mW/g of the specific absorption rate (SAR, a measure of heating produced by the electromagnetic field in tissue), is suitable for most tissues in the body.

We envisage a standalone bladder sensor that also includes a full back-end stage. The sensor will receive the initial settings and send back to the external unit only the signal conveying information about bladder fullness state (low, medium, or high volume/pressure) and, if required,

the volume and pressure values. To this end, both the front- and back-end stages need to be fully deployed in a device that can be conveniently implanted in the trunk near the bladder.

The feasibility of the analog front-end stage has been well demonstrated, including research performed by members of our research group [123]. We have performed this research toward the implementation of a standalone bladder sensor (BS) to assess the feasibility of an implantable back-end system performing the full spike-sorting process and the sensory signal decoding in real-time with low-power consumption. To the best of our knowledge, this will be the first on-chip system performing all these tasks autonomously.

4.2 Bladder sensor deployment

Bladder sensor deployment using an analog back-end processing stage would be highly complex with very limited functional capabilities; therefore, we have chosen a digital signal processing (DSP) approach. The available choices to implement our measurement method are DSP processors, microcontrollers (MCUs), programmable logic, and ASICs.

We have to meet real-time and power consumption constraints and, when needed, improve the system in a fast and cost-effective way. General purpose DSPs and MCUs provide great flexibility but require the large hardware architectures typical of these programmable devices. In contrast, ASICs offer the lowest power consumption due to an optimal use of resources but do not allow fast and cost-effective changes. To account for this trade-off, we chose to deploy our system in a low-power Field Programmable Gate Array (FPGA). This technology enables a more frugal deployment of our custom-logic system, but, unlike ASICs, FPGA balances flexibility and the ability to accommodate design changes during the ongoing R&D process. In addition, the custom-logic approach ensures high reliability and fast response times [140].

The back-end DSP proposed for the BS uses the modular architecture depicted in Figure 4-2A, which allows for optimal maintenance times and the possible reuse of some of the inner modules in other applications. The flowchart in Figure 4-2B shows the main functions performed by the DSP in real-time, which are described in the following sections.

4.2.1 Overall system description

The volume measurement method deployed by the DSP need an input signal from one recording channel that contains at least one neural unit with action potentials from bladder mechanoreceptors exhibiting a Spearman's rank correlation coefficient of 0.6 or better [37]. All of the required parameters for real-time operation of the DSP are determined in an offline training phase using custom-written software in Matlab, Mathwork Inc., MA, USA. During the training phase, a spike sorting process is performed to identify all of the units present on the recorded channel and subsequently spikes waveform templates are computed. The sorted unit exhibiting the best neural activity correlation with the bladder volume is selected for subsequent processing. Next, the baseline of the mechanoreceptors resting activity is determined and an optimal binning process allows finding the binwidth (t_{bw}) that yields the lowest volume estimation error. Finally, the parameters needed for quantitative and qualitative volume estimations are computed and transferred to the DSP. The DSP can detect in real-time performance deterioration to request recalculation of the parameters when needed.

The DSP can operate in two modes: a spike-capture mode used during the training phase, and a processing mode for real-time estimation of the bladder volume or pressure. The whole DSP is driven by the implanted Neurostimulator Control Unit (NCU) and uses the same power supply as the implanted device. The NCU starts the DSP and sends all of the initialization settings required for real-time standalone operation. It is also accountable for relaying data, such as the captured action potentials from the DSP during the training phase, the performance warnings, and the output signals, to the external unit. This latter is intended for the following uses: user interface during the normal operation of the neuroprosthesis, wireless interface during the settings loading in the DSP through the NCU, and the interface with an external PC during the training phase.

The amplified, band-pass filtered and digitized neural signal is continuously fed to the Spike Detector Block (SDB). This signal contains the action potentials (spikes) from all of the neurons close to the selected microelectrode tip (channel). To avoid the need for an input buffer and to provide fast response times, the input signal should be processed within the detected spike time-window of 2.5 ms. Therefore, we have chosen 2.5 ms as the system response-time constraint.

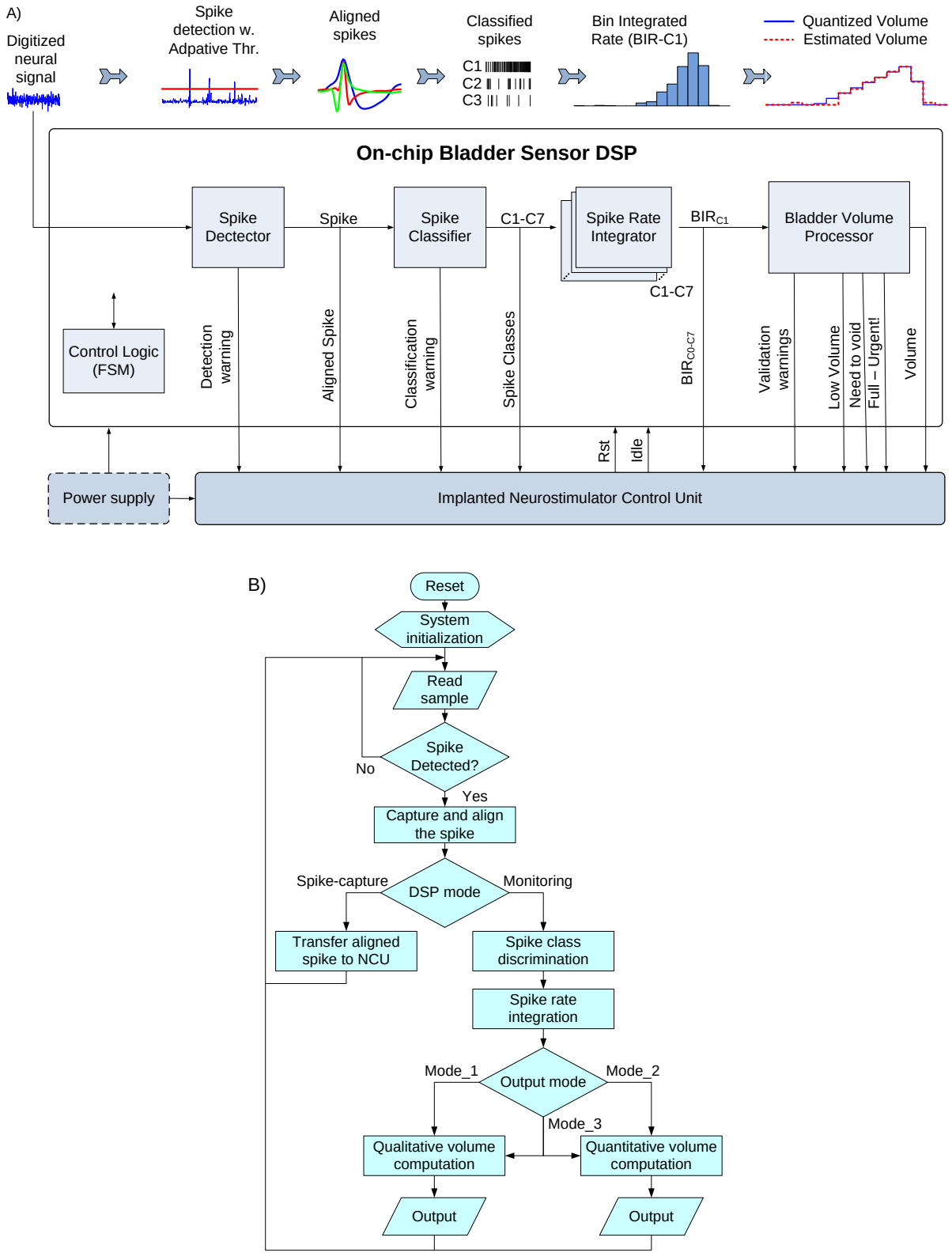

Figure 4-2: Bladder volume sensor. A) DSP system architecture. B) Flowchart of the DSP main functions.

The SDB improves the signal-to-noise ratio (SNR) and adaptively adjusts the detection threshold for a robust detection of the spike over the remaining background noise using a non-linear energy estimator and a moving averaging filter, both described in section 4.2.2.B. The spike is then isolated and aligned using its maximum absolute value within a window of fixed duration. The aligned spike is fed to the next processing block or relayed through the NCU to the external unit during the training phase.

The Spike Classifier Block (SCB) can discriminate up to seven different spike classes (C1 – C7) by computing the weighted distance to the stored templates of each class. The number of spikes classes was chosen considering the foreseen number of neural units that can be recorded in the experiments of our ongoing research and also the reusability of this block in other applications that implement multivariate (multiunit) estimators. One of the eight SCB binary outputs is set to signal the detection of the corresponding spike class. Class 1 (C1) is reserved for the spikes stemming from the neuron that was identified during the training phase as the unit conveying suitable sensory information from the bladder.

The SCB can detect an eventual deterioration in classification quality due to changes in the recorded neural signal over time. To this end, class 0 (C0) is reserved for pre-classified spikes with a distance exceeding the minimal quality criteria set for each class. If the number of spikes reclassified as C0 during a given period (e.g., 60 s) is greater than an established limit, then the flag ‘Spike Detection Failed’ is set and the NCU relays the warning to the external unit. Subsequent signal processing would be aborted until the problem is addressed. The solution could be as simple as changing one parameter, e.g., varying the step size used by the adaptive threshold detector; otherwise, a new training process should provide adjusted settings to match the new conditions.

The bladder volume (or pressure) measurement method deployed by this DSP is based on processing neural information using time-windows, hereafter referred to as bins, of a programmable duration (bin-width).

The Spike Rate Integrator Block (SRI) integrates (counts) the number of the spikes of the selected class (C1) during the programmed bin-width. In the current application, only one SRI for class C1 is required to feed the next block with the Bin Integrated Rate (BIR_{C1}). Up to six

additional counters could eventually be implemented in applications with a decoding method that requires information from more than one neuron.

The last signal processing stage is performed by the Bladder Volume Decoder Block (BVD). This block can operate in three modes: a qualitative volume estimation output (Mode-1), a quantitative volume estimation output (Mode-2), and a combined mode, in which both estimated volume outputs are computed (Mode-3). The qualitative and quantitative methods were fully described and demonstrated in a previous study conducted by our group [37].

In Mode-1 the BVD outputs three qualitative values of bladder fullness that can be used to trigger the neurostimulation or to warn the patient. These binary outputs can indicate low-volume (comfortable level), medium-level (need- to-void within some predefined time), and a full-level (urge to void or a risk of imminent leaking). Correspondingly, three different thresholds can be set as needed. We set the thresholds to a quarter, a half and full bladder capacity, as previously determined by cystometric measurements. The definition of the states and the corresponding fractions were set based on the sensations arising from the lower urinary tract in humans [37],[112], i.e., an undetectable bladder sensation due to a low-urine volume stocked, the filling sensation threshold typically at 250−300 mL, and the detection of urinary urgency, discomfort or pain, which occurs, on average, at 500−600 mL.

In Mode-2, the BVD computes the bladder volume using a regression model of programmable order, with coefficients computed offline during the training phase. Mode-2 is also suitable for feedback purposes and for monitoring applications where an accurate value is required, such as long-term follow-ups for clinical purposes and research studies.

The Control Logic Block (CLB), implemented by a Finite State Machine (FSM), drives the signal processing workflow and receives the settings through the NCU.

The NCU sends the initial Reset and can set the DSP in an Idle state for maximum power savings. The design and implementation of the NCU, which will control the entire neuroprosthetic implant (including the BS and stimulator), wireless data transmission and power supply recovery from an external source, are beyond the scope of this research.

The optimal number of bits required for accurate fixed-point arithmetic operations was chosen as 32 bits based on simulations performed in Matlab/Simulink using the fixed-point toolbox.

4.2.2 Spike Detector Block

Several spike detection methods used in previous studies were analyzed for use in the SDB. The considerations included the effectiveness, the operational performance in real-time, and the complexity of the custom-logic required to deploy each method. Two methods stood out with the given design criteria: Absolute Thresholding Detection (ATD) [111],[141], which is applied directly on the raw but filtered signal, and the Teager (Nonlinear) Energy Operator (indistinctly termed TEO or NEO) [127],[142-147], which preprocesses the signal before the spike detection by using simple thresholding.

Based on published results and considering our own tests outcomes, we chose NEO signal preprocessing to improve the robustness of the spike detection in a non-stationary, noisy environment, such as those which this application should withstand. NEO is a simple but effective operator introduced for digital signal processing by Kaiser et al. [148] that estimates the instantaneous energy of the signal. NEO emphasizes the spike over the background noise, thereby significantly increasing the SNR.

In SDB deployment we used a modified equation (4-1) of the original NEO that we termed kNEO, where the constant k was chosen as 2.0. In (4-1), $\psi[x(n)]$ is the estimated instantaneous energy and $x(n)$ is the input neural signal at the *n*-sample. This modification further improves the SNR of the spikes in the lower frequencies and consequently the probability of their detection is increased.

$$\psi[x(n)] = x^2(n) - x(n+k)\,x(n-k) \tag{4-1}$$

The background noise level of the recorded signal can vary due to interference from other signal sources in the body, external sources, or other factors [111]. Therefore, a robust spike detector should be able to adapt the detection threshold depending on the ongoing signal noise.

One approach to set the threshold to detect the spikes over the background noise is to use a scaled value of the signal standard deviation [149]. This approach may lead to threshold values that increase with the spike rate and the spike amplitude. An improved version that uses the median for estimating the noise significantly reduced this problem under the assumption that the spikes amount to small fraction of all samples [111]. However, the median filtering is not well

adapted to run in real-time and needs large buffers to store the signal over a given period of time. The estimation of the noise level and finding the adaptive threshold by computing the RMS of the NEO signal has been reported to yield good results [147]. Nevertheless, the RMS calculation also needs an input buffer and several operations for each incoming sample.

After running simulation tests using signals with different SNR and giving consideration to the number of operations and the memory size required, we chose a first-order exponential average filter defined by equation (4-2) to extract the estimated noise level *y(n)*. This filter only requires storing the last output and a few mathematical operations. The coefficient (*a*) was computed using a time-window (*t*) of 100 ms with a sampling frequency (f_S) of 24 kHz.

$$y(n) = C(\psi(n) + a\,[y(n-1) - \psi(n)]\,), \tag{4-2}$$

$$a = e^{-1/f_s\, t}$$

The detection threshold (*Thr*) was set to a scaled filter output using a scaling factor (*C*) as shown in (4-3). This factor is determined experimentally by finding the value with the highest probability of detection (P_D) and the lowest probability of false alarms (P_{FA}) while *C* is swept from 1 to 100 with steps of 0.5. The *C* factor is computed offline and stored in DSP registers with the other parameters.

$$Thr(n) = C\; y(n) \tag{4-3}$$

In Figure 4-3A we depict the SDB architecture using the kNEO pre-processor with adaptive thresholding that depends on the ongoing background noise, whereas the main functions workflow driven by the FSM is shown in Figure 4-3B. The input signal of M bits (M = 32) is fed to both the Delay-(D)-states shift register bank (D = 26) and the kNEO processor module (kNEOP) that improves the SNR and sets the 'Spike Detected' flag (SDF) when a spike surpasses the threshold, as computed by the Adaptive Threshold Block. The shift-register bank delays the signal to keep it synchronized with the kNEOP output. This shift-register also stores the samples before the spike amplitude goes above the detection threshold to avoid missing the initial part of

the spike and allow for kNEO computation using future samples. The activation of the SDF starts the FSM process for transferring T samples (T = 72) to the Captured Spike FIFO. Next, the captured spike is fed to the Peak Detector Block to find the absolute peak and its corresponding offset within the T-samples window. This block outputs the Spike Peak Offset (SPO) and sets the 'Peak Detected' flag (PDF). Using the SPO, the Align Spike Block transfers the samples preceding (N_p = 20) and following the absolute peak (N_f = 44) to the next block input-FIFO. In this way, the aligned spike is fitted to a window of N samples ($N = N_p + N_f = 64$).

Once the alignment process has been completed, the 'Spike Ready' flag (SRF) is set, which in turn reset the SDF and PDF flags. The SRF is reset when the aligned spike is transferred, clearing the block for the processing of the next spike. Finally, a watchdog timer is used to monitor spike detection. If no spike is detected during a given period of time, e.g., due to signal recording problems or a threshold set too high, a warning is issued to the NCU to signal the problem. Subsequently, the NCU will acknowledge the problem and run a subroutine to address it, for example, by changing the step used in the threshold self-adjusting circuit. If the problem persists, the NCU can send a code error to the external unit that will properly advise the patient or the physician about the recording problem that must be addressed.

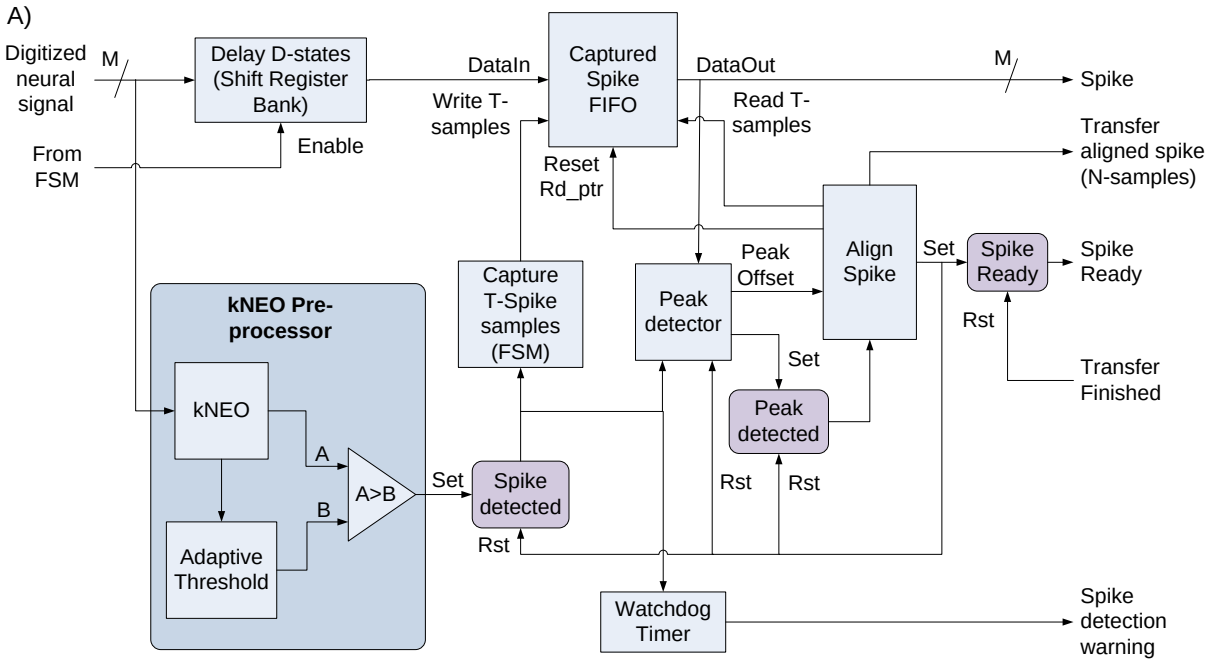

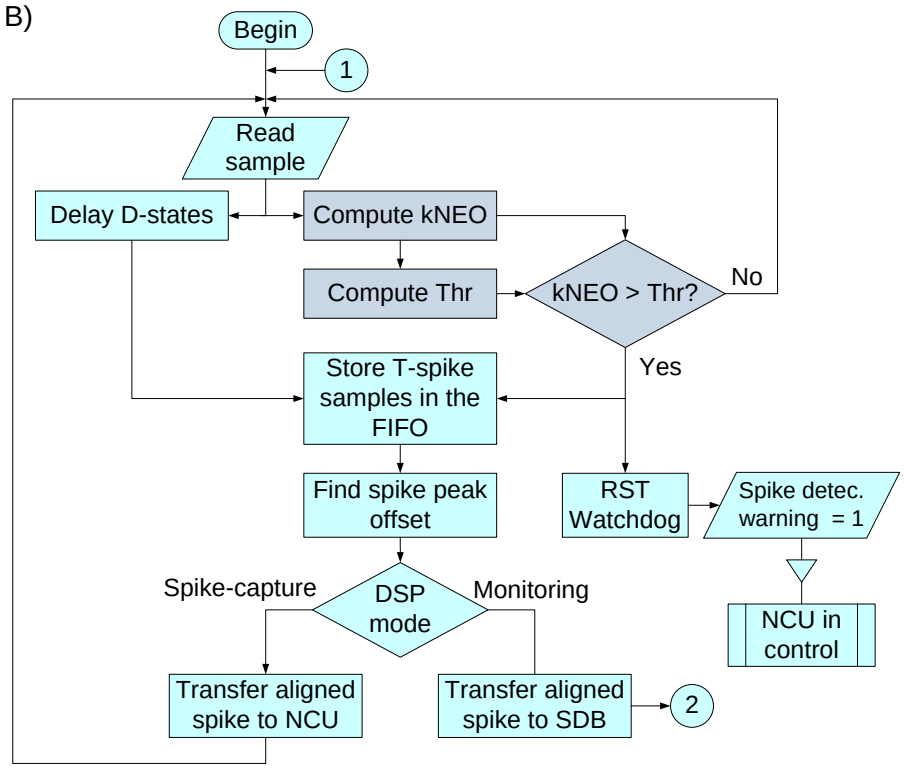

Figure 4-3: Spike detector block (SDB). A) Circuit architecture. B) Flowchart of the SDB main functions.

4.2.3 Spike classification block

We performed an exhaustive literature review to identify algorithms best able to be implemented with custom DSPs that met our constraints on low-power consumption and real-time processing. As in [135], we also found that on-chip spike classification had not been addressed in previously published works, most likely due to the complexity of the algorithms required for deployment with a power consumption/power density within allowable limits.

Many approaches have been proposed for spike classification with different degrees of accuracy, speed and complexity. A useful review of the advantages and limitations of the most common spike classification algorithms used in the past can be found in [150] and [137]. Most of them require spike feature extraction and subsequent dimensionality reduction before the clustering process. Such is the case of the most popular approach used for spike sorting, Principal Component Analysis (PCA) for feature extraction and *K-Means* for clustering. This was the method used by the only study we found implementing the full spike sorting process on-chip, which employed the off-the-shelf embedded system Smartdust iMote2 [135]. However, several

authors have demonstrated that the PCA and *K-Means* spike-sorting method required significant resources and time [146]. Additionally, its classification accuracy has been shown to be lower than other methods [111],[128],[146],[151],[152]. In particular, the power consumption and the latency achieved by a spike sorter module for one channel are still relatively high in the iMote2 spike-sorting implementation [135]: 87 mW and 9.2 ms, respectively. There are no results regarding the classification accuracy achieved.

Neurons from the same class generate the same waveforms [46]. Although the recorded spikes are not identical due to background noise, tissue homogeneity, and electrode properties, among other factors [46], the recorded spikes exhibit waveforms that tend to match patterns in different degrees [152]. Therefore, the algorithms based on template-matching analysis can yield good classification accuracies when the proper spike features or patterns (templates) are chosen [150],[152]. With this method, spike classification is achieved by finding the minimal distance between the features of the unclassified spike and each of the stored templates (the nearest-neighbor clustering method) or by using more complex and robust methods to address bursting neurons, electrode drift, overlapping spikes, and so on, such as Bayesian clustering [150] and superparamagnetic clustering (SPC) [111].

The Euclidean Distance (ED) is the simplest metric that can be used in template matching, but the classification performance decreases when the clusters are elongated and close to each other [152]. In contrast, the Mahalanobis Distance [153] is a metric that takes into account the shape, size, and orientation of the clustered data, thus yielding a better classification accuracy. However, this metric requires the computation of covariance matrices and other mathematical operations, which implies a heavy computational burden and requires significant processing time.

Considering the above arguments, we chose to deploy a spike sorting method comprised of two phases: 1) an offline training phase to be executed in an external computer with the spikes recorded using the implanted system and 2) a real-time unsupervised classification phase to be deployed in the DSP (SCB). During the training phase, the most suitable algorithms can be executed regardless of their complexity to obtain the best templates and parameters.

For the training phase, we used software that was custom-written in Matlab to perform signal filtering followed by spike detection and alignment. For clustering, we used the superparamagnetic function provided by Waveclus [111]. The training phase outputs are the

number of classes and the spike templates, which were computed by averaging all of the spikes from the same class.

For the real-time spike sorting phase, we used lower complexity and a much faster approach, the template-matching method with the Weighted Euclidian Distance (WED) metric shown in equation (4-4). This method does not require an online computation of the covariance matrices and addresses the above mentioned drawbacks of the ED.

In (4-4) S_j is the N-dimensional vector of the spike to be classified (j = 1,...,N), $P_{i,j}$ is the template matrix (i = 1,...,p, p: number of templates/patterns), w_j is the vector of weights, and Δ_{Ci}^2 is the squared WED computed between the spike *S* and the template *P* of class *i*.

$$\Delta_{Ci}^2 = \sum_{j=1}^{N} w_j \left(S_j - P_{i,j}\right)^2 \tag{4-4}$$

We faced the problem of whether it was advantageous to perform the spike features extraction followed by a dimensional reduction or to exploit all available dimensions, i.e., the spike samples (N = 64). After analyzing the various advantages and the results of simulations in Matlab, we decided to use all of the spike samples without feature extraction, which also favors classification accuracy [150]. Because we used custom logic to implement the SCB, both the amount of resources needed for SCB implementation and the processing time were lower in our approach without feature extraction compared to those needing it.

We sought to set the weights so that they emphasized the dimensions where the template differences were significant (usually in the vicinity of the main peak) and in turn minimized the contribution of the dimensions where the differences tended to be non-significant and contaminated to a greater degree by background noise (usually towards both ends of the spike).

To find the vector of weights (w_j) that meet our requirements, we compute the vector of the variance in each dimension of the spike templates (σ_j^2) and next we normalize σ_j^2 by the maximum value for all dimensions, i.e., *max* (σ_j^2).

The spike class (i) is determined by finding the minimal distance (Δ_{Ci}^2) between the spike *S* and the template *P* of class *i*. Subsequently, the spike class is validated by comparing it with the maximum value admitted for each class. If the distance is over this value, then the spike is

reclassified as Class-0 (C0), i.e., the undefined class. The distance allowable values are determined experimentally.

In Figure 4-4A we show the architecture of the SCB implementing the real-time spike classification method described above, whereas in Figure 4-4B, the main functions workflow driven by the FSM is shown. During the block initialization, the templates of all possible spike classes to be identified and the vector of weights are stored in the corresponding FIFO memories. The WED validation limits are also loaded in the Class Validation block. The input to the block is the aligned spike stored by the preceding block (SDB) in the input FIFO. The FSM runs all of the states required to compute the WED, finds the minimal value and sets the preliminary spike class, all of which is performed by the Class Detection block. Next, the FSM executes the class validation in the Class Validation block. This latter check whether, over a given time period, the number of spikes classified as Class-0 is greater than the allowable limits. In such a case, the warning flag 'Spike Classification Warning' is set as a notification that corrective actions are required. The last block, the DEC, generates a short pulse in the corresponding output for each spike class when the FSM activates the signal Output_Class, so that a spike raster is generated for each channel.

4.2.4 The Spike Rate Integrator Block

The SRI block integrates (counts) the number of spike events occurring within a time-window (bin) of a given duration (bin-width, t_{bw}). The optimal t_{bw} is found during the training phase, stored as parameter and transferred to a timer during the system initialization. Therefore, only a counter (14 bits) and the timer for fixing t_{bw} (1–60 s) are required for each decoding channel. To estimate the bladder volume in this application, only one SRI output is needed (BIR_{C1}).

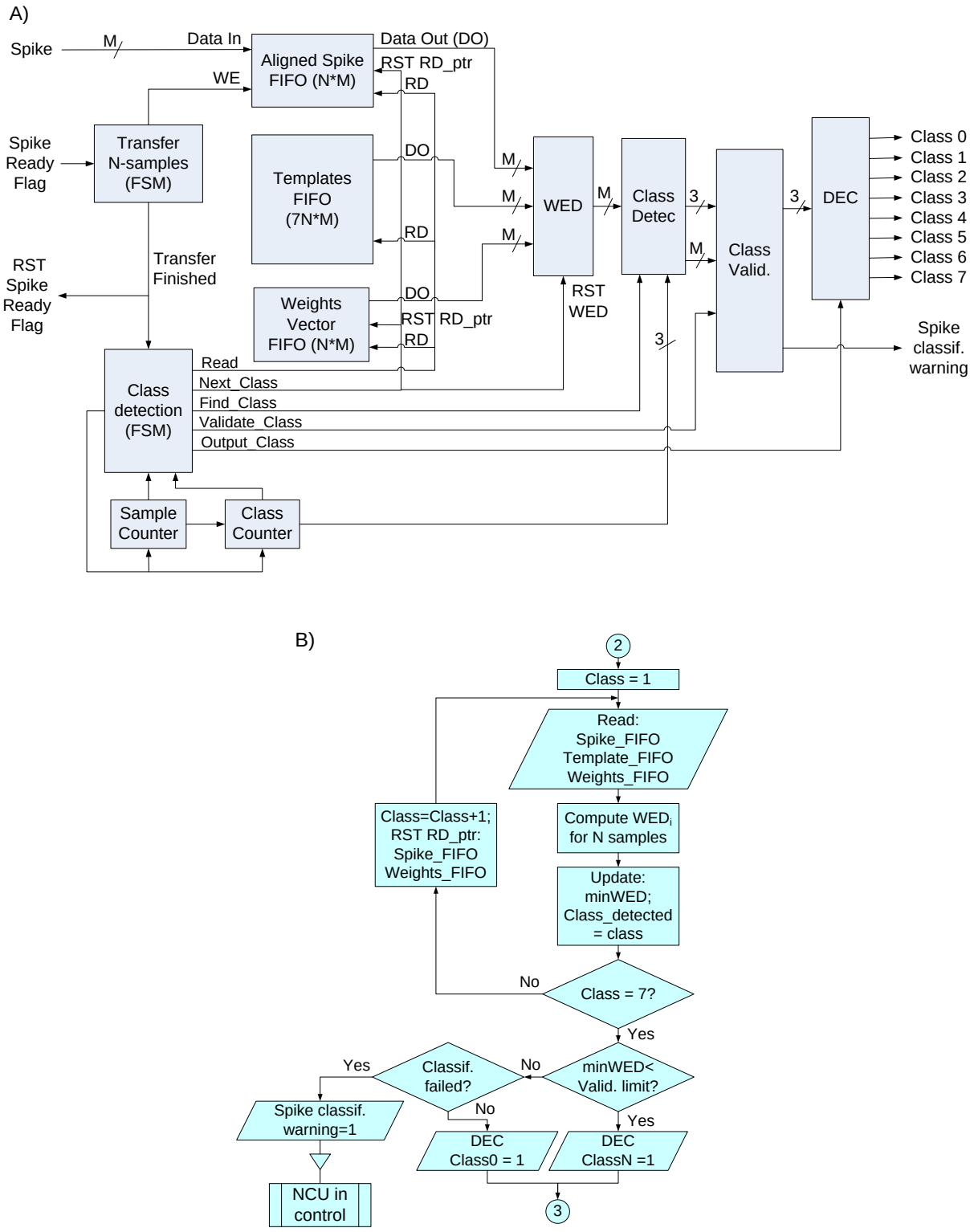

Figure 4-4: Spike classification block (SCB). A) Circuit architecture. B) Flowchart of the SCB main functions.

4.2.5 Bladder Volume Decoder Block

The BVD block is composed of two circuits deploying the decoding methods introduced in section 4.2.1; one for the qualitative volume estimation depicted in Figure 4-5A and another for quantitative volume estimation depicted in Figure 4-5B. Figure 4-5C shows the workflow of both circuits driven by the FSM.

4.2.5.1 Qualitative volume decoding

To implement the qualitative method (Figure 4-5A), three reference fractions of bladder fullness are set as 0.25, 0.5 and 1.0 times the maximum bladder functional capacity. Each fraction corresponds to one of the states defined earlier in section 4.2.1 as low-volume (L), need-to-void (medium, M), and full level (high, H). The three BIR reference values (BIR_{ref}) corresponding to each fullness state (i.e., BIR_0, BIR_1, and BIR_2) are computed during the training phase, and transferred to the BIR_{ref} registers (Figure 4-5A) during system initialization.

The circuit of Figure 4-5A implements the qualitative volume estimation by finding the *arg min* of the absolute difference among the BIR_{C1} and each BIR_{ref}, as shown in (4-5). To reduce the amount of hardware and better meet the real-time latency constraint, only one adder, which was configured to perform subtraction, is used. The FSM feeds the BIR_{ref} input one value at a time and the *arg min* block outputs the offset (0, 1, or 2), which corresponds to the minimal absolute difference. Finally, the Decoder (DEC) activates the binary output corresponding to the bladder fullness state estimated at t_{bw}-intervals.

$$arg\ min_{i\in[0,2]}\ \{|\mathrm{BIR_{C1}}\ -\ \mathrm{BIR_i}|\} \tag{4-5}$$

The output validation logic monitors the three states of bladder filling following the expected order during a filling-voiding cycle, i.e., low, medium and high. If the expected order is not followed, an event counter is updated. When 10 events have been counted, the signal 'Validation_warning_1' is issued.

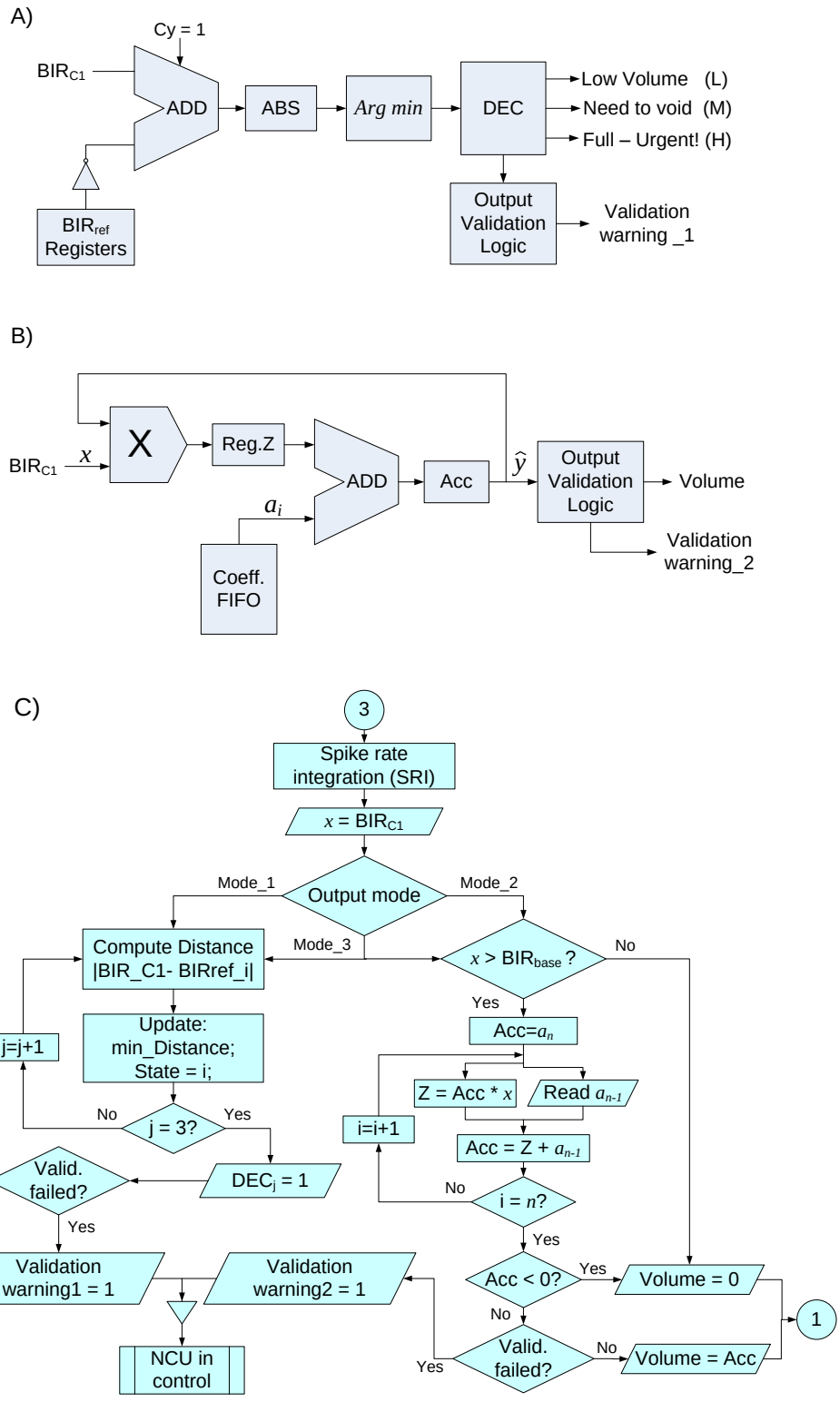

Figure 4-5: Bladder volume decoding (BVD). A) Qualitative estimation circuit. B) Quantitative estimation circuit. C) Flowchart of the BVD main functions.

4.2.5.2 Quantitative volume decoding

The quantitative volume estimation is achieved by a regression model based on a polynomial of order *n* shown in (4-6). We applied Horner's method to reduce the number of operations, the hardware burden, and the errors arising from fixed-point arithmetic with numbers that differ in magnitude [154]. Therefore, only *n* additions and *n* multiplications without exponentiation are required, as shown in (4-7).

$$\hat{y} = \sum_{i=0}^{n} a_i x^i \tag{4-6}$$

$$\hat{y} = x(x(x \dots (a_n x + a_{n-1}) + a_{n-2}) \dots + a_2) + a_1) + a_0 \tag{4-7}$$

The model input (x) is the BIR_{C1} value computed by the SRI block using the optimal t_{bw}. The BIR_{C1} is compared with the resting activity threshold baseline (BIR_{base}), which is found during the training phase and saved in an internal register. If BIR_{C1} is lower than BIR_{base}, the estimated volume output is set to zero; otherwise the volume is computed using (4-7).

The output variable ($\hat{y}$) is the estimated bladder volume of the processed bin. The optimal model order (n) is determined using real signal recordings and considering the trade-off among the allowable latency (2.5 ms) and power density (40 mW/cm^2), the bin-width (a t_{bw} between 1 s and 60 s), and the volume estimation accuracy (>75%). To account for this trade-off, we determine the minimal model order with the shortest t_{bw} that yield the lowest estimation error. The model coefficients (a_i) are computed during the training phase using a bisquare robust fitting method, which assigns lower weights to the outlier values during the fitting process.

The circuit depicted in Figure 4-5B implements (4-7) by using an adder, a multiplier, a temporal register and an accumulator (Acc). The FIFO stores *n* coefficients (a_{n-1} to a_0). The FSM initializes the Acc with (a_n) and loads the adder with the appropriate coefficient stored in the FIFO. The FSM performs *n* multiply-add-accumulate operations starting from the innermost brackets in (4-7). The output volume is computed and updated at regular intervals determined by t_{bw}.

The output validation logic monitors that the output is within the validation limits. If the model output ($\hat{y}$) is negative, the volume is bound to 0. If it is greater than the upper validation limit, the volume is bound to this limit and an event counter is updated. The signal 'Validation_warning_2' is issued when 10 consecutive events have been counted.

The NCU will relay the warnings issued from both circuits in Figure 4-5 to the external unit, which in turn will activate an alarm to signal the patient that corrective actions must be taken to address the problem.

4.3 Results of the validation tests

The DSP depicted in Figure 4-2 was deployed using a low-power FPGA (Igloo AGL1000V2) from Microsemi Co. (Actel), CA, USA. The FPGA was programmed with VHDL using the tools of the development environment Libero SoC.

The FPGA was operated with a core power supply of 1.2 V. Test runs were performed with the clock frequency (f_{clk}) of 333 kHz, which was the f_{clk} value best able to meet the real-time constraint for spike processing within the refractory period, including a security margin.

Two types of signals were used to validate the DSP, realistic synthetic signals and real signals from bladder afferent nerves recorded during acute experiments performed with Sprague-Dawley rats, as described in [37].

To properly assess the spike detection and classification, a signal with a known ground truth is required; i.e., the spike insertion time and its class. A set of 60-s synthetic signals was constructed from an online database of real spike recordings [155]. The synthetic signals constructed from real spikes provide similar features than the real signals recorded during the acute experiments with animal models: similar frequency response (300 - 3000 Hz), spike length (2.5 ms), and the characteristic waveform produced by neuron action-potentials during the resting, depolarization, repolarization and hyperpolarization phases. However, as described below, some sets of the synthetic signals used to assess the spike-sorting circuits displayed more challenging characteristics than those of the real signals recorded, which allowed us to test the circuits under the worst case scenario; i.e. signals

with low SNR and highly correlate spike waveforms. More than 3000 spikes were inserted using a Poisson distribution with the desired firing rate (20 – 100 Hz) and background noise level. Unlike other synthetic signals using non-correlated white-noise, the background noise added to these test signals was generated from a combination of attenuated synthetic signals containing similar spike shapes. Therefore, these synthetic signals more realistically mimicked real signals in which the background noise is dominated by the interference produced by any firing neurons close to the recording microelectrode. Signals with SNRs varying from 1 to 8 were used in our validation tests. The SNR was calculated as in [128]. These signals were used to validate both the Spike Detection and Classification Blocks (SDB and SCB). The outputs of these blocks were compared with the results obtained from Matlab/Simulink simulations using the signals with known ground truths.

Acute experiments carried out on 40 animals to study the measurement method that we proposed in [37] also provided us with real signals for testing the volume estimation in real-time. In these experiments, the rats' bladders were filled to capacity and subsequently voided, while simultaneous recordings from the bladder afferent nerves, intravesical pressure and volume, were performed. The real neural signals were fed to the DSP depicted in Figure 4-2 to test the estimation of the bladder volume in real-time. The DSP outputs were finally compared with the results from the Matlab/Simulink simulations.

Both the synthetic and the real signals used for testing the DSP were bandpass filtered in the range of 300 – 3,000 Hz and discretized with a resolution of 8 bits at 24 kS/s.

4.3.1 Spike Detector Block results

Spike detection is illustrated in Figure 4-6. As input data, we used the synthetic signal with an SNR of 1 dB, which is depicted in Figure 4-6A, along with the absolute threshold (ATD) computed from the median of the entire signal recording (60 s). The pre-processed signal and the detection threshold, computed using (4-1) and (4-3), respectively, is shown in Figure 4-6B. The zoomed-in windows from both signals, depicted in Figure 4-6C and Figure 4-6D, show that the ATD applied on the neural signal is unable to detect the five spikes of the known classes (classes

depicted to the right) within this time-window. In contrast, detection using the preprocessed signal and the adaptive threshold easily detects all the spikes.

To assess the spike detection performance, we used the following metrics: 1) the probability of detection (P_D) computed as the number of the true spikes detected, i.e., the true positives (TP) divided by the actual number of spikes (S) in the signal or $P_D = TP/S$; and 2) the probability of false alarms (P_{FA}) computed as the number of false detections, i.e., the false positives (FP) divided by TP or $P_{FA} = FP/TP$. Additionally, we computed the accuracy index, F_{score} [113], by using (4-8) to assess the overall detection performance by considering both the false detections (FP) and the missed spikes (False negatives, FN).

$$F_{score} = \frac{2TP}{2TP+FP+FN} \tag{4-8}$$

The F_{score} index yields zero when no spike is detected (TP = 0) and unity when all the spikes are properly detected (FP = 0 and FN = 0).

To compare our results with other detection methods, we first determined the optimal scaling factor (C) to be used in (4-3) for each method evaluated: absolute threshold detection with the signal median (ATD_median), as in [111]; simple detection with kNEO preprocessing and its RMS computation (kNEO_RMS), as in [147]; and the simple detection with kNEO preprocessing and its moving average computation (kNEO_MOVAVG), as realized in this work. To this end, we computed the Thr by sweeping C in the interval [1,100] with steps of 0.5. In Figure 4-7A we plotted the averaged F_{score} of each method using signals with SNRs ranging from 1 to 8. The value of C, yielding the highest F_{score}, was chosen as the optimal scaling factor for subsequent calculations.

The F_{score} was also computed using the optimal scaling factor, while the noise level was decreased (SNR ranged from 8 to 1). The F_{score} curves plotted in Figure 4-7B show that for high values of SNR (from 8 to 6), all of the methods performs similarly. However, when the SNR is further decreased, our detection method clearly outperforms the others. Figure 4-7C shows the ROC curves for each method. The area under each ROC curve, also known as the choice probability, was computed using the averaged values obtained from all SNRs. The ATD_median detection method yielded a probability choice of 0.853, the NEO_RMS of 0.972, and NEO_AVG of 0.989.

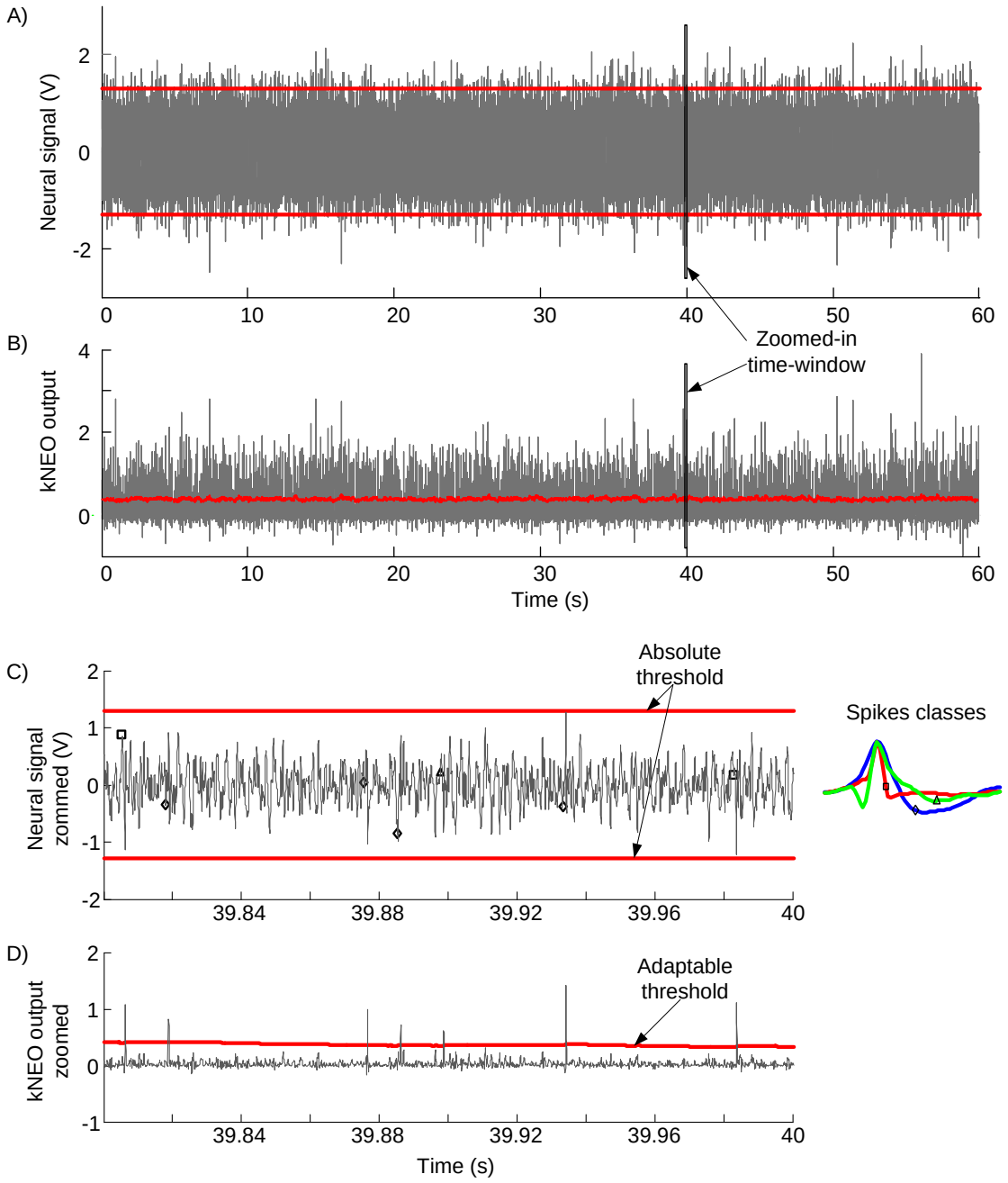

Figure 4-6: Spike detection performance comparison. A) Input neural signal (synthetic) with SNR of 1dB; B) kNEO preprocessor output; C) and D) Zoomed-in signal from A) and B), respectively.

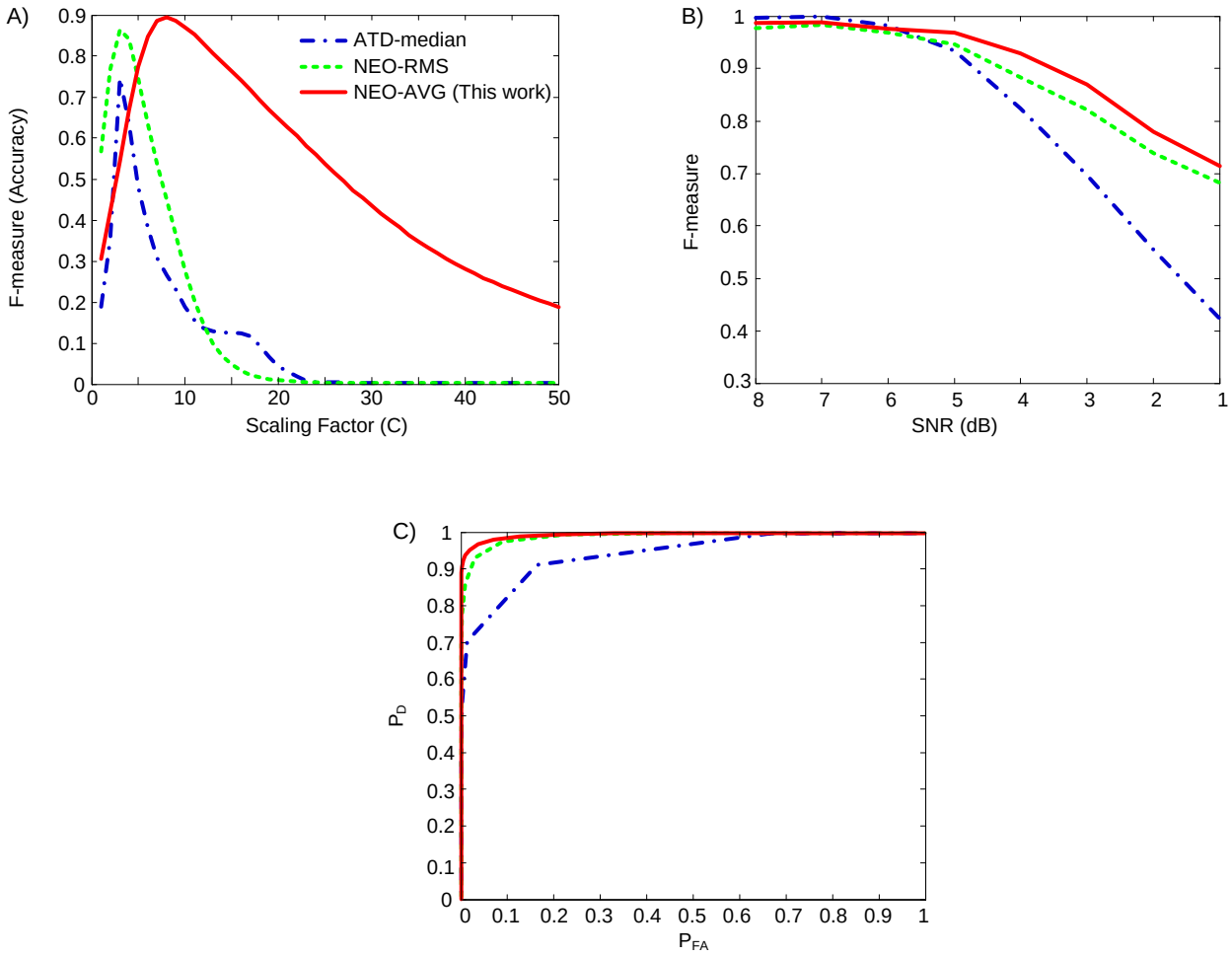

Figure 4-7: Results of the spike detection performed using different methods. A) Detection accuracy (F-score) achieved while the scaling factor C was swept; B) Detection accuracy achieved for signal with different SNR; and C) ROC curves for each method.

4.3.2 Spike Classifier Block results

Classification accuracy is significantly influenced by the degrees of resemblance among the spikes to be classified. Therefore, to assess accuracy, we used two sets of synthetic signals with the specifications mentioned above but also displaying a low and a high degree of resemblance. The top and bottom rows of Figure 4-8 show the classification results for these sets of signals. The degree of resemblance was estimated by computing the averaged value of the Pearson's correlation coefficient (R_{avg}) among all of the templates by pairs (i.e., R_{12}, R_{13}, and R_{23}). Figure

4-8A and Figure 4-8E depict the templates with low and high R_{avg}, respectively, along with the vector of normalized weights emphasizing the dimensions with higher differences among the templates. In Figure 4-8B to 7D (left) and Figure 4-8E to 7H (right), we plotted the Probability Density Function (PDF) corresponding to the WED of all of the classified spikes computed using each template class. It can be observed that the highest densities are achieved for the spikes corresponding to the matching template class. As expected, the PDF of the spikes from classes with a high R are closer. However, the highest probabilities densities are still achieved for the spikes of the matching template class.

Table 4-1 shows the average classification accuracy for both sets of signals with low and high resemblance. The accuracy of the spike classification method proposed in this work compares favorably with PCA/K-Means, which is the method used by the Smartdust iMote2 implementation of the spike sorter [135], and the SPC clustering of wavelets coefficients, which in turn compares favorably with other methods [111]. All methods were tested using the same signals and validated with the known ground truth.

Table 4-1: Classification Accuracy comparison (%)

	PCA/ K-Means	DWT/SPC	This work
Spikes - low R_{avg}	94.3	94.1	96.2
Spikes - high R_{avg}	71.3	84.9	87.7
Average	82.8	89.5	92.0

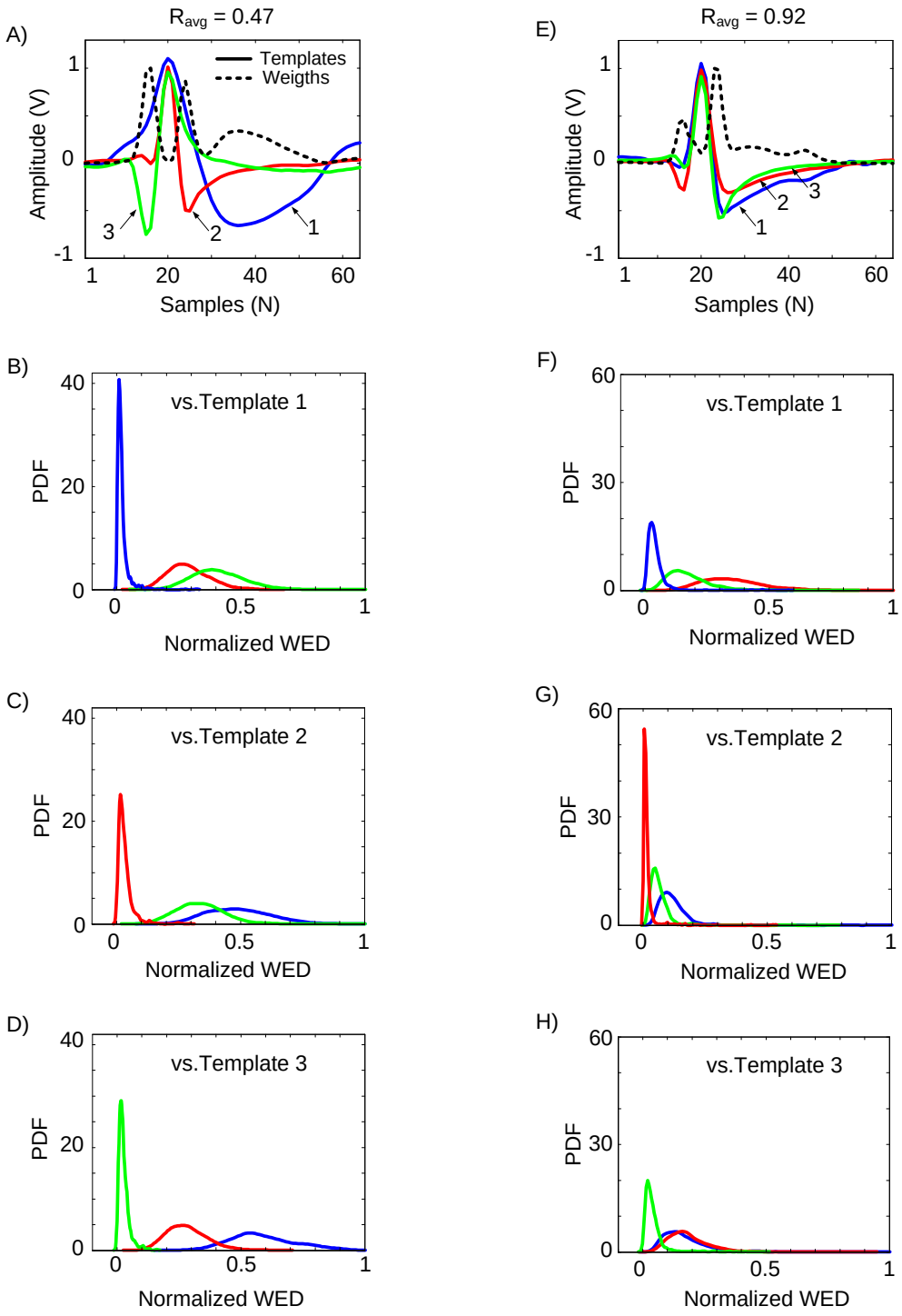

Figure 4-8: Results of the spike classification using the WED method. A) and E) Templates with low and high degree of resemblance, respectively, along with the curve of weights to compute the WED. B) to D) and F) to H) The probability density functions (PDF) corresponding to the WED of all the classified spikes computed with each template class of low and high resemblance, respectively.

4.3.3 Spike Rate Integrator results

This block was tested using both synthetic and real signals. The output of this block using a real signal is illustrated in Figure 4-9. The input real signal used was previously amplified (x10^5), filtered (300 – 3000 Hz), and digitized at 24 kS/s. The spikes in the digital neural signal (Figure 4-9A) are detected and sorted (Figure 4-9B) by the SDB and SCB blocks, respectively. The SRI block computes the BIR_{C1} (Figure 4-9C) the optimal t_{bw} (39 s in this example) that is fed to both volume decoding circuits of Figure 4-5.

4.3.4 Bladder Volume Decoder results

Both the quantitative and qualitative volume estimations are illustrated in Figure 4-9 using a real signal. The quantitative volume estimation output is plotted in Figure 4-9D (solid line), along with the expected value of the discretized volume (dashed line). The accuracy of the quantitative estimation, *Ac*, was computed using the root mean square error (RMSE), as shown in (4-9) and (4-10), where V_{max} is the maximum measured volume of the bladder, V_i is the actual volume (discretized) of the bin i, $\hat{V}_i$ is the estimated bin volume computed using (4-7) and subsequently validated, and b is the total number of bins. Figure 4-9D shows the quantitative volume estimation using a t_{bw} of 39 s that was found during the optimal binning process executed during the training phase, which yielded an *Ac* of 98.4%.

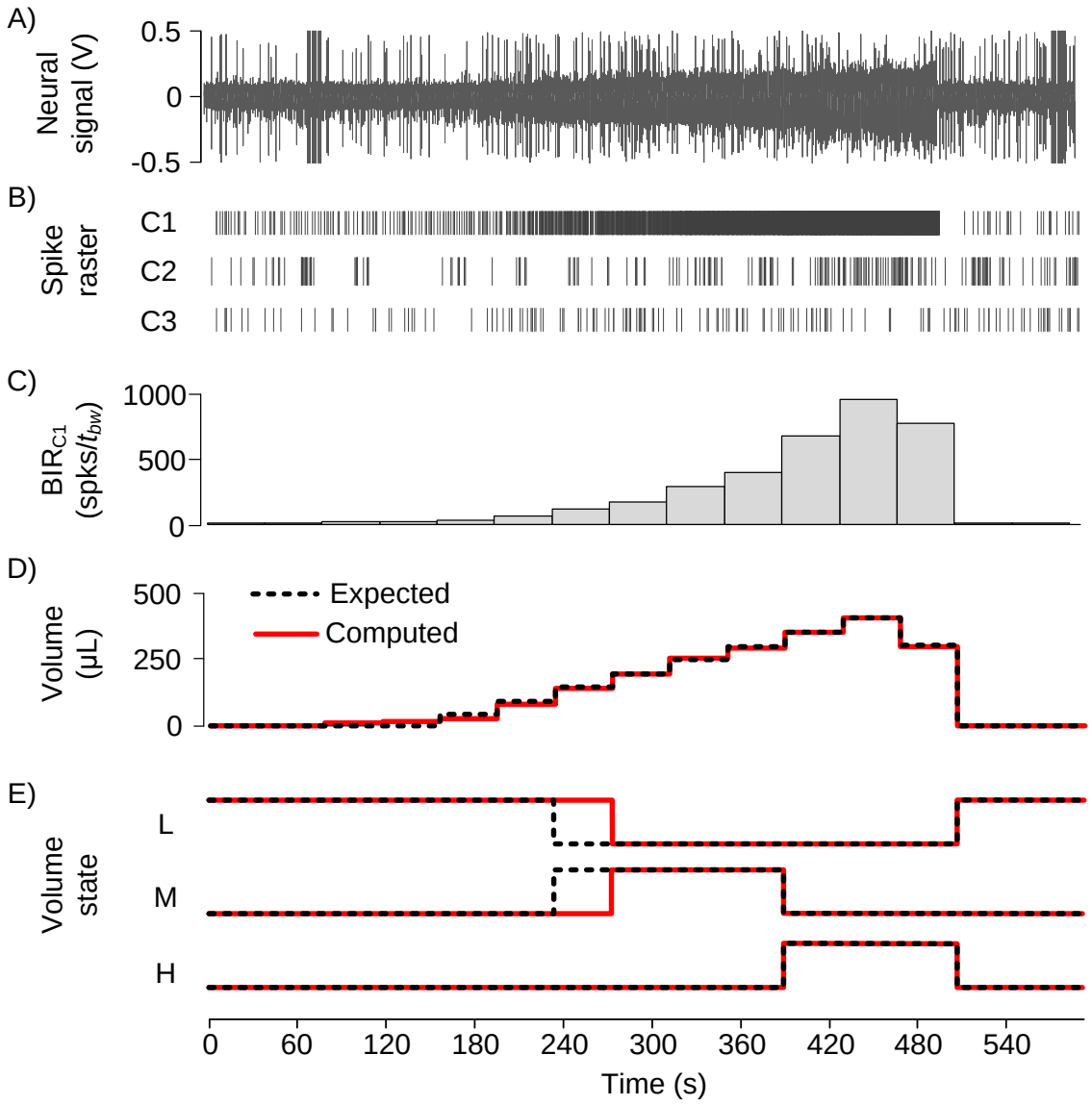

Figure 4-9: Processing stage outputs for the quantitative and qualitative volume estimation. A) Input neural signal previously amplified, filtered, and digitized. B) Spike raster obtained after signal processing performed by the SDB and SCB circuits. C) Output of the SRI circuit using a t_{bw} of 39 s. D) The quantitative volume estimation is compared with the expected output (volume discretized). E) The qualitative degree of fullness computed is compared with the expected output.

$$Ac = (1 - RMSE/V_{max}) * 100\% \tag{4-9}$$

$$\text{RMSE} = \sqrt{\frac{\sum_{i=1}^{b}(V_i - \hat{V}_i)^2}{b}} \tag{4-10}$$

Figure 4-9E shows the binary outputs corresponding to the estimation of the three qualitative states defined previously (L, M, and H) as solid lines. The value of the three binary outputs determines the qualitative state of the bin. The dashed lines are the expected binary value of the qualitative estimation circuit outputs (Figure 4-5A) for each bin according to the actual bladder volume.

The overall success rate (*OSR*) was used to assess the estimation accuracy of this multiclass classification application, as described in [113]. The *OSR* is the ratio of all the correct classifications of the states compared to all of the classifications performed, as shown in (4-11). It is calculated by adding the number of bins (B_i), for which the estimated state of the bin matched the actual state, and dividing by the total number of bins (b). Figure 4-9E shows the qualitative volume estimation using 15 bins (b) with length (t_{bw}) of 39 s, where 14 bins were correctly classified (B_i), yielding an *OSR* of 93.3%.

$$OSR = \frac{\sum_{i=1}^{b} B_i}{b} \tag{4-11}$$

The overall quantitative estimation accuracy from all of the measurement cycles (n = 107) with 40 animals, using the decoding methods employed by the circuits in Figure 4-5, was 94.2 ± 3.1% (mean ± standard deviation). The overall qualitative estimation accuracy was 97.8 ± 3.5%. More details about other experimental results can be found in [37].

To analyze the finite-precision effects arising from the fixed-point arithmetic outputs of the decoding model deployed by the circuit in Figure 4-5A, we compared fixed-point results versus double-precision arithmetic results obtained in Matlab/Simulink. The percentage average error was in the order of 10^{-8}, which is negligible for this application.

4.3.5 FPGA resources, power consumption and latency results

Table 4-2 shows the percentage of cells and the RAM blocks used and the power consumption and latencies achieved. The measured power consumption during the DSP operation was 485 μW. The static power consumed during the Igloo-FPGA Flash-Freeze mode (Idle) was 55.6

μW. The power density achieved, when considering single-side area of the package (1.3 x 1.3 cm = 1.69 cm^2) and the measured power density, was 287 $\mu W/cm^2$.

Table 4-3 contains the performance results of this study and the only study that was found that employed an on-chip, full spike-sorting process [135]. The consolidated results from SDB and SCB are compared with the on-the-fly spike sorting block realized in [135] using the Smartdust iMote2 (Intel processor PXA271), with the minimal core voltage and the minimal core frequency that met system specifications for both cases.

Table 4-2: FPGA Resources usage and Power consumption

	Cells/ (%)	RAM Blocks/(%)	Power (μW)	Latency (μs)
SDB	6069(25)	2(6)	189	1079
SCB	8036(32)	6(19)	34	953
SRI	401(2)	0	1	3
BVD	2070(8)	2(6)	91	32
FSM	224(1)	1	3	0.01
Total	16800(68)	10(32)	318	2067

Table 4-3: Performance comparison of the on-the-fly spike sorting process

	iMote2 PCA/K-Means	This work
Core voltage (V)	0.85	1.2
Allowed core frequency (MHz)	13	0.333
Latency (ms)	9.2	2.0
Power consumption (mW)	87	0.5
Power density (mW/cm^2)	56.5	0.3

4.4 Discussion

The design, prototyping, and testing of a DSP system that deploy the method for real-time volume monitoring from bladder afferent activity that we proposed in [37], allowed us to demonstrate the feasibility of a feedback sensor to be used in a neuroprosthetic implant capable of restoring bladder functions with a conditional stimulation approach.

Our design was driven by power consumption and real-time constraints. Due to the intrinsic features of recorded neural signals as well as the detected spikes' event frequency (< 100 spikes/s), the real-time constraint was achieved using a low system-clock frequency (333 kHz), which favored a reduction in power consumption. Furthermore, the sequential processing approach adopted for the system architecture was easily able to meet the time constraints, allowing for a further reduction of the average power dissipated over time.

Although this sensor is not intended to be used on the cortex but in the lower abdomen or near the targeted spinal root, the 0.3 mW/cm^2 power density showed by this single-channel DSP, which used an off-the-shelf component (Igloo FPGA), was far under the most conservative upper limits reported in literature (40 mW/cm^2) [139]. This may suggest the possible reuse of some of the DSP modules in BCIs. As mentioned earlier, FPGAs provide flexibility and cost advantages that are essential during the research and development process. However, power consumption can be improved by up to an order of magnitude [140] by the eventual deployment of the DSP in ASICs for the neuroprosthetic implant.

The approaches for designing each processing block were chosen by taking into account the results reported in the literature, our own test results using realistic synthetic signals with a known ground truth, and real signals recorded from animal models during the acute experiments reported in [37]. To meet our DSP design requirements, the approach used to deploy each processing stage was improved by proposing solutions capable of running in real-time, without external supervision, and by optimizing the amount of hardware resources required for their implementation.

The DSP presented in this study allowed the reliable detection of spikes immersed in noisy signals with low SNR by emphasizing them over the background noise using a non-linear energy

estimator and a self-adjusting detection threshold circuits. The method and circuits proposed to classify each spike by a weighted Euclidean distance, with coefficients that emphasized the difference among the spike templates, allowed us to achieve an average accuracy of 92% while using a reasonable amount of resources and displaying a processing time fast enough to meet real-time constraints. This spike classification performance compared favorably with studies cited previously that used methods with a much higher computational cost that are currently deployed in general purpose personal computers and, in one particular case, using an embedded system [135].

The appropriate selection of the number of bits used in fixed-point arithmetic operations and a circuit design, which optimized the amount of hardware required for a real-time estimation of the bladder volume, allowed us to match the accuracies achieved during simulations in Matlab/Simulink using double-precision arithmetic with short latencies.

Although it was not imperative to prove the feasibility of sensory decoding in real-time using an standalone system, we included circuits in the DSP that are capable of self-detecting errors to allow for online corrections assisted by the external unit. This will adds more reliability and safety to the neuroprosthetic implant.

Several research studies cited in the introduction have shown that neural recording can be achieved using front-end circuits with a power consumption of a few μW. In forthcoming research, the DSP presented in this paper will be integrated with a front-end recording-stage, and an implantable device will be built to conduct acute and chronic experiments in animal models with induced spinal cord injury.

4.5 Conclusion

Our results demonstrate that it is possible to accurately monitor the bladder volume using a standalone DSP. The proposed DSP is capable of carrying out, in real-time and with low-power consumption, the entire signal processing required for detecting and discriminating the afferent neural activity stemming from a specific source as well as the sensory decoding of the bladder fullness using both qualitative and quantitative methods.

4.6 Acknowledgment

The authors would like to thank Tomonori Minagawa and Jean-Jacques Wyndaele for their valuable collaboration during the animal experiments.

CHAPTER 5 GENERAL DISCUSSION

Sensory feedback to be used with an electronic prosthesis is of great interest due to the multiple potential applications in the medical field in which these devices can be used. However, sensory feedback is still a major challenge due to both technological limitations and the lack of a clear understanding of all relevant physiological processes.

In this thesis, we tackled the problem of finding a suitable method of providing sensory feedback to an intelligent neuroprosthesis. This neuroprosthesis was meant to restore the urinary bladder functions of storing and voiding urine in paraplegic patients or other patients with impaired sensations and lack of voluntary control of the bladder. The adopted methodological approaches allowed us to successfully circumvent each of the problems we faced during the research and to validate the thesis hypotheses H1 and H2. We had to perform both basic biomedical research and applied research to solve problems without known effective solutions.

From the beginning, we realized that some studies that tried to find a solution for chronic bladder monitoring did not consider important anatomical and physiological characteristics that certainly influenced or even prevented the achievement of the expected results. We identified these characteristics and subsequently identified the user needs that a bladder sensor had to meet to be useful in real applications beyond the laboratory boundaries.

Two main choices of measurement principles were carefully studied. One was based on artificial sensors, such as pressure, displacement, ultrasound, and other detection principles reviewed in Chapter 2. The other was based on the natural receptors in the bladder wall, especially those that had been reported to respond specifically to the bladder stretching during filling. Each method reviewed showed advantages and drawbacks that prevented a clear and judicious choice from the common pros and cons analyses that can be found in the introductory section of several of these studies. For instance, the information gathered from artificial sensors tends to be independent of the patient's condition and thus more reproducible among patients and over time; however, these sensors are more invasive, show biocompatibility problems and decreasing reliability over a long period of time. In contrast, the approaches based on natural sensors are less invasive, show fewer biocompatibility issues, and are more reliable in chronic applications; nevertheless, their responses can change for patients with different pathological conditions (e.g., cancer and cystitis) of the patients.

Finally, we considered all of the above mentioned analyses and the results of the systematic assessment of the measurement methods, in which we used the most important user needs as selection criteria. Consequently, we concluded that the natural receptors in the bladder wall were the best choice as the primary measurement principle. Our choice agreed with other renowned authors on this subject who favored the use of biopotentials for neuroprostheses feedback [1]. However, known important issues needed to be addressed: the low signal-to-noise ratio of the recorded signals and the proper identification of the neural source; i.e., the afferent neural activity arising from the bladder mechanoreceptors that were reported to be volume receptors, but there was no proof of their existence at the time. Therefore, a study of the feasibility of this approach was necessary.

In our study using a practical and accessible animal model (Sprague-Dawley rats), we assessed the feasibility of real-time bladder volume monitoring from the afferent activity of bladder mechanoreceptors. We considered important clues from our previous studies on bladder neurophysiology and biomechanics. These clues suggested the presence of volume-specific mechanoreceptors in the bladder inner mucosa [30] and showed the slow dynamic response of the bladder to filling [64].

This study proposed two methods for measuring bladder volume. For a primary transduction principle, these methods used the afferent neural activity produced by mechanoreceptors during slow bladder filling. The proposed measurement methods required identification of the signal source. This included the spike sorting process followed by the selection of the neural unit (axon) that showed a good, but not necessarily linear, correlation with the volume, and subsequent neural activity decoding using the qualitative and quantitative approaches. The former allowed qualitative volume estimations, i.e. three levels of fullness defined as low-volume, a comfortable level; medium level, need-to-void within a proper timeframe; high level, urge-to-void because there is a risk of an imminent leaking. The qualitative method was designed to reduce the computational cost as much as possible; thus, the hardware resources required for its electronic implementation were minimized. This method achieved a high accuracy estimation of the bladder volume (97%) and was able to detect the bladder fullness with a sensitivity of 100%. The qualitative levels were defined based on actual sensations that emanate from the lower urinary tract in humans. These levels appear to be sufficient for proper feedback to an FES device for

restoring bladder function and for providing timely advice to impaired patients about when to urinate.

The quantitative approach was implemented using a regression model that was optimized to run in real-time with much lower computational cost than those found in published studies for decoding sensory information from neural recordings. Our approach allowed the real-time estimation of the volume or pressure value with an accuracy of 94%. The quantitative approach can also be used for accurate FES feedback or in other applications, such as patient warning, differential diagnosis of urinary dysfunction, and clinical research.

During the design of both measurement methods, we considered the physiological characteristics and the previously identified user needs. An important issue that was considered throughout the design was the fact that the firing frequency of the mechanoreceptors increased during bladder distension; however, this increase was not monotonic due to the relatively rapid adaptation of these receptors along with the viscoelastic accommodation of the bladder wall, among other factors discussed in Chapter 3. This behavior of the mechanoreceptors response made it difficult to instantaneously detect the bladder volume or pressure. Therefore, we decided to extract parameters and runs algorithms that addressed this behavior, which was not suitable for our purposes. For instance, the signal was processed using time-windows (bins) of optimally chosen durations (bin-width), and the input parameter for estimating volume was conveniently defined as the bin integrated rate (BIR), which was computed as the number of actions potentials (spikes) produced by a particular neural unit within the time-window. Moreover, we utilized a regression model that estimated volume using the BIR as the input and that considered the non-linear response of the mechanoreceptors. The high accuracy of the obtained estimation results not only demonstrated the efficacy of the measurement method but also suggested that the volume sensory information might be encoded as an average of the sustained activity over a given time-window.

In addition to the experiments that were performed to demonstrate the feasibility of the proposed measurement methods, we carried out other experiments to explore the bladder mechanoreceptor behavior in other situations besides the slow (‘physiological’) filling. Several of the reviewed studies discussed whether it was possible to detect the tonic and phasic responses of the bladder. Most stated that only rapid pressure changes, i.e., phasic responses, could be detected from recordings of the afferent neural activity of the bladder. The isovolumetric measurement trials

that we performed showed that we can accurately quantify the different levels of tonic responses produced by the bladder mechanoreceptors, especially for volumes beyond the sensitivity threshold. These results demonstrated that our method was able to detect not only the phasic responses during gradual filling but also the tonic responses during isovolumetric measurements.

The experimental results of other measurement trials, in which the bladder was passively withdrawn using an additional infusion pump, showed the reversibility of the mechanoreceptors response, i.e., a decrease in the firing frequency during the receptor downloading phase. During the passive withdrawing, the bladder was voided without detrusor contraction; thus, the recorded activity might have arisen from mechanoreceptors that responded specifically to the bladder volume. Although the mechanoreceptors displayed a hysteretic response, the bladder volume could be estimated using our method. These results may contribute to confirming the predicted existence of volume-specific receptors in the bladder wall, which are considered necessary for the voluntary control of the bladder through the storing and voiding pathways [30]. However, further studies with the specific objective of proving the existence of these receptors, which is beyond the scope of the thesis, should be performed to conclusively confirm this finding.

In the last study of this thesis research, we assessed the feasibility of the measurement method implementation using a low-power electronic system capable of performing all of the tasks required for the bladder volume or pressure decoding from afferent neural activity in real-time. Most of the existing methods that we reviewed to detect, discriminate and decode sensory information from afferent neural activity are not well adapted for unsupervised real-time performance. Those that are rely on complex algorithms that represent a heavy burden even for powerful personal computers.

To demonstrate the bladder sensor feasibility, we designed, prototyped, and tested a dedicated DSP system that deployed the methods discussed above using a low-power FPGA (Actel Igloo). The design was driven by real-time and power consumption constraints, which led us to adopt approaches that met these constraints without deterioration of the required accuracy. For instance, the power consumption constraint was satisfied by designing algorithms that are best suited for real-time processing using circuits of low-power consumption and low system-clock frequency and by adopting a sequential processing approach for the global system architecture. The estimated power-density dissipation achieved by our design (0.3 mW/cm^2) was far below the

most conservative upper limits reported in literature for neuroprosthetic implants of 40 mW/cm^2 [139]. This result may suggest the possible reuse of some of the DSP modules in brain-computer interfaces.

To achieve our goal of implementing the bladder sensor using the method proposed in the preceding study, we faced the problem of implementing the spike sorting process in real-time using a standalone electronic system capable of performing all of the required tasks. The approaches for designing each processing block were chosen by taking into account the results reported in the literature, our own test results using realistic synthetic signals with a known ground truth, and real signals recorded from the animal models during our previous acute experiments. We were able to detect spikes immersed in noisy signals with low SNR by emphasizing the spikes over the background noise using a non-linear energy estimator and a spike detection circuit with self-adjusting threshold capability. Moreover, the proposed method and circuits for classifying each spike involved a weighted Euclidean distance approach using coefficients that emphasized the difference among the spike templates. This process allowed us to achieve an average accuracy of 92%, while using a reasonable amount of resources with a processing time fast enough to meet the real-time and power constraints. Our spike-sorting method compared favorably with other high computational-cost approaches that usually are executed offline.

We found only one study [135] that used a system (iMote2) with a general purpose Intel processor, which was programmed in C, to implement the full on-chip spike sorting process. This chip used a well-known spike sorting method (PCA/K-Means) that has shown poor classification accuracy in comparative analyses. Due to the approaches we used in the implementation, we achieved higher classification accuracies and greatly improved the latency and power consumption performance showed in this single study. We did not find any study that implemented both the spike sorting and the sensory decoding that we achieved in our DSP.

The results of the three major studies in our thesis research have allowed us to demonstrate not only the feasibility of an implantable bladder sensor based on the sensory decoding of neural afferent signals but also the advantages of following a systematic methodology which considered the user needs throughout our research process.

CONCLUSION

The recording and decoding of sensory information form afferent neural activity is the measurement principle that best meets the user needs for a neuroprosthetic device for chronic monitoring of the bladder volume or pressure.

Accurate bladder volume and pressure estimates are possible using the measurement methods proposed in this thesis that are based on the neural decoding of the afferent activity of bladder mechanoreceptors recorded at specific spinal roots containing nerves with bladder sensory information.

Both phasic and tonic responses related to bladder activity can be detected using the presented measurement methods.

A standalone bladder sensor running the measurement methods proposed in this thesis can be implemented using a low-power integrated circuit capable of providing feedback to intelligent neurostimulators and timely warns patients with impaired bladder sensations or urinary dysfunctions about when the bladder need to be voided.

The sensory decoding of the bladder volume and pressure can be implemented in a single chip that also runs the spike sorting process satisfying real-time latency and density-power dissipation constraints.

The spikes immersed in a noisy signal can be accurately detected and classified using the optimized algorithms and circuits that we proposed and validated in this thesis. This process can run unsupervised in real-time with low-computational cost and low-power consumption.

Recommendations for future work

This thesis opens the door to future research toward the achievement of an implantable device that can be used in current clinical practice to warn patients or to restore bladder function through conditional functional electrical stimulation.

- The DSP circuit designed in this thesis can be further optimized using MAC units that are more efficient than those provided by the Actel FPGA library.
- The back-end function performed by the DSP should be integrated in a mixed-signal system that also includes the front-end signal conditioning stage (amplifiers and linear-phase filters to avoid spike distortion) and the other internal unit components presented in Chapter 4.
- The system should then be encapsulated in an implantable device to perform chronic experiments in larger animal models (e.g., pigs) before acute and chronic experimentation in paraplegic patients.
- To use the spike sorting module in BCI applications where a high number of channels must be processed simultaneously, the architecture presented in Chapter 4 can be modified to implement pipeline architecture to further reduce the signal processing latencies.

BIBLIOGRAPHY

[1] T. Sinkjaer, M. Haugland, A. Inmann *et al.*, "Biopotentials as command and feedback signals in functional electrical stimulation systems," *Medical Engineering & Physics,* vol. 25, no. 1, pp. 29-40, 2003.

[2] F. Mounaim, and M. Sawan, "Toward A Fully Integrated Neurostimulator With Inductive Power Recovery Front-End," *Biomedical Circuits and Systems, IEEE Transactions on,* vol. 6, no. 4, pp. 309-318, 2012.

[3] H. A. C. Wark, B. R. Dowden, P. C. Cartwright *et al.*, "Selective Activation of the Muscles of Micturition Using Intrafascicular Stimulation of the Pudendal Nerve," *Emerging and Selected Topics in Circuits and Systems, IEEE Journal on,* vol. PP, no. 99, pp. 1-1, 2011.

[4] F. M. J. Martens, J. P. F. A. Heesakkers, and N. J. M. Rijkhoff, "Minimal invasive electrode implantation for conditional stimulation of the dorsal genital nerve in neurogenic detrusor overactivity," *Spinal Cord,* vol. 49, no. 4, pp. 566-572, 2011.

[5] U. Barroso, R. Tourinho, P. Lordêlo *et al.*, "Electrical stimulation for lower urinary tract dysfunction in children: A systematic review of the literature," *Neurourology and Urodynamics,* vol. 30, no. 8, pp. 1429–1436, 2011.

[6] S. Siegel, and N. Kaula, "Pudendal Nerve Neuromodulation: A New Option for Refractory Bladder Overactivity and Pain," *Current Bladder Dysfunction Reports,* 2010.

[7] H. Oh-oka, "Neuromodulation in the Treatment of Overactive Bladder With a Focus on Interferential Therapy," *Current Bladder Dysfunction Reports,* vol. 5, no. 1, pp. 39-47, 2010.

[8] E. E. Horvath, P. B. Yoo, C. L. Amundsen *et al.*, "Conditional and continuous electrical stimulation increase cystometric capacity in persons with spinal cord injury," *Neurourology and Urodynamics,* vol. 29, no. 3, pp. 401-407, 2010.

[9] M. Carmel, M. Lebel, and L. Tu, "Pudendal nerve neuromodulation with neurophysiology guidance: a potential treatment option for refractory chronic pelvi-perineal pain," *International Urogynecology Journal*, vol. 21, no. 5, pp. 613-616, 2010.

[10] N. Kohli, and D. Patterson, "InterStim Therapy: A Contemporary Approach to Overactive Bladder," *Rev Obstet Gynecol.*, vol. 2, no. 1, pp. 18-27., 2009.

[11] H. B. Goldman, C. L. Amundsen, J. Mangel *et al.*, "Dorsal genital nerve stimulation for the treatment of overactive bladder symptoms," *Neurourology and Urodynamics*, vol. 27, no. 6, pp. 499-503, 2008.

[12] L. Bresler, J. S. Walter, A. Jahoda *et al.*, "Effective methods of pelvic plexus nerve and bladder stimulation in anesthetized animal model," *J Rehabil Res Dev*, vol. 45, no. 4, pp. 627-637, 2008.

[13] P. H. Peckham, and J. S. Knutson, "Functional Electrical Stimulation for Neuromuscular Applications," *Annual Review of Biomedical Engineering*, vol. 7, no. 1, pp. 327-360, 2005.

[14] J. W. Middleton, and J. R. Keast, "Artificial autonomic reflexes: using functional electrical stimulation to mimic bladder reflexes after injury or disease," *Autonomic Neuroscience*, vol. 113, no. 1-2, pp. 3-15, 2004.

[15] A. Ba, and M. Sawan, "Integrated programmable neurostimulator to recuperate the bladder functions," in Electrical and Computer Engineering. IEEE CCECE Canadian Conference ON, 2003, pp. 147-150.

[16] N. J. M. Rijkhoff, H. Wijkstra, P. E. V. van Kerrebroeck *et al.*, "Urinary Bladder Control by Electrical Stimulation: Review of Electrical Stimulation Techniques in Spinal Cord Injury," *The Journal of Urology*, vol. 160, no. 3, Part 1, pp. 961-961, 1998.

[17] I. Medtronic. "Clinical Sumary: Medtronic InterStim® Therapy," http://professional.medtronic.com/wcm/groups/mdtcom_sg/@mdt/@neuro/documents/documents/sns-clinical-summary.pdf.

[18] J. Kutzenberger, “Surgical therapy of neurogenic detrusor overactivity (hyperreflexia) in paraplegic patients by sacral deafferentation and implant driven micturition by sacral anterior root stimulation: methods, indications, results, complications, and future prospects,” *Acta Neurochir Suppl.*, vol. 97, no. Pt 1, pp. 333-9., 2007.

[19] N. Y. Siddiqui, J. M. Wu, and C. L. Amundsen, “Efficacy and adverse events of sacral nerve stimulation for overactive bladder: A systematic review,” *Neurourology and Urodynamics*, vol. 29, no. S1, pp. S18-S23, 2010.

[20] S. Jezernik, W. M. Grill, and T. Sinkjaer, “Detection and inhibition of hyperreflexia-like bladder contractions in the cat by sacral nerve root recording and electrical stimulation,” *Neurourology and Urodynamics*, vol. 20, no. 2, pp. 215-230, 2001.

[21] M. D. Craggs, C. W. Lynne, and P. Canio, "Pelvic somato-visceral reflexes after spinal cord injury: measures of functional loss and partial preservation," *Progress in Brain Research*, pp. 205-219: Elsevier, 2006.

[22] J. F. Morrison, "Sensations arising from lower urinary tract," *The physiology of the lower urinary tract*, M. Torrens and J. F. B. Morrison, eds., pp. 89-131, London: Springer Verlag, 1987.

[23] E. A. Tanagho, "Anatomy of the genitourinary tract," *Smith's General Urology*, E. A. Tanagho and J. W. McAninch, eds., pp. 1-16, San Francisco: McGraw Hill, 2007.

[24] S. P. Vasavada, and R. R. Rackley, "Electrical Stimulation for Storage and Emptying Disorders," *Campbell-Walsh Urology*, A. J. Wein, ed., Philadelphia, PA: Saunders Elsevier, 2007.

[25] A. J. Wein, "Pathophysiology and Classification of Voiding Dysfunction," *Campbell-Walsh Urology*, A. J. Wein, ed., pp. ch.57, Philadelphia, PA: Saunders Elsevier, 2007.

[26] A. C. Peterson, and G. D. Webster, "Urodynamic and Videourodynamic Evaluation of Voiding Dysfunction," *Campbell-Walsh Urology*, A. J. Wein, ed., Philadelphia, PA: Saunders Elsevier, 2007.

[27] A. Yoji, “Quality Function Deployment: Integrating Customer Requirements into Product Design ” *Productivity Press*, 1990.

[28] D. Rowan, E. James, A. Kramer *et al.*, “Technical aspects. Produced by the International Continence Society Working Party on Urodynamic Equipment.,” *J Med Eng Technol,* vol. 11, no. 2, pp. 57-64, 1987.

[29] W. Schäfer, P. Abrams, L. Liao *et al.*, “Good urodynamic practices: Uroflowmetry, filling cystometry, and pressure-flow studies,” *Neurourology and Urodynamics,* vol. 21, no. 3, pp. 261-274, 2002.

[30] J. F. Morrison, “The activation of bladder wall afferent nerves,” *Experimental Physiology,* vol. 84, no. 1, pp. 131-136, 1999.

[31] J. F. Morrison, “The physiological mechanisms involved in bladder emptying,” *Scandinavian journal of urology and nephrology. Supplementum,* vol. 184, pp. 15-8, 1997.

[32] J. N. Sengupta, and G. F. Gebhart, “Mechanosensitive properties of pelvic nerve afferent fibers innervating the urinary bladder of the rat,” *Journal of Neurophysiology,* vol. 72, no. 5, pp. 2420-2430, 1994.

[33] V. K. Shea, R. Cai, B. Crepps *et al.*, “Sensory Fibers of the Pelvic Nerve Innervating the Rat's Urinary Bladder,” *Journal of Neurophysiology,* vol. 84, no. 4, pp. 1924-1933, 2000.

[34] N. Yoshimura, and M. B. Chancellor, “Neurophysiology of lower urinary tract function and dysfunction,” *Reviews in urology,* vol. 5 Suppl 8, pp. S3-S10, 2003.

[35] Z. S. Zumsteg, C. Kemere, S. O'Driscoll *et al.*, “Power feasibility of implantable digital spike sorting circuits for neural prosthetic systems,” *IEEE Transactions on Neural Systems and Rehabilitation Engineering,* vol. 13, no. 3, pp. 272-279, Sep, 2005.

[36] A. Mendez, and M. Sawan, “Chronic monitoring of bladder volume: a critical review and assessment of measurement methods,” *The Canadian journal of urology,* vol. 18, no. 1, pp. 5504-16, 2011.

[37] A. Mendez, M. Sawan, T. Minagawa *et al.*, “Estimation of Bladder Volume from Afferent Neural Activity,” *Neural Systems and Rehabilitation Engineering, IEEE Transactions on,* vol. 21, no. 5, 2013.

[38] A. Mendez, A. Belghith, and M. Sawan, “Dedicated On-chip Processor for Sensing the Bladder Volume through Afferent Neural Pathways,” *IEEE Transactions on Biomedical Circuits and Systems,* vol. (Submitted), May, 2013, 2013.

[39] K. D. Farrell, L. M. Robinson, S. A. Baydock *et al.*, “A Survey of Canadian Websites Providing Information About Female Urinary Incontinence,” *J Obstetric and Gynecology of Canada,* vol. 28, no. 8, 2006.

[40] L. Stothers, D. H. Thom, and E. Calhoun, "Urinary Incontinence in Men " NIH Publication No. 07–5512 P. H. S. Urologic Diseases in America. US Department of Health and Human Services, National Institutes of Health, National Institute of Diabetes and Digestive and Kidney Diseases, ed., US Government Printing Office, 2007, pp. 195-219.

[41] I. Nygaard, D. H. Thom, and E. Calhoun, "Urinary Incontinence in Women " NIH Publication No. 07–5512 P. H. S. Urologic Diseases in America. US Department of Health and Human Services, National Institutes of Health, National Institute of Diabetes and Digestive and Kidney Diseases, ed., US Government Printing Office, 2007, pp. 159-186.

[42] M. Bettez, L. M. Tu, K. Carlson *et al.*, “2012 Update: Guidelines for Adult Urinary Incontinence Collaborative Consensus Document for the Canadian Urological Association,” *Canadian Urological Association Journal,* vol. 6, no. 5, pp. 354–363, October 2012, 2012.

[43] M. P. W. Offermans, M. F. M. T. Du Moulin, J. P. H. Hamers *et al.*, “Prevalence of urinary incontinence and associated risk factors in nursing home residents: A systematic review,” *Neurourology and Urodynamics,* vol. 28, no. 4, pp. 288-294, 2009.

[44] A. Farry, and D. Baxter, *The Incidence and Prevalence of Spinal Cord Injury in Canada: Overview and estimates based on current evidence*, Rick Hansen Institute and Urban Future, 2010.

[45] S. N. Vigod, and D. E. Stewart, "Major Depression in Female Urinary Incontinence," *Psychosomatics*, vol. 47, 2006.

[46] Momokazu Gotoh, Yoshihisa Matsukawa, Yoko Yoshikawa *et al.*, "Impact of urinary incontinence on the psychological burden of family caregivers," *Neurourology and Urodynamics*, vol. 28, no. 6, pp. 492-496, 2009.

[47] N. Yoshimura, and M. Chancellor, "Physiology and Pharmacology of the Bladder and Urethra," *Campbell-Walsh Urology*, A. J. Wein, ed., Philadelphia, PA: Saunders Elsevier, 2007.

[48] N. C. I. National Institutes of Health, "The Urinary System," 2013, http://training.seer.cancer.gov/anatomy/urinary/, 2013].

[49] M. R. Margaret, "Neurophysiology in neurourology," *Muscle & Nerve*, vol. 38, no. 1, pp. 815-836, 2008.

[50] C. J. Fowler, D. Griffiths, and W. C. de Groat, "The neural control of micturition," *Nat Rev Neurosci*, vol. 9, no. 6, pp. 453-466, 2008.

[51] N. J. M. Rijkhoff, T. Sinkjaer, S. Jezernick *et al.*, *Overacting bladder control method involves activating inhibitory spinal reflex by stimulating afferent nerve fibers in response to detection of onset of bladder contraction*, Overacting bladder control method involves activating inhibitory spinal reflex by stimulating afferent nerve fibers in response to detection of onset of bladder contraction. WO200025859-A; WO200025859-A1; AU9964653-A; US6836684-B1,to UNIV AALBORG (UYAA-Non-standard) NEUROCON APS (NEUR-Non-standard), Patent, 2000.

[52] J. G. Blaivas, H. P. Sinha, A. A. Zayed *et al.*, "Detrusor-external sphincter dyssynergia," *J Urol.*, vol. 125, no. 4, pp. 542-4., 1981.

[53] N. Simforoosh, F. Dadkhah, S. Y. Hosseini *et al.*, “Accuracy of Residual Urine Measurement in Men: Comparison Between Real-Time Ultrasonography and Catheterization,” *The Journal of Urology*, vol. 158, no. 1, pp. 59-61, 1997.

[54] R. A. Gaunt, A. Prochazka, C. W. Lynne *et al.*, "Control of urinary bladder function with devices: successes and failures," *Progress in Brain Research*, pp. 163-194, 2006.

[55] S.-S. Byun, H. H. Kim, E. Lee *et al.*, “Accuracy of bladder volume determinations by ultrasonography: are they accurate over entire bladder volume range?,” *Urology*, vol. 62, no. 4, pp. 656-660, 2003.

[56] E. Koomen, E. Bouman, P. Callewaerdt *et al.*, “Evaluation of a non-invasive bladder volume measurement in children,” *Scandinavian Journal of Urology and Nephrology*, vol. 42, no. 5, pp. 444 - 448, 2008.

[57] J. D. Bronzino, *The Biomedical engineering handbook. Medical devices and systems*, 3rd ed., Boca Raton, FL: CRC/Taylor & Francis, 2006.

[58] J. G. Webster, *Encyclopedia of medical devices and instrumentation*, 2nd ed., Hoboken, N.J.: Wiley-Interscience, 2006.

[59] S. Boyer, M. Sawan, M. Abdel-Gawad *et al.*, “Implantable selective stimulator to improve bladder voiding: design and chronic experiments in dogs,” *Rehabilitation Engineering, IEEE Transactions on*, vol. 8, no. 4, pp. 464-470, 2000.

[60] T. M. Bruns, N. Bhadra, and K. J. Gustafson, “Variable Patterned Pudendal Nerve Stimuli Improves Reflex Bladder Activation,” *Neural Systems and Rehabilitation Engineering, IEEE Transactions on*, vol. 16, no. 2, pp. 140-148, 2008.

[61] M. Sawan, A. Ba, F. Mounaim *et al.*, “Biomedical circuits and systems dedicated for sensing and neurostimulation: Case study on urinary bladder dysfunctions,” *Turkish Journal of Electrical Engineering and Computer Sciences*, vol. 16, no. 3, pp. 171-187, 2008.

[62] F. M. J. Martens, H. J. M. v. Kuppevelt, J. A. C. Beekman *et al.*, "Limited value of bladder sensation as a trigger for conditional neurostimulation in spinal cord injury patients," *Neurourology and Urodynamics,* vol. (Published online in advance by Wiley InterScience), 2009.

[63] B. E. Westerhof, J. V. de Bakker, and W. A. van Duyl, "High resolution detector for micromotion in smooth muscle strips," in Engineering in Medicine and Biology Society, 1996. Bridging Disciplines for Biomedicine. Proceedings of the 18th Annual International Conference of the IEEE, Year, pp. 138-139 vol.1.

[64] I. Korkmaz, and B. Rogg, "A simple fluid-mechanical model for the prediction of the stress–strain relation of the male urinary bladder," *Journal of Biomechanics,* vol. 40, no. 3, pp. 663-668, 2007.

[65] K. Takayama, M. Takei, T. Soejima *et al.*, "Continuous monitoring of bladder pressure in dogs in a completely physiological state," *Urology*, vol. 60, no. 5, pp. 428-32., 1987.

[66] E. L. Koldewijn, P. E. V. Van Kerrebroeck, E. Schaafsma *et al.*, "Bladder pressure sensors in an animal model," *The Journal of urology,* vol. 15 no. 5, pp. 1379-1384, 1994.

[67] J. Coosemans, and R. Puers, "An autonomous bladder pressure monitoring system," *Sensors and Actuators A: Physical,* vol. 123-124, pp. 155-161, 2005.

[68] R. B. Northrop, "Plethysmography," *Noninvasive instrumentation and measurement in medical diagnosis*, M. R. Neuman, ed., CRC Press LLC, 2002, pp. 241-252.

[69] F. M. Waltz, G. W. Timm, and W. E. Bradley, "Bladder Volume Sensing by Resistance Measurement," *Biomedical Engineering, IEEE Transactions on,* vol. BME-18, no. 1, pp. 42-46, 1971.

[70] J. C. Denniston, and L. E. Baker, "Measurement of urinary bladder emptying using electrical impedance," *Medical and Biological Engineering,* vol. 13, no. 2, pp. 305-6, 1975.

[71] P. Doyle, and D. Hill, "The measurement of residual urine volume by electrical impedance in man," *Medical and Biological Engineering and Computing,* vol. 13, no. 2, pp. 307-308, 1975.

[72] J. Abbey, and L. Close, "Electrical impedance measurement of urinary bladder fullness," *J Microw Power,* vol. 18, no. 3, pp. 305-314, 1983.

[73] A. Yamada, M. Fuse, T. Aoyagi *et al.*, "Preventive equipment for urinary incontinence: a device employing lower abdominal impendance changes.," *International Journal of Artificial Organs,* vol. 17, no. 3, pp. 146-150, 1994.

[74] B. C. Gill, P. C. Fletter, P. J. Zaszczurynski *et al.*, "Feasibility of fluid volume conductance to assess bladder volume," *Neurourology and Urodynamics,* vol. 27, no. 6, pp. 525-531, 2008.

[75] P. Hua, E. J. Woo, J. G. Webster *et al.*, "Bladder fullness detection using multiple electrodes," in Engineering in Medicine and Biology Society, 1988. Proceedings of the Annual International Conference of the IEEE, Year, pp. 290-291 vol.1.

[76] B. Provost, and M. Sawan, "Proposed new bladder volume monitoring device based on impedance measurement," *Medical and Biological Engineering and Computing,* vol. 35, no. 6, pp. 691-694, 1997.

[77] M. Sawan, K. Arabi, and B. Provost, "Implantable Volume Monitor and Miniaturized Stimulator Dedicated to Bladder Control," *Artificial Organs,* vol. 21, no. 3, pp. 4, 1997.

[78] C. T. Kim, T. A. Linsenmeyer, H. Kim *et al.*, "Bladder volume measurement with electrical impedance analysis in spinal cord-injured patients," *American Journal of Physical Medicine & Rehabilitation,* vol. 77, no. 6, pp. 498-502, 1998.

[79] A. Keshtkar, A. Mesbahi, and P. Mehnati, "The effect of bladder volume changes on the measured electrical impedance of the urothelium," *International Journal of Biomedical Engineering and Technology,* vol. 1, no. 3, pp. 287-92, 2008.

[80] S. Rajagopalan, M. Sawan, E. Ghafar-Zadeh *et al.*, "A Polypyrrole-based Strain Sensor Dedicated to Measure Bladder Volume in Patients with Urinary Dysfunction," *Sensors,* vol. 8, no. 8, pp. 5081-5095, 2008.

[81] J. Upfal, and A. Roberts, *Anatomical sensor*, World Intellectual Property Organization WO2004037082-A1; AU2003273617-A1,to Urovid Pty Ltd, 2004.

[82] P. Petrican, and M. A. Sawan, "Design of a miniaturized ultrasonic bladder volume monitor and subsequent preliminary evaluation on 41 enuretic patients," *Rehabilitation Engineering, IEEE Transactions on,* vol. 6, no. 1, pp. 66-74, 1998.

[83] P. Beauchamp-Parent, and M. Sawan, "New reconfigurable ultrasonic enuresis monitoring system," in Proceedings of the 20th Annual International Conference of the IEEE EMBS, Hong Kong. China, Year, pp. 789-792.

[84] N. Kristiansen, J. Djurhuus, and H. Nygaard, "Design and evaluation of an ultrasound-based bladder volume monitor," *Medical and Biological Engineering and Computing,* vol. 42, no. 6, pp. 762-769, 2004.

[85] T. Sinkjaer, "Integrating Sensory Nerve Signals Into Neural Prosthesis Devices," *Neuromodulation,* vol. 3, no. 1, pp. 34-41, 2001.

[86] X. Navarro, T. B. Krueger, N. Lago *et al.*, "A critical review of interfaces with the peripheral nervous system for the control of neuroprostheses and hybrid bionic systems," *Journal of the Peripheral Nervous System,* vol. 10, no. 3, pp. 229-258, 2005.

[87] S. Jezernik, W. E. N. Jian Guo, N. J. M. Rijkhoff *et al.*, "Analysis of bladder related nerve cuff electrode recordings from preganglionic pelvic nerve and sacral roots in pigs," *The Journal of Urology,* vol. 163, no. 4, pp. 1309-1314, 2000.

[88] G. A. M. Kurstjens, A. Borau, A. Rodríguez *et al.*, "Intraoperative recording of electroneurographic signals from cuff electrodes on extradural sacral roots in spinal cord injured patients," *The Journal of Urology,* vol. 174, no. 4, pp. 1482-1487, 2005.

[89] T. Sinkjaer, N. Rijkhoff, M. Haugland *et al.*, "Electroneurographic (ENG) signals from intradural S3 dorsal sacral nerve roots in a patient with a suprasacral spinal cord injury," in The 5th Annual IFESS2000 Conference and The Neural Prostheses, Aalborg, Denmark Year, pp.

[90] B. J. Wenzel, J. W. Boggs, K. J. Gustafson *et al.*, "Detecting the onset of hyper-reflexive bladder contractions from the electrical activity of the pudendal nerve," *IEEE Transactions on Neural Systems and Rehabilitation Engineering,* vol. 13, no. 3, pp. 428-435, 2005.

[91] S. Jezernik, and T. Sinkjaer, "Detecting sudden bladder pressure increases from the pelvic nerve afferent activity," in Proceedings of the 20th Annual International Conference of the IEEE EMBS, Hong Kong, China, Year, pp. 2532-5.

[92] A. Harb, M. Sawan, and M.-A. Crampon, "Monitoring Bladder Activities in Paralysed Dogs: System Design and Acute Experiments. ," in 4th Annual Conference of the International Functional Electrical Stimulation Society (IFESS), Sendai, Japon, Year, pp.

[93] A. Saleh, M. Sawan, E. A. Elzayat *et al.*, "Detection of the bladder volume from the neural afferent activities in dogs: experimental results," *Neurological Research,* vol. 30, no. 1, pp. 28-35, 2008.

[94] W. M. Grill, S. E. Norman, and R. V. Bellamkonda, "Implanted Neural Interfaces: Biochallenges and Engineered Solutions," *Annual Review of Biomedical Engineering,* vol. 11, pp. 1-24, 2009.

[95] S. Micera, L. Citi, J. Rigosa *et al.*, "Decoding information from neural signals recorded using intraneural electrodes: toward the development of a neurocontrolled hand prosthesis," *Proceedings of the IEEE,* vol. 98, no. 3, pp. 407-17, 2010.

[96] A. Bonfanti, T. Borghi, R. Gusmeroli *et al.*, "A low-power integrated circuit for analog spike detection and sorting in neural prosthesis systems," *Biomedical Circuits and Systems Conference, BioCAS IEEE,* 2008, pp. 257-260.

[97] D. N. Durand, W. Tesfayesus, and P. B. Yoo, “Peripheral nerve signals for neural control,” *2007 Ieee 10th International Conference on Rehabilitation Robotics*, vol. 1, pp. 999-1002, 2007.

[98] J. A. Woltjen, G. W. Timm, F. M. Waltz *et al.*, “Bladder Motility Detection Using the Hall Effect,” *Biomedical Engineering, IEEE Transactions on*, vol. BME-20, no. 4, pp. 295-299, 1973.

[99] J. Wang, C. Hou, W. Zhang *et al.*, “Micturition alert device dedicated to neurogenic bladders,” *U.S. National Library of Medicine English Abstracts*, vol. 22, no. 5, pp. 597-601, 2008.

[100] J. Korinek, J. Vitek, P. P. Sengupta *et al.*, “Does Implantation of Sonomicrometry Crystals Alter Regional Cardiac Muscle Function,” *Journal of the American Society of Echocardiography*, vol. 20, no. 12, pp. 1407-1412, 2007.

[101] R. W. Stadler, W. J. Combs, and D. Lipson, *Implantable medical device employing sonomicrometer output signals for detection and measurement of cardiac mechanical function* US2004176810-A1; US7082330-B2,to Medtronic Inc (Medt), 2004.

[102] L. Martel, A. Bélanger, and J.-M. Berthelot. "Loss and recovery of independence among seniors," Vol. 13, No. 4, Catalogue 82-003.

[103] A. Branner, R. B. Stein, E. Fernandez *et al.*, “Long-term stimulation and recording with a penetrating microelectrode array in cat sciatic nerve,” *Biomedical Engineering, IEEE Transactions on*, vol. 51, no. 1, pp. 146-157, 2004.

[104] T. M. Bruns, R. A. Gaunt, and D. J. Weber, “Estimating bladder pressure from sacral dorsal root ganglia recordings,” in Annual International Conference of the IEEE-EMBC, Year, pp. 4239-4242.

[105] G. A. Clark, N. M. Ledbetter, D. J. Warren *et al.*, “Recording sensory and motor information from peripheral nerves with Utah Slanted Electrode Arrays,” in Engineering in Medicine and Biology Society,EMBC, 2011 Annual International Conference of the IEEE, Year, pp. 4641-4644.

[106] J. Rigosa, D. J. Weber, A. Prochazka *et al.*, "Neuro-fuzzy decoding of sensory information from ensembles of simultaneously recorded dorsal root ganglion neurons for functional electrical stimulation applications," *Journal of Neural Engineering,* vol. 8, no. 4, pp. 046019, 2011.

[107] X. Navarro, N. Lago, M. Vivo *et al.*, "Neurobiological evaluation of thin-film longitudinal intrafascicular electrodes as a peripheral nerve interface," *2007 Ieee 10th International Conference on Rehabilitation Robotics* vol. 1 and 2, pp. 643-649, 2007.

[108] J. J. Wyndaele, "Investigating Afferent Nerve Activity From the Lower Urinary Tract: Highlighting Some Basic Research Techniques and Clinical Evaluation Methods," *Neurourology and Urodynamics,* vol. 29, no. 1, pp. 56-62, 2010.

[109] S. Matsuura, and J. W. Downie, "Effect of anesthetics on reflex micturition in the chronic cannula-implanted rat," *Neurourology and Urodynamics,* vol. 19, no. 1, pp. 87-99, 2000.

[110] K. Iijima, Y. Igawa, and J.-J. Wyndaele, "Mechanosensitive Primary Bladder Afferent Activity in Rats With and Without Spinal Cord Transection," *The Journal of Urology,* vol. 182, no. 5, pp. 2504-2510, 2009.

[111] R. Q. Quiroga, Z. Nadasdy, and Y. Ben-Shaul, "Unsupervised Spike Detection and Sorting with Wavelets and Superparamagnetic Clustering," *Neural Computation,* vol. 16, no. 8, pp. 1661-1687, 2004.

[112] M. D. Craggs, "Objective measurement of bladder sensation: use of a new patient-activated device and response to neuromodulation," *BJU International,* vol. 96, no. s1, pp. 29-36, 2005.

[113] I. H. Witten, and E. Frank, *Data Mining: Practical Machine Learning Tools and Techniques, 2nd ed.*, pp. 170-172, San Fransisco, CA: Elsevier Inc., 2005.

[114] H. Motulsky, and A. Christopoulos, *Fitting Models to Biological Data Using Linear and Nonlinear Regression: A Practical Guide to Curve Fitting*, pp. 89-90, New York: Oxford, 2004.

[115] H. Akaike, “A new look at the statistical model identification,” *Automatic Control, IEEE Transactions on,* vol. 19, no. 6, pp. 716-723, 1974.

[116] R. R. Harrison, R. J. Kier, C. A. Chestek *et al.*, “Wireless neural recording with single low-power integrated circuit,” *IEEE transactions on neural systems and rehabilitation engineering,* vol. 17, no. 4, pp. 322-9, 2009.

[117] R. Sarpeshkar, W. Wattanapanitch, S. K. Arfin *et al.*, “Low-Power Circuits for Brain-Machine Interfaces,” *Ieee Transactions on Biomedical Circuits and Systems,* vol. 2, no. 3, pp. 173-183, Sep, 2008.

[118] S. B. Brian, and M. L. Marie Carmela, “Prevalence of Urinary Incontinence in Men, Women, and Children—Current Evidence: Findings of the Fourth International Consultation on Incontinence,” *Urology,* 2010.

[119] Z. Fan, J. Holleman, and B. P. Otis, “Design of Ultra-Low Power Biopotential Amplifiers for Biosignal Acquisition Applications,” *Biomedical Circuits and Systems, IEEE Transactions on,* vol. 6, no. 4, pp. 344-355, 2012.

[120] W.-S. Liew, X. Zou, L. Yao *et al.*, “A 1-V 60-uW 16-channel interface chip for implantable neural recording,” in Custom Integrated Circuits Conference, 2009. CICC '09. IEEE, 2009, pp. 507-510.

[121] C. Prior, C. Rodrigues, A. Aita *et al.*, “Design of an integrated low power high CMRR instrumentation amplifier for biomedical applications,” *Analog Integrated Circuits and Signal Processing,* vol. 57, no. 1, pp. 11-17, 2008.

[122] W. Wattanapanitch, M. Fee, and R. Sarpeshkar, “An Energy-Efficient Micropower Neural Recording Amplifier,” *Biomedical Circuits and Systems, IEEE Transactions on,* vol. 1, no. 2, pp. 136-147, 2007.

[123] B. Gosselin, M. Sawan, and C. A. Chapman, “A Low-Power Integrated Bioamplifier With Active Low-Frequency Suppression,” *Biomedical Circuits and Systems, IEEE Transactions on,* vol. 1, no. 3, pp. 184-192, 2007.

[124] S. Micera, and X. Navarro, "Bidirectional Interfaces with the Peripheral Nervous System," *International Review of Neurobiology*, R. Luca, I. Dario and S. Leopold, eds., pp. 23-38: Academic Press, 2009.

[125] A. Rodriguez-Perez, J. Ruiz-Amaya, M. Delgado-Restituto *et al.*, "A Low-Power Programmable Neural Spike Detection Channel With Embedded Calibration and Data Compression," *Biomedical Circuits and Systems, IEEE Transactions on*, vol. 6, no. 2, pp. 87-100, 2012.

[126] D. Loi, C. Carboni, G. Angius *et al.*, "Peripheral Neural Activity Recording and Stimulation System," *Biomedical Circuits and Systems, IEEE Transactions on*, vol. 5, no. 4, pp. 368-379, 2011.

[127] B. Gosselin, and M. Sawan, "A low-power integrated neural interface with digital spike detection and extraction," *Analog Integrated Circuits and Signal Processing*, vol. 64, no. 1, pp. 3-11, 2010.

[128] A. M. Kamboh, and A. J. Mason, "On-chip feature extraction for spike sorting in high density implantable neural recording systems," in Biomedical Circuits and Systems Conference, BioCAS IEEE, 2010, pp. 13-16.

[129] S. Hiseni, C. Sawigun, W. Ngamkham *et al.*, "A compact, nano-power CMOS action potential detector," in Biomedical Circuits and Systems Conference, BioCAS IEEE, 2009, pp. 97-100.

[130] M. S. Chae, Z. Yang, M. R. Yuce *et al.*, "A 128-Channel 6 mW Wireless Neural Recording IC With Spike Feature Extraction and UWB Transmitter," *IEEE Transactions on Neural Systems and Rehabilitation Engineering*, vol. 17, no. 4, pp. 312-321, 2009.

[131] T.-C. Chen, W. Liu, and L.-G. Chen, "128-channel spike sorting processor with a parallel-folding structure in 90nm process," in ISCAS, 2009, pp. 1253-1256.

[132] V. Karkare, S. Gibson, and D. Markovic, "A 130-uW 64-channel spike-sorting DSP chip," in Solid-State Circuits Conference, A-SSCC. IEEE Asian, Year, pp. 289-292.

[133] Y. Perelman, and R. Ginosar, “An integrated system for multichannel neuronal recording with spike/LFP separation, integrated A/D conversion and threshold detection,” *IEEE Transactions on Biomedical Engineering,* vol. 54, no. 1, pp. 130-137, Jan, 2007.

[134] R. H. Olsson, and K. D. Wise, “A three-dimensional neural recording microsystem with implantable data compression circuitry,” *Solid-State Circuits, IEEE Journal of,* vol. 40, no. 12, pp. 2796-2804, 2005.

[135] Y. Sun, S. Huang, J. J. Oresko *et al.*, “Programmable Neural Processing on a Smartdust for Brain-Computer Interfaces,” *Biomedical Circuits and Systems, IEEE Transactions on,* vol. 4, no. 5, pp. 265-273, 2010.

[136] C.-C. Peng, P. Sabharwal, and R. Bashirullah, “Neural cache: A low-power online digital spike-sorting architecture,” in Engineering in Medicine and Biology Society, EMBS. Conference of the IEEE, 2008, pp. 2004-2007.

[137] L. F. Nicolas-Alonso, and J. Gomez-Gil, “Brain Computer Interfaces, a Review,” *Sensors,* vol. 12, no. 2, pp. 1211-1279, 2012.

[138] T. M. Seese, H. Harasaki, G. M. Saidel *et al.*, “Characterization of tissue morphology, angiogenesis, and temperature in the adaptive response of muscle tissue to chronic heating,” *Laboratory investigation; a journal of technical methods and pathology,* vol. 78, no. 12, pp. 1553-1562, 1998.

[139] P. D. Wolf, "Thermal Considerations for the Design of an Implanted Cortical Brain–Machine Interface (BMI)," *Indwelling Neural Implants: Strategies for Contending with the In Vivo Environment*, Chapter 3, R. WM, ed., CRC Press, 2008.

[140] B. I. Rapoport, L. Turicchia, W. Wattanapanitch *et al.*, “Efficient Universal Computing Architectures for Decoding Neural Activity,” *PLoS ONE,* vol. 7, no. 9, pp. e42492, 2012.

[141] I. Obeid, and P. D. Wolf, “Evaluation of spike-detection algorithms fora brain-machine interface application,” *Biomedical Engineering, IEEE Transactions on,* vol. 51, no. 6, pp. 905-911, 2004.

[142] S. Mukhopadhyay, and G. C. Ray, "A new interpretation of nonlinear energy operator and its efficacy in spike detection," *Biomedical Engineering, IEEE Transactions on,* vol. 45, no. 2, pp. 180-187, 1998.

[143] J. H. Choi, H. K. Jung, and T. Kim, "A new action potential detector using the MTEO and its effects on spike sorting systems at low signal-to-noise ratios," *Biomedical Engineering, IEEE Transactions on,* vol. 53, no. 4, pp. 738-746, 2006.

[144] Q. Wang, J. Dai, H. Zhang *et al.*, "Spike detection and sorting based on nonlinear energy operator and matched filter," *Chinese Journal of Scientific Instrument,* vol. 32, no. 1, pp. 81-86, 2011.

[145] J. Holleman, A. Mishra, C. Diorio *et al.*, "A micro-power neural spike detector and feature extractor in .13um CMOS," in Custom Integrated Circuits Conference, 2008. CICC 2008. IEEE, Year, pp. 333-336.

[146] S. Gibson, J. W. Judy, and D. Markovic, "Comparison of spike-sorting algorithms for future hardware implementation," in Engineering in Medicine and Biology Society Conference, EMBS IEEE, 2008, pp. 5015-5020.

[147] Z. Yang, Q. Zhao, and W. Liu, "Neural signal classification using a simplified feature set with nonparametric clustering," *Neurocomputing,* vol. 73, no. 1-3, pp. 412-422, 2009.

[148] J. F. Kaiser, "On a simple algorithm to calculate the `energy' of a signal," in Acoustics, Speech, and Signal Processing, 1990. ICASSP-90., 1990 International Conference on, Year, pp. 381-384 vol.1.

[149] D. L. Donoho, "De-noising by soft-thresholding," *Information Theory, IEEE Transactions on,* vol. 41, no. 3, pp. 613-627, 1995.

[150] M. S. Lewicki, "A review of methods for spike sorting: the detection and classification of neural action potentials," *Network: Computation in Neural Systems,* vol. 9, no. 4, pp. 53 - 78, 1998.

[151] E. Chah, V. Hok, A. Della-Chiesa *et al.*, "Automated spike sorting algorithm based on Laplacian eigenmaps and k -means clustering," *Journal of Neural Engineering,* vol. 8, no. 1, pp. 016006, 2011.

[152] D. M. Schwarz, M. S. A. Zilany, M. Skevington *et al.*, "Semi-supervised spike sorting using pattern matching and a scaled Mahalanobis distance metric," *Journal of Neuroscience Methods,* vol. 206, no. 2, pp. 120-131, 2012.

[153] P. C. Mahalanobis, "On the generalised distance in statistics," in Proceedings National Institute of Science, India, 1936, pp. 49-55.

[154] R. G. Lyons, *Understanding Digital Signal Processing*, 3rd. ed., pp. 772-773, NJ: Pearson Education Inc., 2010.

[155] J. Martinez, C. Pedreira, M. J. Ison *et al.*, "Realistic simulation of extracellular recordings," *Journal of Neuroscience Methods,* vol. 184, no. 2, pp. 285-293, 2009.

APPENDICES

APPENDIX 1 – BLADDER SENSOR: USER NEEDS

Medical Needs

1. The bladder sensor (BS) is able to measure properly the volume of urine inside the bladder:
   - Continuously in chronic basis
   - Placed in the patient during a single minimally invasive procedure
   - With side-effects acceptable for chronic use, including pain and discomfort and considering the benefits vs. risks ratio
   - Avoiding biocompatibility problems
   - Regardless of patient sex
   - Regardless of neurological and others patient health problems including the urinary tract organs, the genital organs and other related organs (i.e. kidneys, ureters, bladder, urethra, pelvic floor, prostate)
   - Regardless of bladder anatomical or physiological problems (e.g. inflammation, overactivity)
   - Regardless patient postural position and during and after postural changes
   - During and after urge stress condition (e.g. coughing, sneezing, vomiting)
   - At any bladder volume and intravesical pressure (Pves = Pdetrusor + Pabdom.)
   - At any bladder wall compliance including spastic and flaccid bladder
   - At any urine chemical composition and conductivity
   - At any bladder size and shape
2. The sensor inform appropriately in advance when the real functional bladder capacity (determined in a previous urometric evaluation) is reached.
3. The sensor alert when the intravesical pressure or volume are beyond safe values during the storing and voiding phases.
4. The sensor detects overactivity (onset detrusor contractions) during the storing phase.

5. The sensor do not produce unacceptable overload to the bladder during the measurement.
6. The sensor is easily calibrated and adjusted to patient particular conditions (obtained from urodynamic evaluation).

Technical Needs

1. The sensor is able to provide feedback signals to other systems that need it, i.e. to the implanted neurostimulator or the external unit.
2. The sensor is autonomous (standalone operation).
3. The volume and shape of the system package and transducers allow an uncomplicated and safe implantation procedure.
4. The power consumption allows the sensor operation for long-time periods (months).
5. The electromagnetic and radiofrequency radiations of the implant, if any, are harmless.
6. The sensor temperature rising does not affect the surrounding medium and the measurement accuracy.
7. The deleterious effects over the tissue produced by the sensor, if any, are clinically acceptable.
8. The sensor is maintenance-free.
9. Discarding the sensor is uncomplicated and safe to the environment.

Ergonomic Needs

1. The sensor is easy, comfortable and safe to wear.
2. The sensor calibration and setting up can be readily made by trained medical personnel.
3. The sensor communication with the patient (alerts) is easily detectable regardless patient's impairment.

EVALUATION OF USER NEEDS

The medical and technical needs are regrouped in order to facilitate the evaluation. The group label can be used as primary need instead of the separate needs which will be considered as second level needs. However, this do not necessarily means less important but regrouped needs.

The relative importance has been set carefully considering trade-offs among the needs, technological limitations and real expectations for a first version of an effective but non ideal sensor.

The Table A1-1 shows the scale and criteria considered in the needs evaluation. The scale ranges from 5 to 0, being 5 the most important.

Table A1-1: Scale and criteria to evaluate system needs

Value	Meaning
5	It is essential, the sensor will not works properly without 100% satisfaction of this need
4	It is important, the sensor will perform properly with partially satisfaction of this need (>80%)
3	It is desirable, but the system can achieve the main goal without total or partial satisfaction of this need
2	It is optional, it would enhance the sensor functions
1	It is less important, and should be implemented only if no additional cost or R&D effort is required
0	It is not important at all and should not be considered

The relative importance system needs for the bladder sensor (BS) implementation were assessed and regrouped are presented in the Table A1-2.

Table A1-2: Assessment of system needs

No.	Need	Relative Importance
1	**The BS measure the volume of urine inside the bladder <u>effectively</u>**	**5**
	– Continuously in permanent or chronic basis	5
	– Regardless of patient sex	5
	– Regardless of neurological and others patient health problems including the urinary tract organs, the genital organs and other related organs (e.g. kidneys, ureters, bladder, urethra, pelvic floor, prostate)	4
	– Regardless of bladder anatomical or physiological problems (e.g. inflammation, overactivity)	4
	– Regardless patient postural position and during and after postural changes	5
	– During and after urge stress condition (e.g. coughing, sneezing, vomiting)	4
	– At any bladder volume and intravesical pressure	5
	– At any bladder wall compliance including spastic and flaccid bladder	4
	– At any urine chemical composition and conductivity	5
	– At any bladder size and shape	5
2	**The BS measure the volume of urine inside the bladder <u>efficiently</u>**	**4**
	– The power requirement is such that allow the system operate for long-time periods (months)	4
	– The deleterious effects over the tissue, if any, caused by the sensor and the transducers are clinically acceptable	5
	– The BS temperature rising does not has an effect on the surrounding medium or on the measurement accuracy	4
	– The BS do not produce overload to the bladder during the measuring	4
3	**The BS measure the volume of urine inside the bladder <u>safely</u>**	**5**
	– It can be placed in patient during a single minimally invasive procedure	3
	– The volume and shape of the system package and transducers allow an uncomplicated and safe implantation procedure	4
	– The side-effects are acceptable in chronic use including pain and discomfort and considering the benefits vs. risks ratio	5
	– Avoiding biocompatibility problems	5

No.	Need	Relative Importance
4	**The BS is easy to use**	**4**
	– The system is easy, comfortable and safe to wear	4
	– The system calibration and setup can be readily made by trained medical personnel	4
	– The system communication with the patient (alerts) is easily detectable regardless patient's impairment	5
5	**The BS inform appropriately in advance when the real functional bladder capacity is reached (determined in a previous cystometric evaluation)**	**5**
6	**The BS alert when the intravesical pressure or volume are beyond safe values**	**3**
7	**The BS is easily calibrated and adjusted to patient particular parameters (obtained from urodynamic evaluation).**	**5**
8	**The BS detects overactivity (onset detrusor contractions) during the storing phase**	**5**
9	**The BS is able to provide feedback signals to other systems that need it, i.e. to the neurostimulator or the external unit**	**4**
10	**The BS is autonomous (standalone operation)**	**3**
11	**The BS is maintenance-free**	**4**
12	**Discarding the BS is uncomplicated and safe to the environment**	**3**

APPENDIX 2 – TARGET TECHNICAL SPECIFICATIONS

Technical specifications are the translation of needs into metrics and values that are used to establish system attributes. Target values are set initially to guide the measurement method research. To accomplish this translation the House of Quality (HoQ) shown in Figure A2-1 was developed following the proposed methodology for the Quality Function Deployment method [27].

The specifications were obtained considering a comprehensive literature review and the application of QFD method. The proposed targets specifications shown in Table A2-1 are the result of HoQ analysis. The evaluation of correlation degree among needs and metrics, among the metrics themselves and the setting of the needs weighting, allow identifying the most relevant specifications and the trade-offs to consider in subsequent research stages.

The results are shown in Table A2-1 with some comments, when needed, for better understanding of the targeted value. We also included the International Continent Society (ICS) standards for urodynamic instrumentation used in clinical diagnosis [28],[29]. However, it is worth noting that these standards have been established for urodynamic instruments used for diagnosis in clinical labs facilities for non-wearable and non-chronic applications, as it is the case of the device researched. Hence, it would be unreal to expect that these standards can be completely fulfilled by implantable devices, considering the present limitations in both medical knowledge and technological feasibility. However, when possible, some ICS standards were considered as references in order to improve the design as much as possible.

Table A2-1: BS target technical specifications

Metrics	Units	Target Value	Reference (ICSS)	Comments
Volume monitoring				
Range	mL	0 - 650	0 - 1000	Lower value for monitoring purpose but with safety factor over maximum physiological limit
Accuracy	mL	≤ ±10	±10	Volume values are recommended to be rounded to nearest multiple of 10 mL.
Precision (or repeatability)	%	≤ ±5	N/A	To ensure resolution in the worst case
Resolution	mL	≤ 10	10	Volume values are recommended to be rounded to nearest multiple of 10 mL. The resolution can be inferred as 10 mL
Pressure monitoring				
Range	cmH_2O	0 - 250	0 - 250	Physiological intravesical pressure (including stress conditions as coughing)
Accuracy	cmH_2O	≤ ±5	±1	Lower for monitoring purpose: for physiological intravesical pressure (including stress conditions as coughing)
Precision (or repeatability)	%	≤ 1	N/A	
Resolution	cmH_2O	≤ 1	1	Minimum value required to detect onset contractions
Frequency response	Hz	0 - 10	0-10	Meet bladder pressure frequency of changes
Power consumption	mW	≤ 10		
Alerts				
Detection of bladder overactivity		Yes		Filling pressure rising slope > value determined in cystometric study
Detection of fullness		Yes		Adjustable percentage of volume max.
Detection of volume max.		Yes		Maximum cystometric capacity
Detection of pressure max.		Yes		Cystometric Leakage Pressure Point
Alerting signals		3		Visual, audible and mechanical (vibration) alerts
Programmable		Yes		Easy to program
Biocompatible		Yes		
Autonomous		Yes		Standalone operation
Communication with neurostimulator system		Yes		
Safety		Yes		Meet IEC 60101 standards, Health Canada standard, CSE, and CE
Usability		very good		Easy to use, straight forward and intuitive handling
Easy Calibration		very good		
Maintenance-free		Yes		
Safe to discard after life-cycle or damage		Yes		

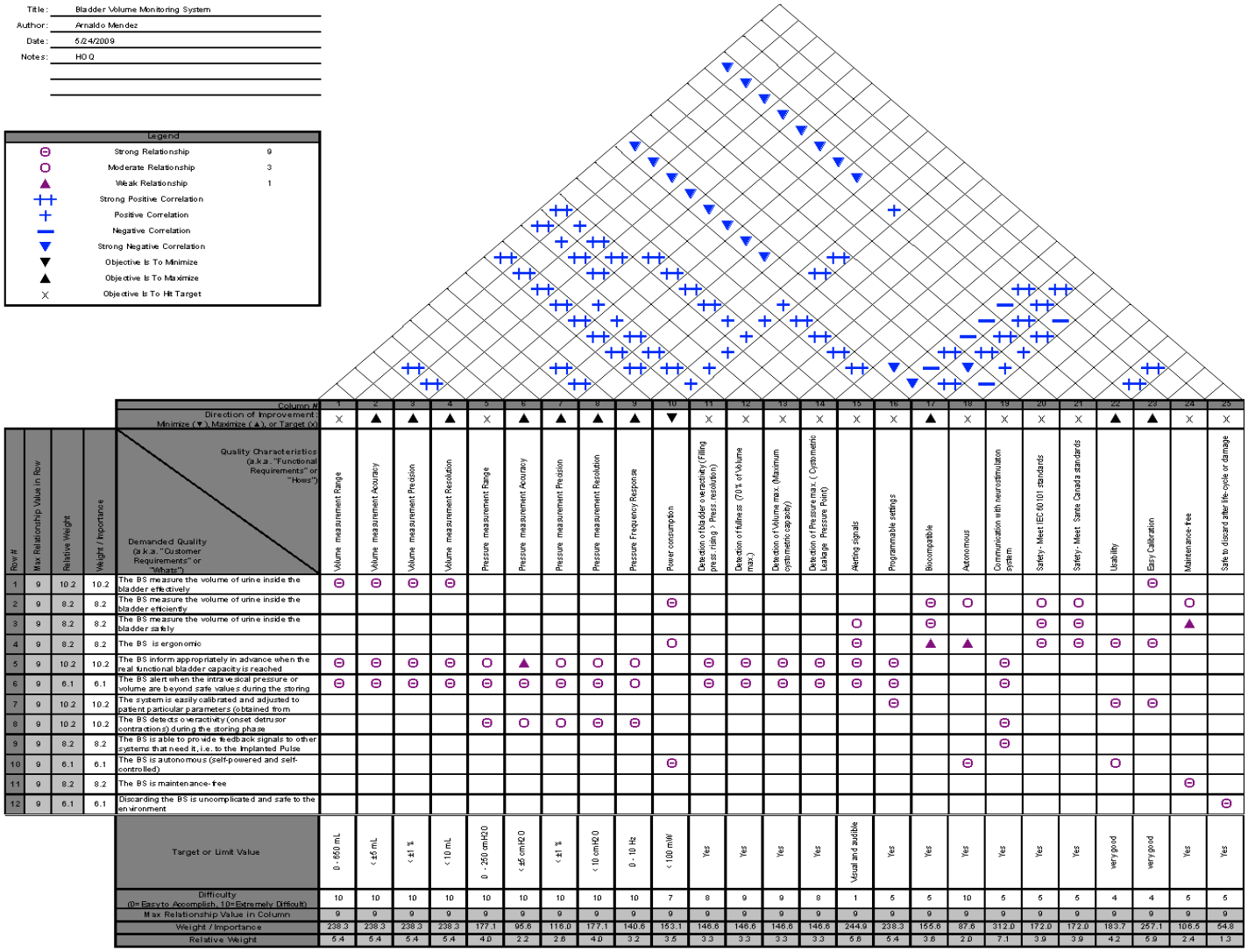

Figure A2-1: House of Quality (HoQ)

APPENDIX 3 – ADDITIONAL INFORMATION ON THE ASSESSMENT OF THE MEASUREMENT METHODS

Results shown in Table 2-1 were obtained using the set weights of shown in Table A3-1 and the Rates shown in Table A3-2.

Table A3-1: Set of weights used for the selection criteria used to assess the measurement methods.

Selection Criteria	Set 1	Set 2	Set 3	Set 4	Set 5
Effectiveness in chronic use	10	10	10	10	10
Immunity to postural changes, urge stress, urine conductivity and temperature and other artifacts	10	10	10	10	10
Easy to calibrate and adjust to patient's particularities	5	5	5	5	10
Easiness of implantation (minimally invasive)	10	20	10	10	10
Safe to use with minimal deleterious effects	10	10	20	10	10
Efficacy of volume measurement (accuracy)	5	5	5	5	10
Precision of volume measurement (reproducibility)	20	10	10	10	10
Detection of bladder overactivity	10	10	10	10	10
Low power consumption	10	10	10	10	10
Availability and cost of materials and components	10	10	10	20	10

Table A3-2: Rates given to the measurement methods for each evaluation criterion.

Selection criteria	IVP	EIP	SGP	WUS	EMP	ENG
Effectiveness in chronic use	2	2	3	3	4	5
Immunity to postural changes, urge stress, urine conductivity and temperature and other artifacts	1	1	4	2	2	4
Easy to calibrate and adjust to patient's particularities	4	4	2	4	2	3
Easiness of implantation (minimally invasive)	3	3	2	5	3	4
Safe to use with minimal deleterious effects	3	1	3	5	4	4
Efficacy of volume measurement (accuracy)	1	2	5	4	3	2
Precision of volume measurement (reproducibility)	1	2	5	4	4	3
Detection of bladder overactivity	5	3	5	4	3	4
Low power consumption	3	2	1	2	5	5
Availability and cost of materials and components	4	5	1	4	4	4

APPENDIX 4 – CORRELATION COEFFICIENT COMPARISON

The Pearson's (PCC), Spearman's (SCC) and Kendall's (KCC) correlation coefficient means among the recorded ENG signals and the infused volume were computed and analyzed to find the most suitable one for unit class selection; that is, the nerve that conveys the most reliable source of sensory information of the bladder volume. Figures A3-1 to A3-4 depict the results of a Multiple Comparison test among the groups of coefficients using a one-way ANOVA with bin-widths of 1 s, 10 s, 30 s, and 60 s, respectively (n = 107).

We found a significant difference among these three coefficients for a bin-width (BW) of 1 s, which is the timeframe used to select the best unit (worst case scenario). For a BW ≥ 30s the SCC and KCC did not show significant difference between them but both were significant different from PCC. The SCC displayed always the best values of correlation even for the shortest BW.

In all fiber recordings where more than one unit exhibited good Pearson's and Spearman's correlation coefficients, using the minimal BW of 1 s, the best unit chosen when using PCC instead of SCC was not the unit that yielded the lowest estimation error. On the other hand, SCC peaked before KCC while BW was swept from 1 s to 60 s, which matched roughly the bin-width mean yielding the lowest estimation error RMSE throughout the experiments.

Based on these result the Spearman's rank correlation coefficient was chosen as the most suitable to select the neural unit for decoding the bladder volume.

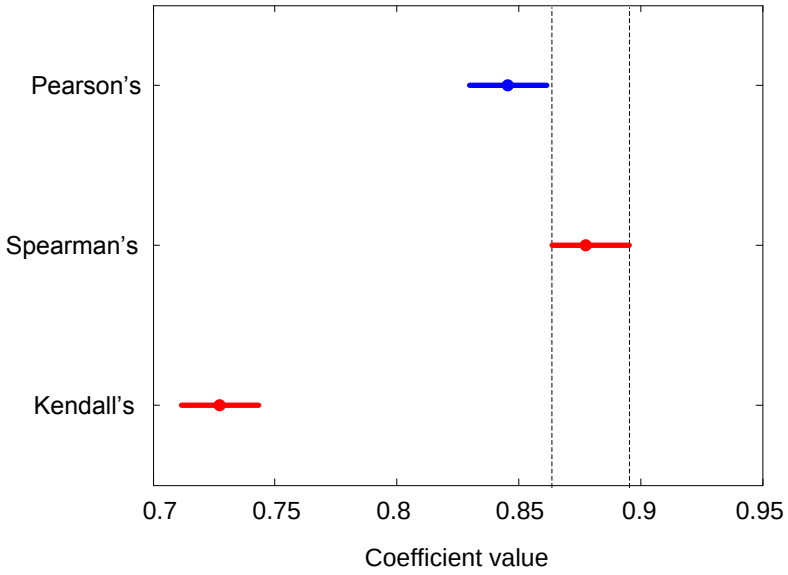

Figure A4-1: Multiple Comparison test among the groups of coefficients using a one-way ANOVA with a bin-width of 1 s. Pearson's, Spearman's and Kendall's correlation coefficient means showed a statistically significant difference among them ($p < 0.05$).

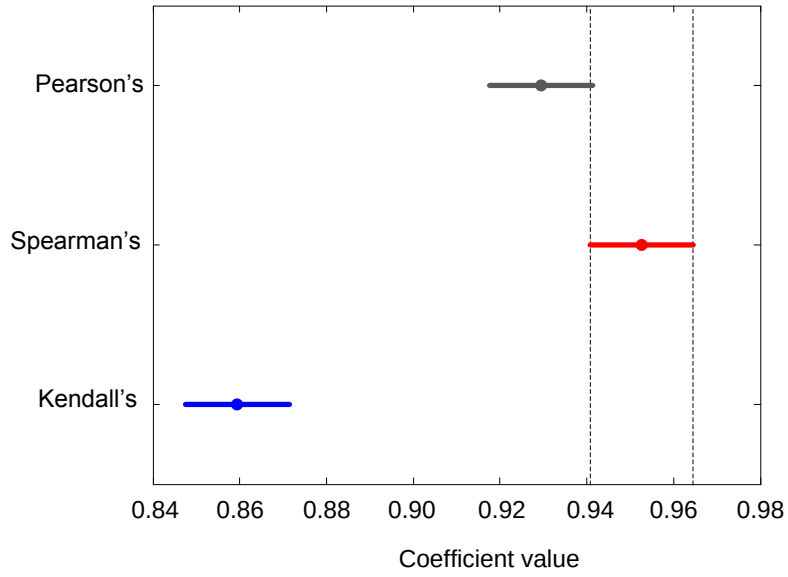

Figure A4-2: Multiple Comparison test among the groups of coefficients using a one-way ANOVA with a bin-width of 10 s. Pearson's and Spearman's correlation coefficient means showed a statistically significant difference with Kendall's ($p < 0.05$).

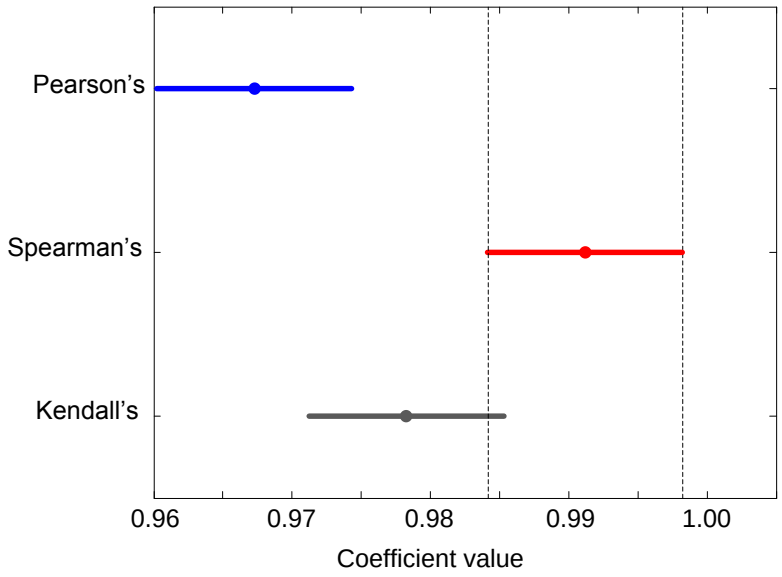

Figure A4-3: Multiple Comparison test among the groups of coefficients using a one-way ANOVA with a bin-width of 30 s. Spearman's and Pearson's correlation coefficient means were statistically significant different ($p < 0.05$).

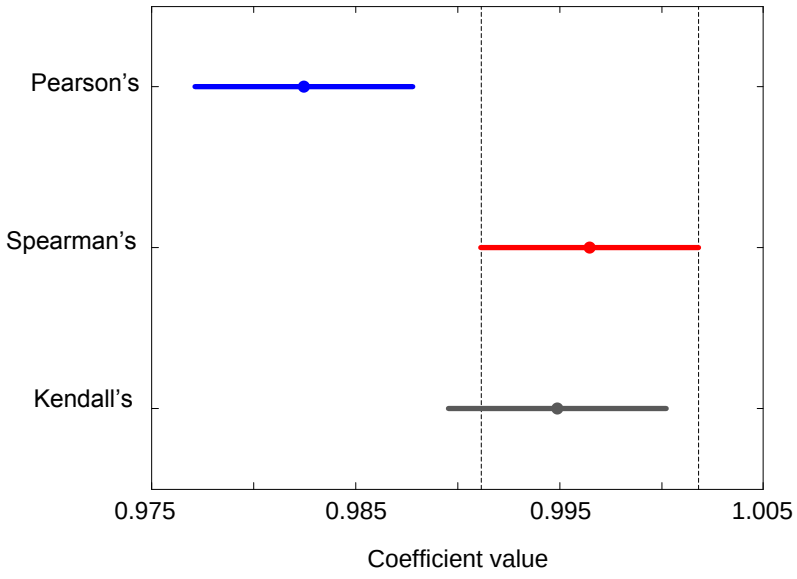

Figure A4-4: Multiple Comparison test among the groups of coefficients using a one-way ANOVA with a bin-width of 60 s. Spearman's and Kendall's correlation coefficient means showed a statistically significant difference with Pearson's coefficient ($p < 0.05$).